Cellular and Molecular Analysis of NDR and LATS Kinases in *Dictyostelium*

Peter Michael Kastner

Dissertation

der Fakultät für Biologie

der Ludwig-Maximilians-Universität München

zur Erlangung des akademischen Grades

„Doktor der Naturwissenschaften"

(Dr. rer. nat.)

vorgelegt von

Peter Michael Kastner

aus Schongau

München, 2010

Gutachter: 1. Prof. Dr. Michael Schleicher

                      2. Prof. Dr. Dirk Eick

Datum der Einreichung: 31. Aug. 2010

Mündliche Prüfung: 01. Dez. 2010

Ehrenwörtliche Versicherung

Ich versichere hiermit ehrenwörtlich, dass die vorgelegte Dissertation von mir selbständig und ohne unerlaubte Hilfe angefertigt ist.

München, den 31. August 2010

Peter Michael Kastner

Ort der Durchführung

Der experimentelle Teil dieser Dissertation wurde durchgeführt im Labor von Prof. Dr. Michael Schleicher am Institut für Anatomie und Zellbiologie der Ludwig-Maximilians-Universität München unter Betreuung von PD Dr. Annette Müller-Taubenberger.

Publications

Articles

Kastner, P.M., M. Schleicher, and A. Müller-Taubenberger. 2010. The NDR family kinase NdrA of *Dictyostelium* localizes to the centrosome and is required for efficient phagocytosis. *Traffic*, *in press*.

Müller-Taubenberger, A., H.C. Ishikawa-Ankerhold, P.M. Kastner, E. Burghardt, and G. Gerisch. 2009. The STE group kinase SepA controls cleavage furrow formation in *Dictyostelium*. *Cell Motil. Cytoskeleton*. 66:929-39.

Talks

Dictyostelium meeting. 2009. MRC, Cambridge, United Kingdom
Kastner P., M. Schleicher, A. Müller-Taubenberger. 2009. Insights into NDR kinases from *Dictyostelium.*

International *Dictyostelium* meeting. 2008. Tsukuba, Japan
Kastner P., M. Schleicher, A. Müller-Taubenberger. 2008. Functional analysis of NDR kinases in *Dictyostelium discoideum*.

DGZ Young scientist meeting. 2007. Münster, Germany
Kastner P., M. Schleicher, A. Müller-Taubenberger. 2007. NDR kinases and regulation of cytokinesis in *Dictyostelium discoideum.*

Poster presentations

50th Annual DGZ Meeting. 2010. Regensburg, Germany
Kastner P., M. Schleicher, A. Müller-Taubenberger. 2010. Characterization of the centrosomal NDR kinases NdrA and NdrB in *Dictyostelium discoideum. Eur. J. Cell Biol.* 89:S2-26.

ASCB 49th Annual Meeting. 2009. San Diego, California
Kastner P.M., M. Schleicher, A. Müller-Taubenberger. 2009. Characterization of the centrosomal NDR kinases NdrA and NdrB in *Dictyostelium discoideum*. *Mol. Biol. Cell* 20(suppl):1097/B255.

49th Annual DGZ Meeting. 2009. Konstanz, Germany

Kastner P., M. Schleicher, A. Müller-Taubenberger. 2009. Characterization of NDR kinases in *Dictyostelium discoideum*. *Eur. J. Cell Biol.* 88:SE-10.

ASCB 48th Annual Meeting. 2008. San Francisco, California

Kastner P.M., M. Schleicher, A. Müller-Taubenberger. 2008. Characterization of NDR kinases in *Dictyostelium discoideum*. *Mol. Biol. Cell* 19(suppl):1939/B402.

DFG Molecular Cell Dynamics. 2008. Münster, Germany

Kastner P.M., M. Schleicher, A. Müller-Taubenberger. 2008. NDR kinases in *Dictyostelium discoideum*.

48th Annual DGZ Meeting. 2008. Jena, Germany

Kastner P., M. Schleicher, A. Müller-Taubenberger. 2008. Regulation of cytokinesis in *Dictyostelium discoideum* by a SIN-related pathway. *Eur. J. Cell Biol.* 87:S3-9.

ASCB 47th Annual Meeting. 2007. Washington D.C.

Kastner P.M., M. Schleicher, A. Müller-Taubenberger. 2007. Cytokinesis in *Dictyostelium discoideum* is regulated by a SIN-related pathway. *Mol. Biol. Cell* 18(suppl):2245/B597.

EMBO workshop "Molecular Mechanisms of Cell Cycle Control". 2007. Spetses, Greece

Kastner P.M., M. Schleicher, A. Müller-Taubenberger. 2007. NDR kinases and regulation of cytokinesis in *Dictyostelium discoideum*.

47th Annual DGZ Meeting. 2007. Frankfurt, Germany

Kastner P., M. Samereier, M. Schleicher, A. Müller-Taubenberger. 2007. Exploring the role of NDR kinases in *Dictyostelium discoideum* cytokinesis. *Eur. J. Cell Biol.* 86:S1-36.

Table of contents

Summary

Dictyostelium discoideum is a well established haploid model organism to gain insights into the mechanisms and the regulatory machinery controlling essential cellular functions. The main objective of this study was the characterization of NDR/LATS (nuclear Dbf2-related)/(large tumor suppressor) kinases of *Dictyostelium*. The NDR/LATS kinases NdrA, NdrB, and Lats2 (NdrC) of *Dictyostelium* were investigated to specify the regulatory networks of NDR/LATS kinases with respect to their functional roles. NDR/LATS kinases were identified in both uni- and multicellular organisms as key regulators of processes such as morphological changes, mitotic exit, cytokinesis, as well as development, cell growth and secretion.

For both, NdrA and NdrB the localization to the centrosome was shown by fluorescence microscopy. NdrA, which is enriched at the centrosomal corona was also identified in isolated centrosome preparations. The localization of NdrA and NdrB is regulated during the cell cycle. In prophase, NdrA disappears from the centrosome, forms a cloud-like structure around the spindle, and is totally absent during later stages of mitosis. NdrB localizes to the mitotic spindle and spindle poles. MobB, a member of the Mob1 family of coactivators specific for the NDR/LATS family of protein kinases, forms a complex with NdrB, and *in vitro* analysis showed an interaction of MobA and MobB with NdrA.

Deletion of NdrA causes impaired cell growth on bacteria which is due to reduced phagocytosis. The detailed analysis of NdrA-null cells revealed that the formation of phagocytic cups is delayed. NdrA co-precipitates with EmpC, a member of the p24 family of cargo receptors of Golgi complex derived vesicles which are supposed to be involved in membrane trafficking towards the cell cortex. The results suggest that a signal originating from the NdrA kinase at the centrosome triggers the efficiency of phagocytosis. It is assumed that in NdrA-null cells the defects in phagocytosis may be caused by an impairment of vesicle trafficking which is involved in providing new membrane at the sites of particle uptake.

For the NdrB-MobB complex a number of potential interactors could be identified. Both, NdrB and MobB were found to interact with PI3Kc kinases, which are important for phosphoinositol-phosphate turnover at the cleavage furrow or the front of moving cells. Furthermore, binding of RacE and its putative activator ElmoB suggests an involvement of NdrB in the regulation of actin filament assembly and cell morphology. The activity of NdrB

may be regulated by the putative interactors Aurora kinase AurK and the Ste20-like kinase KrsA.

Lats2 was found to function in the regulation of cytokinesis and to be involved in centrosome duplication. The detailed microscopic analysis of Lats2-null cells revealed large multinucleate cells that are characterized by an excess number of centrosomes. Multinucleated Lats2-null cells undergo synchronous mitosis but are unable to proceed through cytokinesis. Thus the results obtained in this study suggest a role for Lats2 rather in the regulation of cytokinesis than of mitosis.

Interaction studies of Lats2 specified the oncogenic Ras family of small GTPases as novel interactors of NDR/LATS kinases. The amount of activated RasB and RasG was upregulated in the absence of Lats2. The activity of RasB and RasG in cell division has been shown previously as well as the regulation of RasB and RasG by the RasGAP NF1. This RasGAP is a putative Lats2 interactor, and is also involved in the regulation of cytokinesis. RasB and RasG as well as the Ras binding domain RBD of Lats2 localize to the plasma membrane, whereas Lats2 without the RBD is cytoplasmic.

The data suggest a novel regulatory mechanism of cell division that involves the tumor suppressor homolog Lats2 and members of the oncogenic Ras family of GTPases, RasB and RasG, under the control of the RasGAP NF1. It is also tempting to speculate that Lats2 plays a role in *Dictyostelium* SIN (septation initiation network)-related signal transduction, triggering cell division.

Zusammenfassung

Der haploide Modellorganismus *Dictyostelium discoideum* ermöglicht die direkte Analyse regulatorischer Mechanismen bei essentiellen zellulären Prozessen. In dieser Arbeit wurden die NDR/LATS (nuclear Dbf2-related)/(large tumor suppressor) Kinasen NdrA, NdrB, und Lats2 in *Dictyostelium* charakterisiert. NDR/LATS Kinasen wurden in ein- sowie mehrzelligen Organismen als Schlüssel-Regulatoren der Zell-Dynamik, morphologischer Veränderungen wie dem Übertritt von der Mitose in die Zytokinese, Entwicklungsvorgängen sowie von Zell-Wachstum und Sekretion beschrieben.

Die Lokalisation von NdrA und NdrB am Centrosom konnte mittels Fluoreszenz-Mikroskopie gezeigt werden. NdrA befindet sich in der centrosomalen Corona und wurde in aufgereinigten Centrosomen nachgewiesen. Für beide Kinasen ist die Lokalisation Zellzyklus-abhängig reguliert. Während der Prophase löst sich NdrA vom Centrosom und befindet sich in der Umgebung der mitotischen Spindel, während es in den späteren Stadien nicht mehr nachgewiesen werden kann. NdrB hingegen lokalisiert an der mitotischen Spindel und den beiden Spindel-Polen. *In vitro* Untersuchungen zeigten, dass NdrB einen Komplex mit MobB bildet, einem Mitglied der Mob1-Familie von Co-Aktivatoren. Für NdrA wurde die Bindung von MobA und MobB gezeigt.

Die Deletion von NdrA beeinträchtigt das Wachstum auf Bakterien, verursacht durch reduzierte Phagozytose-Raten. Die detaillierte Analyse von NdrA-null Zellen zeigte die verzögerte Ausbildung der phagozytotischen Cups. NdrA ko-präzipitiert mit EmpC, einem Cargo-Rezeptor der p24-Familie. Vesikel mit p24-Membran-Proteinen haben ihren Ursprung im Golgi Komplex und sind beteiligt am Membran-Transport zum Zell-Cortex. Die beschriebene Rolle für NdrA weist auf ein Signal hin, welches von der centrosomal lokaliserten Kinase NdrA ausgeht und die Effizienz der Phagozytose beeinflusst. Es ist anzunehmen, dass der für NdrA-null Zellen beobachtete Defekt der Phagozytose auf eingeschränkten Vesikel-Transport zum Nachschub zusätzlicher Membran an die Stellen der Partikel-Aufnahme zurückzuführen ist.

Bei der Untersuchung des NdrB-MobB Komplexes wurden unterschiedliche Interaktoren identifiziert. NdrB und MobB binden Mitglieder der PI3Kc Kinasen, die beteiligt sind am Umsatz von Phosphatidylinositol-Phosphat an der Teilungsfurche oder der Front sich bewegender Zellen. Die Bindung von RacE sowie dessen vermutlichen Aktivators ElmoB lässt eine Rolle für NdrB in der Regulation des Actin-Zytoskeletts und der Zell-

Morphologie vermuten. Desweiteren bindet NdrB die konservierten NDR/LATS-Kinase Regulatoren Aurora Kinase AurK und die Ste20-ähnliche Kinase KrsA.

In dieser Arbeit wurden die regulatorische Funktion von Lats2 in der Zytokinese und dessen Beteiligung an der Duplikation von Centrosomen gezeigt. Die detaillierte mikroskopische Analyse von Lats2-null Zellen wies große multinukleäre Zellen auf, die durch eine erhöhte Zahl an Centrosomen charakterisiert sind. Vielkernige Lats2-null Zellen durchlaufen die Mitose synchron, sind jedoch nicht in der Lage sich zu teilen. Diese Ergebnisse lassen vermuten, dass der Schwerpunkt der Funktion von Lats2 eher in der Regulation der Zytokinese als der Mitose liegt.

Mittels Interaktionsstudien für Lats2 wurde die Ras GTPase Familie als neue Gruppe von NDR/LATS Kinase bindenden Proteinen spezifiziert. Zudem ist der Anteil an aktiviertem RasB und RasG in Lats2-knockout-Zellen hochreguliert. Zuvor wurden bereits die Aktivität von RasB und RasG in der Zell-Teilung sowie die Regulation von RasB und RasG durch das RasGAP NF1 gezeigt. Der potentielle Lats2-Interaktor NF1 ist ebenfalls an der Regulation der Zytokinese beteiligt. RasB und RasG sowie die Ras-bindende Domäne RBD von Lats2 lokalisieren an der Plasmamembran, wohingegen Lats2 ohne die RBD im Zytoplasma angereichert ist.

Aufgrund dieser Ergebnisse kann ein bisher unbekannter regulatorischer Mechanismus für die Regulation der Zellteilung durch das Tumor-Suppressor-Homolog Lats2 beschrieben werden. Lats2 reguliert, vermittelt durch das RasGAP NF1, die Aktivität von RasB und RasG, und spielt somit eine essentielle Rolle bei der Kontrolle der Zell-Teilung. Zusätzlich kann eine Rolle von Lats2 in der *Dictyostelium* SIN (septation initiation network)-verwandten Signaltransduktion, welche die Einleitung der Zellteilung im Anschluss an die Mitose reguliert, angenommen werden.

1 Introduction

1.1 The model system *Dictyostelium discoideum*

Dictyostelium discoideum is a eukaryotic model organism for studying essential cellular processes. *Dictyostelium* serves as a very suitable system for the analysis of the regulation of cellular dynamics as chemotaxis, cell adhesion and phagocytosis (Figure 1A,B) as well as the required signaling processes; for example the regulator of the actin cytoskeleton coronin was first described in *Dictyostelium* (de Hostos et al., 1991). Moreover, *Dictyostelium* facilitates gaining insights into the mechanisms and the regulatory machinery controlling mitosis and cell division. Furthermore, *Dictyostelium* can be employed for the functional characterization of human disease genes or pharmacological studies. *Dictyostelium* belongs to the social amoebae and can be phylogenetically positioned next to animals and fungi but is more distant from plants. First described in 1869 by Oskar Brefeld (Brefeld, 1869), the genus *Dictyostelium* was classified as cellular slime molds. In 1935 Kenneth Raper described the species *Dictyostelium discoideum* (Raper, 1935), which as well as descendant strains became a versatile model for diverse scientific questions.

Social amoebae are characterized by a developmental cycle, in which the transition from an autonomously living single cell to a higher organized multicellular organism occurs. In its natural habitat, *Dictyostelium* cells live in the soil and feed on bacteria (Figure 1A,B). Deprivation of nutrients causes a developmental switch, which induces the aggregation of single cells mediated by chemotaxis (Figure 1C). Later on, these aggregates can undergo morphological changes and form slug-shaped bodies with the ability to phototax towards light (Figure 1D). During culmination, the slug rises from the underlying substratum and forms a fruiting body consisting of a basal disk, stalk and the spore head, containing spores (Figure 1E). The later ones are stable forms for enduring unfavorable periods as starvation conditions. Due to its ability to differentiate and aggregate to multicellular structures *Dictyostelium* became an amenable model for cell differentiation.

The sequencing of the genome, which comprises six chromosomes with a total size of 34 Mb, revealed that *Dictyostelium* contains about 12.000 genes, i.e. the genome is almost as big as the fruit fly *Drosophila* genome and harbors twice the number of genes found in the yeast genome (Eichinger et al., 2005). The haploid genome is easily susceptible to

manipulation by recombinative methods. Since *Dictyostelium* is tractable by genetic and biochemical analyses it also became an important model organism to study biomedical questions (Williams et al., 2006) and it is one of the model organisms chosen by the NIH.
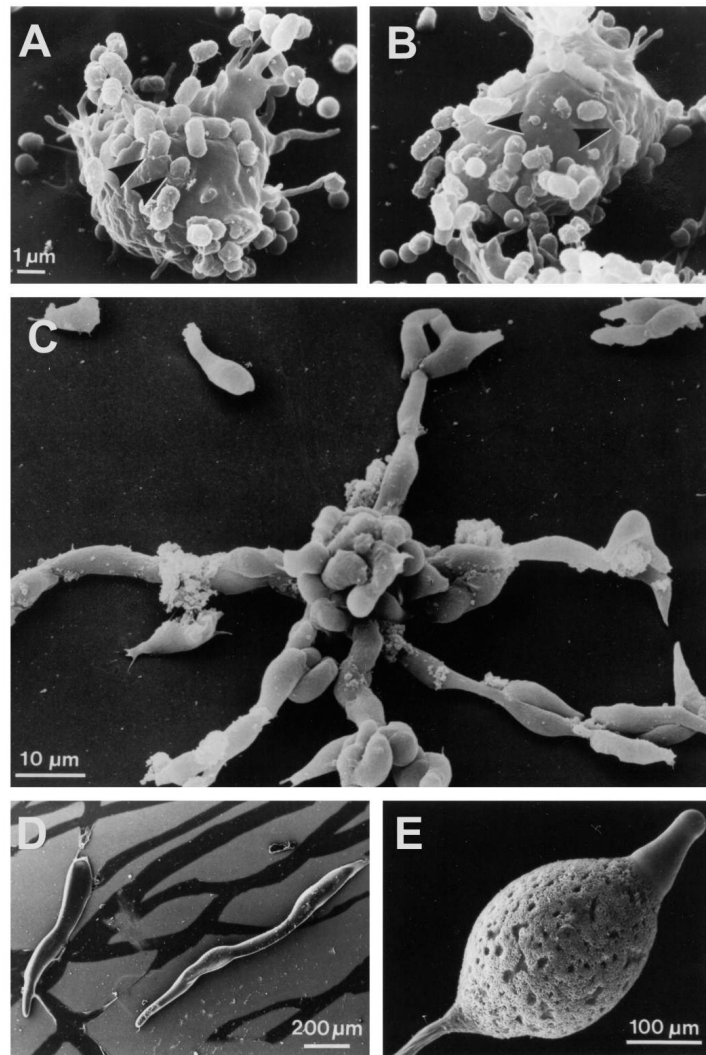
Figure 1: Developmental stages of *Dictyostelium*

Images of different stages of the *Dictyostelium* life cycle taken by scanning electron microscopy. (**A**, **B**) Single amoebae feeding on bacteria by phagocytosis. (**C**) Aggregating cells. (**D**) Slugs moving on a solid substratum. (**E**) Spore head of an almost completely differentiated fruiting body. Images taken from (Müller-Taubenberger and Maniak, 2004).

1.2 The phagocytosis machinery

The major routes for uptake of extracellular materials into the interior of eukaryotic cells can be distinguished as caveolae- or clathrin-mediated endocytosis, macropinocytosis and phagocytosis (Doherty and McMahon, 2009). Clathrin-mediated endocytosis is linked to specific receptors and involves the formation of clathrin-coated vesicles. Formation of caveolae is a more specialized form of endocytosis and not found in all eukaryotic cells, like for instance *Dictyostelium*. Macropinocytosis describes the internalization of fluids, while phagocytosis is the uptake of solid material. Both processes are regulated by complex signaling pathways and require an extensive remodeling of the actin cytoskeleton as well as recycling of membranes and receptors (Huynh et al., 2007; Ravanel et al., 2001).

In metazoans, phagocytosis enables scavenger cells like macrophages or neutrophils to take up pathogens, foreign particles or apoptotic bodies. Also in unicellular organisms like amoebae, phagocytosis is the major road for the uptake of solid food particles (Figure 1A, B). The soil amoeba *Dictyostelium* is a professional phagocyte and is employed as a model for studying the sequence of events during phagocytosis. The mechanisms of particle recognition, the involvement of the cytoskeleton during the internalization, the generation of phago-lysosomes, and the retrieval of membrane share common features between *Dictyostelium* and mammalian phagocytes. However, each of these steps is highly complex and involves numerous proteins that contribute with different functionalities to efficient phagocytosis. This complexity was also confirmed by proteomics approaches that led to the identification of a large number of factors that are of importance for phagocytosis (Garin et al., 2001; Gotthardt et al., 2006; Gotthardt et al., 2002).

The structural rearrangements that underlie phagocytosis, in particular the cytoskeletal rearrangements that accompany the formation of a phagocytic cup, have been studied in detail in *Dictyostelium* (Janssen and Schleicher, 2001; Konzok et al., 1999; Maniak et al., 1995). However, the process of membrane remodeling at the phagocytic cup and the signaling components that participate in the regulation of phagocytosis are less well explored. It is generally accepted that phosphoinositide 3-kinases are essential for membrane trafficking (Lindmo and Stenmark, 2006) by providing PI(3)P to phagosomal, and later on, to phago-lysosomal membranes. PI(3)P has also been shown to serve as a common marker for the early endosomal compartment in *Dictyostelium* (Clarke et al., 2010). Furthermore, the process of lipid vesicle trafficking towards the sites of phagocytic

uptake to provide supplies of membrane has been demonstrated to be required for phagosome maturation (Swanson, 2008).

1.3 Mechanisms of cytokinesis

At the end of the cell cycle, immediately following mitosis, the mother cell is cleaved into two daughter cells. This mechanical process which divides the cell body is called cytokinesis. Models predestined for the investigation of cytokinesis are the yeasts *Saccharomyces cerevisiae* (budding yeast) and *Schizosaccharomyces pombe* (fission yeast), the amoeba *Dictyostelium*, as well as higher eukaryotes as animals and plants. Due to the high complexity of multicellular organisms, work with single cells as yeast or *Dictyostelium* is of high benefit to understand basic principles. Whereas *S. cerevisiae* forms buds, cell division occurs symmetrical in *Dictyostelium* and *S. pombe*, thus provides optimal conditions for studying cytokinesis.

In *Dictyostelium*, chromosomes are segregated by an intranuclear spindle during closed mitosis (Effler et al., 2006); the centrosomes move towards the incipient daughter cells powered by motor proteins on aster microtubules that are linked to the cell cortex (Neujahr et al., 1997). Eukaryotic cells go through a number of shape changes during cytokinesis. After rounding up, cells elongate and ingression of the furrow occurs, then a bridge forms between the two daughter cells, which produces two individual cells after constriction (Robinson and Spudich, 2004). The force required for ingression of the contractile ring at the cleavage furrow is generated by myosin-II and actin. In *Dictyostelium* a number of components of the actin cytoskeleton have been identified that are required for successful cytokinesis (Gerisch et al., 2004).

Regulation of cell division is an essential feature of all organisms from protozoa to highly organized metazoans. In mitosis duplicated genetic material is distributed to two daughter nuclei, a process coordinated by the microtubule network. At the end of mitosis cell division takes place, which is controlled by the cortical actin cytoskeleton. Mediated by the acto-myosin ring at the cell cortex contraction of the cell body starts and leads to division into two independent cells (Glotzer, 1997; Glotzer, 2001; Rajagopalan et al., 2003). Defects and disorders of cell division cause severe cellular alterations and the development of tumors.

While regulation of mitosis and the performance of cytokinesis are described in detail for the yeasts, the signaling processes connecting the spindle to the site of cytokinesis are

largely unknown in higher eukaryotes. Uncontrolled growth and cell division occurs when the molecular interplay between oncogenes and regulating tumor suppressors is disrupted. Altered regulation of tumor suppressing kinases such as for instance the mammalian NDR/LATS kinases, results in misregulated centrosome duplication (Hergovich et al., 2009; Hergovich et al., 2007). Centrosomal aberrations foster chromosomal instability, and thus directly contribute to development of tumors (Nigg, 2006).

In-depth understanding of cytokinesis is of major importance for the investigation and development of potential drug target candidates for the treatment of cancer (Robinson and Spudich, 2004). One assumption is that the signals controlling the mechanical events of cell division are emerging from the mitotic spindle. However, the transduction of these signals and the biochemical feedback control are of major interest for future investigations.

1.4 General features of NDR/LATS kinases

The NDR (nuclear Dbf2-related) and LATS (large tumor suppressor) group of kinases belongs to the AGC (protein kinase A / G / C -like) class of serine/threonine protein kinases controlling important cellular processes from yeast to human (Hergovich et al., 2006). The general characteristics of NDR/LATS kinases are the central catalytic kinase domain consisting of 12 subdomains (Hanks and Hunter, 1995), an N-terminal regulatory domain (NTR) and a C-terminal hydrophobic motif (HM). Common features of NDR/LATS kinases and AGC kinases are the activation segment in the catalytic domain as well as the highly conserved hydrophobic motif, both of which are activated by phosphorylation (Figure 2). The catalytic kinase domain has an insert (I) between subdomain VII and VIII, containing a putative auto-inhibitory sequence (AIS) of 30-60 amino acid residues, which is required by NDR/LATS kinases for the regulation of their activity by auto-phosphorylation (Tamaskovic et al., 2003). The auto-inhibitory sequence is followed by the positively charged activation segment (AS) in subdomain VIII harboring a conserved phosphorylation site which is a target for autophosphorylation (Bichsel et al., 2004; Mah et al., 2001). The NDR/LATS kinase specific N-terminal regulatory domain binds the co-activator Mob1 (Hou et al., 2004). This interaction releases the kinase from auto-inhibition by the auto-inhibitory sequence, thus promoting autophosphorylation at the activation segment (Figure 2), which in turn causes partial activation of the NDR/LATS kinase

(Hergovich et al., 2005). At the C-terminus, a regulatory threonine phosphorylation site is embedded in a hydrophobic motif that is a target for upstream Ste20-like kinases, reported to phosphorylate mammalian NDR/LATS kinases (Stegert et al., 2005).

Some NDR/LATS kinases were reported to localize to the centrosome as for example the mammalian NDR/LATS homologs NDR1 and NDR2 and are regulated by Mob1 proteins. Similar to mammalian NDR/LATS kinases, the *S. pombe* NDR homologous kinase Sid2 localizes to the spindle pole body and also binds a Mob1 co-activator (Hou et al., 2000). The structure of human (Stavridi et al., 2003) and *Xenopus laevis* (Ponchon et al., 2004) Mob1 was resolved and led to the determination of the negatively charged surface of Mob1, which interacts with the positively charged residues of the NDR/LATS-N-terminal regulatory domain. Moreover it was described that phosphorylation of Mob1 by MST kinases is required for the activation of NDR1 (Bao et al., 2009; Hirabayashi et al., 2008).
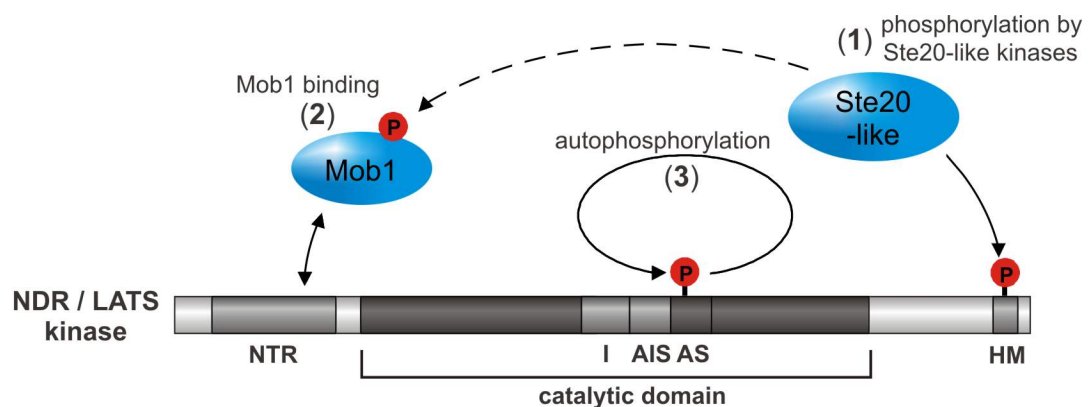
Figure 2: NDR/LATS kinase model of activation

Common features of NDR/LATS kinases are the N-terminal regulatory domain (NTR) which binds Mob1, the central catalytic domain and a C-terminal hydrophobic motif (HM). Activity is regulated by autophosphorylation of a positively charged activation segment (AS) in the catalytic domain next to the specific insert (I), containing the auto-inhibitory sequence (AIS). A threonine residue, located in the conserved hydrophobic motif of the C-terminus is a putative target of Ste20-like kinases. Ste20-like kinases are thought to phosphorylate the hydrophobic motif and most likely Mob1 proteins (**1**), Mob1-coactivators can bind the N-terminal regulatory domain (**2**) and trigger activation of the catalytic kinase domain by autophosphorylation (**3**).

# 1.5 NDR/LATS kinase signaling in yeast, fly and mammals

1.5.1 Regulation of the cell cycle by SIN and MEN signaling in yeast

General key players of cytokinesis are the cyclin-dependent kinase Cdk1 and the Polo family kinase Plk1 (Nigg, 2001). Cdk1 phosphorylates structural components and regulates the proteolytic machinery that controls the timely degradation of mitotic regulators, whereas Plk1 is regulating the microtubule system and controlling cytokinesis. Downstream of these master regulators, regulatory cascades that were described are the mitotic exit network (MEN) of *S. cerevisiae* (budding yeast) and the septation initiation network (SIN) in *S. pombe* (fission yeast), both consisting of kinases and GTPases. These signaling pathways are involved either in the regulation of mitotic events and/or the signaling towards the initiation of cytokinesis. To complete mitosis, it is essential to assure the correct distribution of the duplicated genome to the two daughter cells, followed by constriction of the acto-myosin ring, which leads to division into two independent cells (Glotzer, 1997; Glotzer, 2001; Rajagopalan et al., 2003). The contraction is initiated by signals transduced by the SIN network. In contrast to the SIN, the MEN network plays a major role in regulating the exit from mitosis. This is achieved by controlling the degradation of cyclin-dependent kinases as part of the spindle checkpoint. The signaling molecules involved in SIN and MEN show a high degree of conservation between the two yeasts (Simanis, 2003) and some of the proteins have also been identified in other eukaryotes.

The SIN pathway couples the mitotic exit to cytokinesis. After inactivation of the mitotic CDKs, the SIN pathway becomes active (Guertin et al., 2002). The Polo kinase Plk1 at the spindle pole body (Tanaka et al., 2001) indirectly or via a G-protein switch triggers the activity of the GTPase Spg1. Activated GTP-bound Spg1 associates with the kinase Cdc7 (Mehta and Gould, 2006). Cdc7 further regulates the activity of Sid1. The NDR/LATS kinase Sid2 is activated by the kinase Sid1. Sid2 interacts with Mob1 (Hou et al., 2000) and relocates to the division site (Figure 3A).

The MEN in *S. cerevisiae* is triggered by the spindle checkpoint. Here also a GTPase (Tem1) downstream of the Polo kinase Cdc5 transmits the signal to the core kinases of the cascade, Cdc15 and the NDR/LATS kinase Dbf2, interacting with Mob1. Like Sid2 in the SIN pathway, Dbf2 is triggering cell division. The Dbf2-Mob1 complex activates Cdc14, which initiates the exit of mitosis and is involved in activating the cytokinesis machinery (Figure 3B).
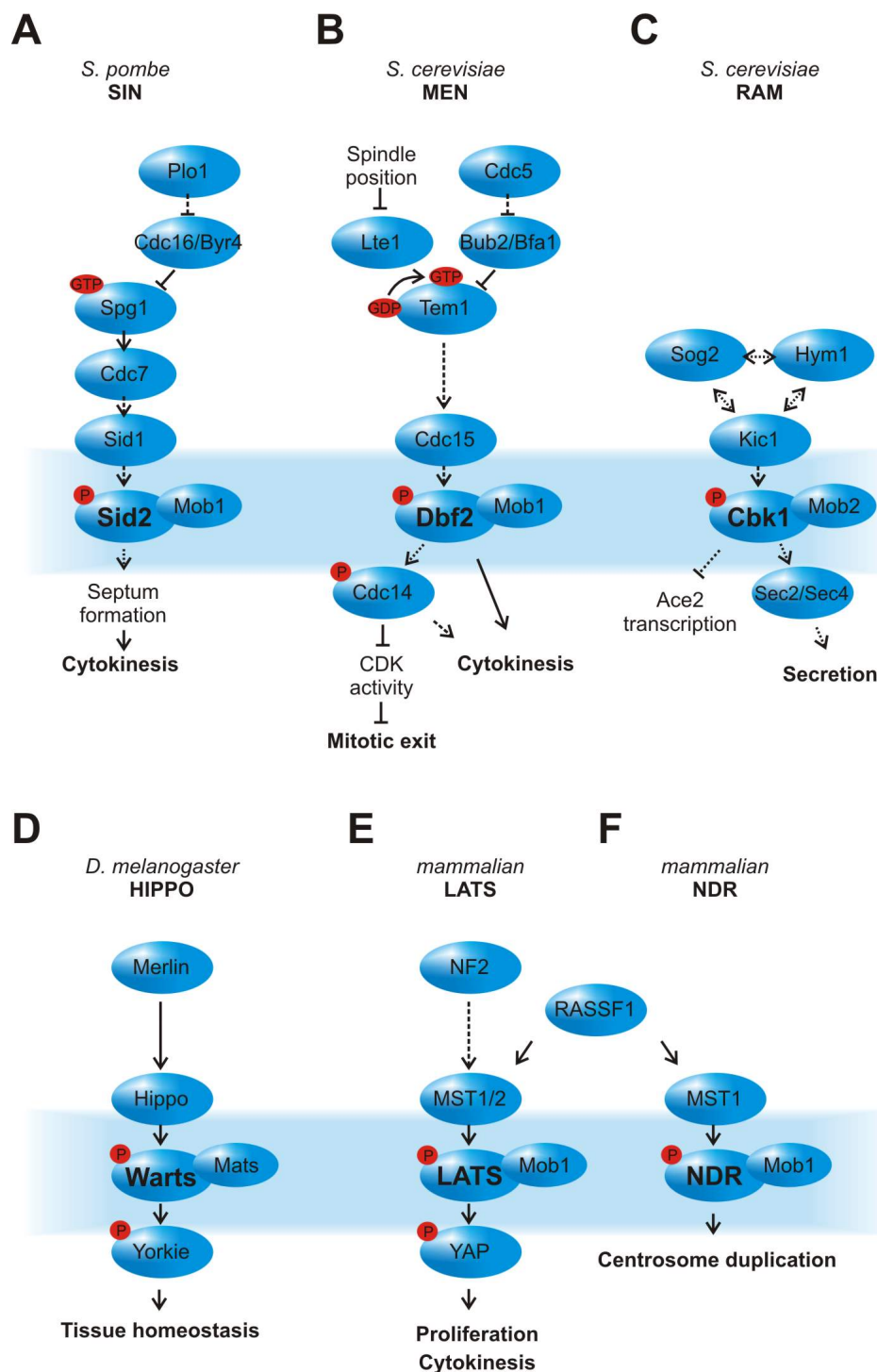
Figure 3: The core elements of NDR/LATS kinase signaling

The NDR/LATS kinases Sid2 and Dbf2 are central regulators of the closely related septation initiation network (SIN) of *S. pombe* (**A**) and the mitotic exit network (MEN) of *S. cerevisiae* (**B**) (Bardin and Amon, 2001; Nigg, 2001). (**C**) Regulation of Ace2 and morphogenesis (RAM) and secretion by Cbk1 (Hergovich et al., 2006; Nelson et al., 2003). (**D**) Tissue homeostasis in fly requires Warts in the Hippo signaling cascade (Hergovich and Hemmings, 2009). The tumor suppressors LATS (**E**) and NDR (**F**) in mammals are responsible for the regulation of proliferation and cytokinesis as well as centrosome duplication (Hergovich and Hemmings, 2009).

1.5.2 Regulation of secretion by the *S. cerevisiae* RAM network

Members of the group of NDR/LATS kinases in other organisms are involved in regulating secretion or cell growth. In *S. cerevisiae* the so-called RAM (regulation of Ace2 activity and cellular morphogenesis) signaling network was described to integrate cell fate determination and morphogenesis, and involves the NDR/LATS kinase Cbk1 (Dohrmann et al., 1996; Jansen et al., 2006). In addition, Cbk1 was shown to regulate growth in budding yeast via Golgi-dependent glycosylation and secretion (Kurischko et al., 2008). During bud emergence, Cbk1 is required for cell wall deposition and influences exocytosis events by interfering with Sec2 and Sec4, two regulators of secretion (Kurischko et al., 2008). Cbk1 phosphorylates Sec2 and thereby triggers Sec4-dependent exocytosis. Together with the upstream Ste20-like kinase Kic1 and its interactors Sog2 and Hym1, Cbk1 regulates growth and secretion via the RAM signaling network (Figure 3C). In the same line, mutants lacking the NDR/LATS kinase COT1 of *N. crassa*, a homolog of *S. cerevisiae* Cbk1, also exhibit growth defects and altered cell wall composition (Ziv et al., 2009).

1.5.3 *Drosophila* Hippo signaling in development

The NDR/LATS kinase homolog Warts (Lats) together with its upstream regulator Hippo, a Ste20-like kinase, plays a fundamental role in connecting the regulation of organ size during eye development in the fly (Edgar, 2006; Zhao et al., 2008) (Figure 3D). Upon phosphorylation by the Hippo kinase, Warts bound to the Mob1 protein Mats is controlling tissue growth and development in the Hippo pathway (Wu et al., 2003). This leads to the activation of a downstream component of Warts, the transcriptional co-activator Yorkie, which is responsible for the transcriptional regulation of Cyclin E and Diap1 (Huang et al., 2005). The loss of Warts or Hippo results in increased rates of cell proliferation and cancer.

1.5.4 Mammalian NDR/LATS kinases act as tumor suppressors

Mammalian NDR and LATS kinases have been described as essential regulators of mitosis, cell growth and development (Hergovich and Hemmings, 2009). In addition, in mammalian cells an implication of NDR kinases in cancer has been established (Hergovich et al., 2006; Tamaskovic et al., 2003). The mammalian NDR/LATS kinases are divided in two groups, NDR1 and NDR2 as well as LATS1 and LATS2.

Misregulation of NDR kinases is linked to tumorigenesis. Upregulation of NDR1 was reported for melanoma cells (Adeyinka et al., 2002). Besides the role of NDR2 in neuronal growth and differentiation (Stork et al., 2004), levels of NDR2 are raised in lung-cancer cells (Ross et al., 2000). Human NDR kinases are responsible for centrosome duplication, indicating a molecular link between cancer and NDR kinases (Hergovich et al., 2007). Disruption of NDR1 in mice causes a high likelihood for development of T cell lymphomas (Cornils et al., 2010).

The kinases LATS1 and LATS2 are responsible for the control of cell size in organs in a pathway closely related to *Drosophila* Hippo signaling (Zhao et al., 2008). Furthermore, in many human sarcomas, ovarian carcinomas, breast cancer or leukaemia, downregulation of the levels of LATS1 and LATS2 have been observed (Hergovich et al., 2006; Takahashi et al., 2005). Detailed analysis led to the finding that Lats1 interacts with CDC2 (cyclin B) and established a role of LATS1 as a mitotic exit network kinase (Bothos et al., 2005; Tao et al., 1999; Yang et al., 2001) that also regulates cell cycle progression (Yang et al., 2004) and genomic integrity (Iida et al., 2004). LATS1-null mice spontaneously develop tumors and show hypersensitivity to carcinogenic treatment (St John et al., 1999). LATS2 was reported to control cell proliferation (Li et al., 2003) and mice depleted of LATS2 are inviable due to defects of genome stability and proliferation control (McPherson et al., 2004).

The interaction with Mob1 proteins is necessary for releasing the kinases from auto-inhibition (Hergovich et al., 2005) and is a prerequesite for the functionality of NDR and LATS. Phosphorylation by mammalian sterile 20-like (MST) kinases is required for maximal activation of NDR/LATS kinases. MST1 and MST2 phosphorylate LATS (Chan et al., 2005), whereas MST1 and MST3 phosphorylate NDR (Hergovich et al., 2009; Stegert et al., 2005). The upstream components MST1 and MST2 are activated by interaction with the tumor suppressor GTPase RASSF1 (Ras association domain-containing protein 1) (Avruch et al., 2009) (Figure 3E, F).

1.6 SIN-homologous signaling in *Dictyostelium*

In an attempt to identify proteins important for cell division a screen using restriction enzyme mediated integration (REMI) mutagenesis was made (Guerin and Larochelle, 2002). Screening for large, multinucleated cells revealed the gene *sepA*, a homolog of *S. pombe cdc7*, a central kinase of the septation initiation network. SepA-null cells are

deficient in growth and cell division, caused by incomplete formation of cleavage furrows (Müller-Taubenberger et al., 2009).

Sequence homology searches for proteins involved in both, the MEN or SIN pathway against the *Dictyostelium* genome database (Chisholm et al., 2006; Eichinger et al., 2005) revealed a number of components with high similarities to the network (Figure 3). These are the Polo-family kinase Plk, the GAP Bub2, its downstream GTPase Spg1 (Müller-Taubenberger, unpublished) and possible effector of the kinase SepA (Müller-Taubenberger et al., 2009).

Though clear homologs for the components upstream of SepA were identified, an assignment of putative downstream targets by homology is difficult, given that NDR/LATS kinases are represented by four members in *Dictyostelium* and putative regulators of the Ste20-like group of kinases comprise 17 kinases (Arasada et al., 2006; Goldberg et al., 2006). Studies on the Ste20-like Severin-kinase SvkA (Rohlfs et al., 2007) revealed a strong defect in cytokinesis with a similar multinucleated phenotype as in SepA-null cells. The putative downstream components of NDR/LATS kinases together with members of the Mob1 family of coactivators are yet unknown.

Dictyostelium comprises four members of the NDR/LATS group Ser/Thr kinases (NdrA, NdrB, Lats2 (NdrC) and Lats1 (NdrD) (Goldberg et al., 2006), which are putative downstream regulators in a SIN related pathway in the regulation of cytokinesis in *Dictyostelium*.

1.7 Goals of the thesis

NDR/LATS kinases have been shown to function as key regulators of mitotic exit and cytokinesis in both, yeast and mammals. The activity of NDR/LATS homologous kinases in mammals is crucial for cell viability and of major importance for the suppression of cancerous cell growth. Moreover, NDR/LATS kinases are important regulators of tissue homeostasis and morphogenesis (Hergovich et al., 2006).

The genome of *Dictyostelium* comprises four NDR/LATS family kinases, the NDR-related NdrA and NdrB, and the LATS-related kinases Lats2 (NdrC) and Lats1 (NdrD). Conserved components of NDR/LATS signaling pathways are present in *Dictyostelium* and highly related to regulatory networks that have been described in simple organisms like yeast, but are also present in higher eukaryotes. Thus, for more profound understanding of the NDR/LATS kinase signaling pathways, I wanted to characterize the activities and

regulatory mechanisms mediated by NDR/LATS kinases in *Dictyostelium*. This work should focus on the functional investigation of NdrA, NdrB and Lats2 with the main objective on the characterization of NdrA and Lats2. In parallel, Lats1 activities should be investigated in collaboration with the laboratory of Prof. Gerald Weeks (UBC, Vancouver, Canada).

In order to achieve these major goals, knockout mutants had to be generated and analyzed by functional and cell biological studies employing biochemical and microscopy tools.

2 Materials and methods

2.1 Materials

2.1.1 Instruments

BioDocAnalyze	BioMetra
Dounce homogenisor	Braun/Wheaton
Eagle Eye II	Stratagene
Gene pulse electroporator	BioRad
Spectral-Photometer LS55	PerkinElmer
Swin-Lok plastic holder and filters	Whatman
PCR-thermocycler Uno	Biometra
pH-Meter pH526	WTW
Photometer Ultrospec 2100 pro	Amersham
Protein-transfer Trans-Blot SD	Peqlab
Thermomixer R	Eppendorf
Ultrasonicator 820/H	Elma
UV-transilluminator IL-200-M	Bachofer
Vortex	Bender & Hobein
Waterbath	GFL. Ika. Infors. Kühner

Microscopes:

LSM 510 Meta confocal microscope	Zeiss
M200	Zeiss
CFL 40	Zeiss
SteREO Discovery.V8	Zeiss

Objectives:

10x A-Plan 0.25 Ph1	Zeiss
20x LD A-Plan 0.30 Ph1	Zeiss
40x LD A-Plan 0.50 Ph2	Zeiss
63x Neofluar 1.4 oil immersion objective	Zeiss
100x Neofluar 1.3 oil immersion objective	Zeiss

Centrifuges:

GS-6KR	Beckman
J2-21M/E	Beckman
J6-HC	Beckman
Microcentrifuge 5415	Eppendorf
Microfuge R	Beckman
Optima LE-80K	Beckman
Rotina 420 R	Hettich
TL ultracentrifuge	Beckman

Rotors:

JA-10, JA-14, JA-20,	Beckman
Ti 35, Ti 45, Ti 70,	Beckman
TLA 100.3	Beckman

2.1.2 Computer programs

Acrobat 9.0	Adobe Systems
AxioVision	Carl Zeiss Vision GmbH
BioDoc Analyze	Biometra
CorelDraw 12	Corel Corporation
Endnote 8.0.1	Thomson Reuters
FL WinLab	Perkin Elmer
ImageJ 1.34n	Wayne Rasband
Microsoft Office 2003	Microsoft
Photoshop CS2	Adobe Systems
T-Coffee	www.ch.embnet.org
ZEN	Zeiss

2.1.3 Laboratory consumables

Cell culture plates, 24 wells	Nunc
Cell culture dishes, 100 mm	Greiner bio-one
Dialysis tubings type 8	BioMol
Gel-blotting-paper GB002	Whatman
Nitrocellulose membrane Protran BA85	Whatman

Parafilm	American National Can
PCR tubes ThermoTube 0.2 ml	Peqlab
Pipettes 10 ml, 25 ml	Nunc, Sarstedt
1.5 ml-centrifuge tubes	Sarstedt
Pipette tips	Gilson
Plasmid DNA Purification Kit - Maxi	Macherey Nagel, Qiagen
Plasmid DNA Purification Kit - Midi	Qiagen
QIAprep Spin Miniprep and Gel Extraction kits	Qiagen
Quartz cuvettes	Starna
Sterile filter, 0.22 µm Millex GV	Sarstedt
Tubes 15 ml, 50 ml	Greiner, Sarstedt
X-ray film X-omat AR 5	GE Healthcare

2.1.4 Reagents

Standard laboratory chemicals were purchased from BioMol, Fluka, Merck, Roth, Serva or Sigma and had the degree of purity "p.a." unless otherwise mentioned. Media and buffers used in this study were prepared with de-ionised water (Millipore), sterilized either by autoclaving or passing through a micro-filter.

Adenosine-5'-trisphosphate-Na$_2$-salt	Serva
Acrylamide (30% acrylamide with 0.8% bisacrylamide)	Roth
Agar-Agar, type RG Euler	BD
Agarose (SeaKem LE)	BMA
Ammoniumpersulfate (APS)	Roth
AX medium pH 6.7 (#AXM0102)	Formedium
Bacto-peptone/-tryptone	Oxoid
BCIP (5-bromo-4-chloro-3-indolyl phosphate)	Gerbu
Blasticidin-S	ICN Biomedicals Inc.
BSA (bovine serum albumin fraction V)	PAA
Coomassie brilliant blue R 250, G 250	Roth, Sigma-Aldrich
Complete EDTA-free protease inhibitor cocktail tablets	Roche
DAPI (4',6-diamidino-2- phenylindoldihydrochlorid)	Sigma-Aldrich
DE52 (diethylaminoethyl-cellulose)	Whatman
Dideoxyribonucleic acids (ATP, TTP, GTP, CTP)	Roche, NEB

DPH (Diphenylhexatriene)	Invitrogen
Disodiumpyrophosphate	Sigma-Aldrich
DMSO (dimethylsulfoxide)	Serva
DNA polymerase Phusion	NEB
DNA polymerase Amplitaq	Applied Biosystems
DNA restriction enzymes	Roche, NEB
DSP (dithiobis[succinimidylpropionate]) crosslinker	Thermo-Pierce
DTT (1,4-Dithio-D, L-threitol)	Gerbu
EDTA (ethylenediaminetetraacetic acid)	Biomol
EGTA (ethyleneglycolbis[2-aminoethylether]tetraacetic acid)	Sigma-Aldrich
Ethidium bromide	Sigma-Aldrich
Gerbu100 adjuvant	Gerbu Biochemicals
GFP-Trap-kit	ChromoTek
Glutathione-sepharose	Sigma-Aldrich
G 418 disulfate	Sigma-Aldrich
HEPES (4-[2-hydroxyethyl]-1-piperazineethanesulfonic acid)	Roth
HL5-C medium pH 7.5 (#HLC0102)	Formedium
IPTG (Isopropyl-β-D-thiogalactopyranoside)	Gerbu
LB-broth (#LBX0102)	Formedium
n-Octylpolyoxyethylene	Bachem
NBT (nitrobluetetrazolium)	Sigma-Aldrich
NP-40 (octyl phenoxylpolyethoxylethanol)	Fluka
Oligonucleotides	ThermoFischer
PhosStop phosphatase inhibitor	Roche
2-Propanol	Roth
Proteose peptone	Oxoid
SDS (sodium dodecylsulfate)	Serva
Silicon dioxide	Sigma-Aldrich
TEMED (tetramethylethylendiamine)	Pierce
TO-PRO-3 iodide	Invitrogen
TRITC (tetramethylrhodamine-isothiocyanate)	Invitrogen
TRITC-dextran	Invitrogen
Triton X-100	Roth
Yeast extract	Oxoid

2.1.5 Antibodies

Polyclonal antibodies generated in the course of this study:

NdrA   (412)

NdrB   (432)

MobB   (433)

Published polyclonal antibody used in this study:

GFP   (Müller-Taubenberger et al., 2009)

Published monoclonal antibodies used in this study:

α-tubulin   (YL1/2)   Chemicon

CP224   (Gräf et al., 1999)

p23   (H194)   (Ravanel et al., 2001)

p25   (H72)   (Ravanel et al., 2001)

cortexillin I (241-438-1)   (Faix et al., 1996)

coronin   (176-3-6)   (de Hostos et al., 1993)

GFP   (K3-184-2)   (Noegel et al., 2004)

Secondary antibodies:

goat anti-rat IgG Alexa-488-conjugated   Invitrogen

goat anti-rabbit IgG Alexa-488-conjugated   Invitrogen

goat anti-rabbit IgG Alexa-568-conjugated   Invitrogen

goat anti-mouse IgG Alexa-488-conjugated   Invitrogen

goat anti-mouse IgG Alexa-568-conjugated   Invitrogen

goat anti-mouse IgG Cy3-conjugated   Invitrogen

goat anti-mouse IgG Cy5-conjugated   Invitrogen

anti-rabbit alkaline-phosphatase-conlugated   Dianova

anti-mouse alkaline-phosphatase-conlugated   Dianova

2.1.6 Vectors

Constructs generated in the course of this study:

NdrA knockout construct   resistance: blasticidin-S

GFP-NdrA   blasticidin-S

NdrB knockout construct   blasticidin-S

GFP-NdrB   blasticidin-S

pGEX 6P-1-NdrA(1-110)

pGEX 6P-1-NdrB

pGEX 6P-1-MobA

pGEX 6P-1-MobB

pGEX 6P-1-MobC

Constructs made available by Dr. Annette Müller-Taubenberger (LMU München):

456-22   blasticidin-S

GFP-NdrA-T497E   G 418

EmpC-GFP   blasticidin-S

GFP-MobA   blasticidin-S

GFP-MobB   blasticidin-S

GFP-Lats2(435-1335)   G418

GFP-Lats2(2-300)   blasticidin-S

RasB-GFP   blasticidin-S

GFP-RasB   blasticidin-S

GFP-RasB-G12T   G 418

GFP-RasG   blasticidin-S

GFP-RasG-G12T   blasticidin-S

pGEX 6P-1-Lats2(2-300)

Constructs made available by Dr. Meino Rohlfs (LMU München):

GFP-NdrA   G 418

GFP-NdrA-T497E   G 418

GFP-NdrA-T497A   G 418

Constructs made available by Prof. Dr. Gerald Weeks (UBC Vancouver, Canada):

Lats2 knockout construct   blasticidin-S

Published constructs used in this study:

pGEX 6P-1   GE Healthcare

pLPBLP   (Faix et al., 2004)

GFP-cortexillin I   (Weber et al., 1999)

LimEΔ-GFP   (Bretschneider et al., 2004)

pDEX-27-GFP   (Müller-Taubenberger et al., 2006)

pDEX-61-GFP   (Müller-Taubenberger et al., 2006)

mRFP-Histone2B   (Müller-Taubenberger et al., 2009)

2.1.7 Bacteria strains

Klebsiella aerogenes   (Ushiba and Magasanik, 1952; Williams, 1978)

E. coli JM 105   Invitrogen

E. coli NEB-5α   New England Biolabs

E. coli BL21-RIL   Stratagene

2.1.8 Yeast strains

S. cerevisiae YSC-II   Sigma-Aldrich

2.1.9 *Dictyostelium* strains

Strains generated in the course of this study:

NdrA-null

NdrA-null + GFP-NdrA

NdrA-null + GFP-NdrA-T497E

NdrA-null + GFP-NdrA-T497A

NdrA-null + LimEΔ-GFP

AX2 + GFP-NdrA

AX2 + GFP-NdrB

Lats2-null

Lats2-null + GFP-Lats2(435-1335)

Strains made available by Dr. Annette Müller-Taubenberger (LMU München):

AX2 + EmpC-GFP

AX2 + GFP-MobA

AX2 + GFP-MobB

AX2 + RasB-GFP

AX2 + GFP-RasB

AX2 + GFP-RasB-G12T

AX2 + GFP-RasG

AX2 + GFP-RasG-G12T

AX2 + GFP-Lats2(2-300)

AX2 + GFP-Lats2(435-1335)

Published strains used in this study:

AX2-214 wild-type   (Watts and Ashworth, 1970)

AX2 + LimEΔ-GFP   (Bretschneider et al., 2004)

2.2 Methods

2.2.1 Molecular biological methods

Expression vectors were generated using standard molecular biological methods. Genomic DNA from *Dictyostelium* wild-type or mutant AX2 was isolated by phenol/chloroform purification followed by ethanol precipitation or by using lysis buffer LyB (10 mM Tris, pH 8.3, 50 mM KCl, 2.5 mM $MgCl_2$, 0.45% NP-40, and 0.45% Tween 20, containing proteinase K) (Charette and Cosson, 2004). PCR (polymerase chain reaction) was performed with either Amplitaq-polymerase (Applied Biosystems), Phusion DNA polymerase (NEB) or home made Taq-polymerase in PCR buffer (10 mM Tris pH 8.8, 50 mM KCl, 2 mM $MgCl_2$, 0.1 mg/ml BSA, 2% DMSO). PCR products were cloned into expression constructs using standard restriction enzyme mediated cloning. Plasmid DNA was obtained from *E. coli* by alkaline lysis miniprep (Holmes and Quigley, 1981) or the silica-based anion-exchange midi-/maxiprep kits. Chemically competent *E. coli* cells were prepared according to the $CaCl_2$ method (Dagert and Ehrlich, 1979). The sequence of the resulting constructs was confirmed by sequencing using sequence specific primers (MWG, Ebersberg).

2.2.2 Cell biological methods

2.2.2.1 Cell culture and transformation of *Dictyostelium*

Cells of the *Dictyostelium* wild-type strain AX2-214, or mutant cells derived from it were cultivated at 21°C in nutrient HL5 medium (Formedium), either in shaking culture with 150 rpm or submerged in Petri dishes or on lawns of *K. aeorogenes*.

To generate NdrA-null or Lats2-null mutants, $2x10^7$ wild-type AX2 cells were transformed with gene replacement constructs by electroporation using a Bio-Rad gene pulser at 0.8-0.9 kV and 3 µF in 4-mm cuvettes. Several independent transformants were selected by addition of 10 µg/ml of blasticidin-S. Transformants were cloned by spreader dilutions on lawns of non-pathogenic *K. aerogenes*. Mutants were identified by PCR using a combination of primers located 5′ or 3′ of the recombination site and within the blasticidin-S resistance cassette or the replaced genomic region of the genes *ndrA* or *ndrC* and in the case of NdrA confirmed by Western blotting with polyclonal antibodies recognizing NdrA.

Wild-type AX2, NdrA-null cells (clone #4) or Lats2-null cells (clone A2) (Chapter 2.1.9) were transformed with constructs for the expression of fluorescently tagged proteins as C- or N-terminal GFP or mRFP tags for visualization of protein localization by live-cell microscopy (Chapter 2.1.6). Transformants were selected by addition of either 10 µg/ml G418 (Sigma-Aldrich) or 7.5 µg/ml blasticidin-S. All GFP- or mRFP-constructs were expressed under the actin-15 promoter.

2.2.2.2 Generation of polyclonal antibodies

The sequences encoding amino acid residues 1 to 100 of NdrA, full length NdrB, amino acid residues 2 to 300 of Lats2, full length MobA or full length MobB were cloned into the bacterial expression vector pGEX-6P1 (GE Healthcare).

These constructs enable expression of:

- GST-NdrA(1-110)   (NdrA N-terminal regulatory domain)
- GST-NdrB   (full-length NdrB)
- GST-Lats2(2-300)   (Lats2 Ras binding domain)
- GST-MobA   (full-length MobA)
- GST-MobB   (full-length MobB)

GST-fusion proteins were purified using glutathione-sepharose and eluated via addition of glutathione. The purified recombinant proteins were used to immunize a female white New Zealand rabbit together with the adjuvant Gerbu100 (Gerbu Biochemicals). The sera were affinity purified against the recombinant proteins used for immunization.

2.2.2.3 Live-cell microscopy of *Dictyostelium*

Cells were transferred into an open glass-bottomed chamber and washed twice with phosphate buffer (PB, 14.6 mM KH_2PO_4, 2 mM Na_2HPO_4, pH 6.1). Confocal images were

taken using an inverted LSM 510 Meta confocal microscope (Zeiss) equipped with a 63x Neofluar 1.4 or a 100x Neofluar 1.3 oil immersion objective. For excitation, the 488-nm argon ion laser line, the 543-nm and the 633-nm helium neon laser lines were used, and emission was collected using 510-525 nm band-pass, 585-615 nm band-pass or a 650-nm long pass filter.

For recording of phagocytosis, cells were incubated with a suspension of heat-killed cells of the yeast *S. cerevisiae* (Sigma-Aldrich) labeled with TRITC (tetramethyl rhodamine isothiocyanate) (Sigma) in PB for 20 min (Maniak et al., 1995), and recorded at 10-seconds intervals using a LSM 510 Meta confocal microscope (Zeiss). Under-agar recordings were performed as described previously (Gerisch and Müller-Taubenberger, 2003).

2.2.2.4 Immunofluorescence microscopy

For immunolabeling, AX2 wild-type or mutant cells settled onto glass coverslips, previously washed with 5% HCl, or cells grown on coverslips were fixed in ice-cold methanol for 10 min or with paraformaldehyde/picric acid (2% paraformaldehyde, 10 mM Pipes, 15% saturated picric acid, pH 6.0) for 20 min and post-fixed with 70% ethanol for 10 min, followed by PBS/glycine and PBG (0.5% BSA, 0.05% fish gelatine, 1xPBS, passed through 0.5 µm filter) followed by three washing steps. Fixed preparations were incubated with monoclonal or polyclonal antibodies, washed three times with PBG and labelled by fluorescence dye-coupled secondary antibodies. F-actin was stained with TRITC-labelled phalloidin. Nuclei were detected with either TO-PRO-3 iodide or DAPI. After staining, coverslips were embedded in either Gelvatol or Mowiol (Longin et al., 1993).

2.2.2.5 Phagocytosis and pinocytosis measurements

Rates of phagocytosis of fluorescently labelled TRITC-yeast, or pinocytosis of TRITC-dextran (Invitrogen) were measured according to a modified protocol of (Rivero and Maniak, 2006). The measurements were in PB instead of HL-5 medium. *Dictyostelium* cells were washed twice with PB and the experiments were peformed in PB at 22°C. The fluorescence measurements were aquired at a wavelength of 544 nm for excitation and 574 nm for emission using an Ultrospec 2100 pro photometer (Amersham). Samples were taken every 15 min.

2.2.2.6 Analysis of development and phototaxis

To induce development, cells were washed twice in 17 mM PB and shaken at a density of 10^7 cells per ml in the buffer. Lysates of cells were taken every three hours over a period of 24 h to determine protein expression during development by Western blot analysis employing specific antibodies.

Development and the ability to phagocytose bacteria were assessed on bacterial lawns of *K. aerogenes* grown on SM-agar plates (90 mg agar, 100 mg peptone, 50 mM glucose, 10 mg yeast extract, 4 mM $MgSO_4$, 16 mM KH_2PO_4 and 5.7 mM K_2HPO_4, ad H_2O to 10 ml, pH 6.5). Alternatively, development of wild-type and mutant cells was induced on nutrient-free phosphate agar plates to document developmental stages by time-lapse photography.

Phototaxis assays were performed by spotting equal numbers of wild-type or mutant cells onto water agar plates that were incubated for 48 h at 21°C in a dark box with a 2-mm slot that served as a light source. For visualization of slugs and slug tracks, cells were transferred onto Nitrocellulose membrane and stained with amido black.

2.2.3 Biochemical methods

2.2.3.1 Purification of centrosomes and analysis

Centrosomes of *Dictyostelium* cells were isolated by purification of nuclei followed by pyrophosphate treatment and sucrose density centrifugation (Schulz et al., 2006). The nuclei fraction with the associated centrosomes was disintegrated by pyrophosphate and passage through a 5 µm mesh polycarbonate filter. Centrosomes were isolated via two consecutive sucrose step gradients of 80% and 50%, followed by 80%, 70%, 55% and 50% steps in SW-40 tubes (Beckman) by centrifugation at 55,000 x g for 1 h at 4°C.

Immunostaining of methanol-fixed centrosomes was performed with anti-CP224 and anti-GFP antibodies. The primary antibodies were visualized with either Alexa Fluor 568 anti-mouse IgG or Alexa Fluor 488 anti-rabbit IgG.

The ratio of centrosomes per nuclei was determined by analyzing the number of nuclei and centrosomes per cell for wild-type and mutants by counting DAPI-stained nuclei and centrosomes immunostained with anti-α-tubulin antibodies and visualization with Alexa Fluor 568 anti-rat IgG.

2.2.3.2 Immunoprecipitation

For identification of interacting proteins the GFP-Trap-kit (ChromoTek) was employed. 3 x 10^7 GFP-NdrA-expressing cells were lysed in 250 µl buffer (10 mM Tris/HCl, pH 7.5, 150 mM NaCl, 0.5 mM EDTA, 0.5% NP40, supplemented with protease inhibitor (Complete; Roche)). The lysate was centrifuged for 15 min at 16,000 x g and incubated with 15 µl GFP-Trap agarose beads under slight agitation for 1 h at 4°C. The beads were washed according to the manufacturer's protocol, and bound proteins were eluted by boiling in SDS-sample buffer. Proteins were separated by SDS-PAGE and stained with Coomassie brilliant blue-R. Bands of interest were cut out from the gel and analyzed further by MALDI-TOF or Orbitrap mass spectrometry (ZfP, LMU München).

2.2.3.3 SDS gel electrophoresis and Western blotting

Protein was separated by standard SDS-PAGE. Western blot analysis was performed applying a semi dry blotting system using transfer buffer (25 mM Tris pH 8.5, 190 mM glycine, 20% methanol, 0.02% SDS) and nitrocellulose membranes. The membranes were blocked with 1% BSA or non-fat milk in NCP buffer (10 mM Tris pH 7.3, 150 mM NaCl, 0.05% Tween20), incubated with specific primary antibodies, washed in NCP buffer and treated with enzyme-linked secondary antibodies, followed by developing with either alkaline phosphatase/BCIP or light emission using NBT.

2.2.3.4 Expression and purification of recombinant proteins

Recombinant proteins were expressed using pGEX vectors were transformed into the expression strain BL21 RIL (Kaelin et al., 1992). Overnight-cultures (37°C) were diluted 1:20, grown at 37°C to an OD_{600} of 0.4-0.8 and induced by addition of 0.5 mM IPTG. Cells were grown at temperatures of 22, 30 or 37°C. Bacteria were pelleted, resuspended in PBS (+ 2 mM DTT, 1 mM EDTA, 5 mM benzamidine, 100 µM PMSF, Complete protease inhibitors (Roche)) and lyzed by sonication in the presence of 0.5 mg/ml lysozyme. Lysates were centrifuged (35,000 g for 45-60 min at 4°C) and supernatants were incubated with glutathione-sepharose for 3-4 h. After washing the sepharose with lysis buffer for three times, the bound protein was eluted with lysis buffer containing 30 mM reduced glutathione and dialysed against PBS. By SDS-PAGE analysis purity and quality of the eluted protein were determined.

2.2.3.5 *In vitro* GST pull-down assays

To test the specific interaction or the identification of novel interactors of GST-tagged proteins or protein-domains, 5 x 10^7 wild-type AX2 cells or AX2 cells expressing GFP-tagged target protein were lysed in lysis buffer (LB; 25 mM Tris/HCl, pH 7.5, 150 mM NaCl, 5 mM EDTA, 1% Triton X-100, 1 mM DTT and 5 mM ATP, supplemented with Complete protease inhibitors (Roche) and Phosstop phosphatase inhibitors (Roche)). Membrane and nuclear-enriched pellet fraction were separated by centrifugation at 100,000 g for 30 min at 4°C. The cytoplasmic fraction was added to equal amounts of GST-tagged protein bound to beads for the pull-down reaction and incubated for 1 h at 4°C. Beads were washed three times with wash buffer (25 mM Tris/HCl, pH 7.5, 150 mM NaCl, and 5 mM EDTA). The pull-down eluates were analyzed by Western blot analysis using specific antibodies or were stained with Coomassie. For Western blotting, lysates were separated via SDS-PAGE and blotted on a Nitrocellulose membrane (Schleicher & Schuell). Bands resulting from Coomassie-stained SDS-PAGE gels were analyzed by MALDI mass spectrometry. For testing the interaction of the GST-Lats2-RBD with GFP-RasG and the GFP-control, the crosslinker Dithiobis[succinimidylpropionate] DSP (Thermo-Pierce) was added during incubation of cell lysate and GST-Lats2-RBD.

3 Results

3.1 NDR/LATS kinases in *Dictyostelium*

The NDR/LATS kinases belong to the AGC subfamily of protein kinases (Pearce et al., 2010). AGC kinases are represented by 21 members in *Dictyostelium* and comprise four NDR/LATS kinases. The NDR/LATS group kinases of *Dictyostelium* were annotated as NdrA, NdrB, Lats2 (NdrC), and Lats1 (NdrD) and are encoded by *ndrA* (DDB_G0278457), *ndrB* (DDB_G0288753), *ndrC* (DDB_G0284839) and *ndrD* (DDB_G0289543) (Goldberg et al., 2006). The NDR/LATS group of kinases in *Dictyostelium* was classified by sequence comparisons using BLASTp (Altschul et al., 1990) or phylogenetic sequence alignments based on the sequences of the catalytic domains (Corpet, 1988) of NDR/LATS kinases from man and other organisms, suggesting the separation into two groups (Figure 5). The performed *in silico* studies indicated that NdrA and NdrB are more related to the man NDR-related kinases NDR1 and NDR2, while Lats2 and Lats1 are closer to the LATS-related kinases LATS2 and LATS1 of human (Figure 4). The *Dictyostelium* protein kinase NdrA comprises 530 amino acid residues (61.0 kDa); NdrB has a size of 542 amino acid residues (63.6 kDa). *Dictyostelium* Lats2 comprises 1335 amino acid residues (149.4 kDa), whereas Lats1 has a size of 2112 amino acid residues (233.8 kDa). Both
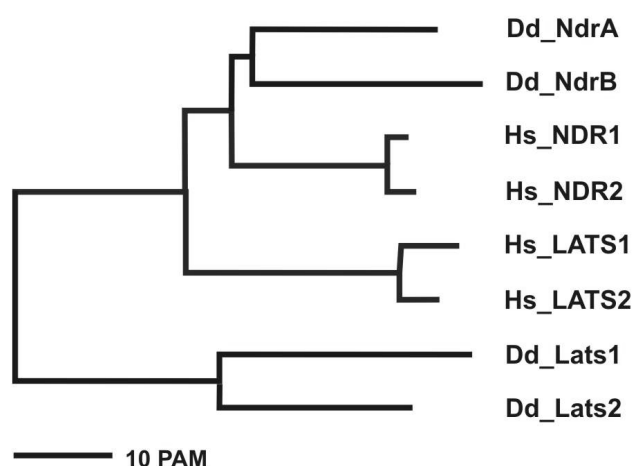
Figure 4: Phylogenetic tree of human and *Dictyostelium* NDR/LATS kinases

Phylogenetic sequence alignment of human (Hs) and *Dictyostelium* (Dd) NDR/LATS kinases. The tree was computed for the sequences of the catalytic domains (Corpet, 1988). Closely linked NDR- and LATS-related kinases of *Dictyostelium* and man group together. PAM = percent accepted mutations.

Dictyostelium LATS-related kinases are carrying long asparagine-rich stretches. Moreover, the differing protein sizes between the *Dictyostelium* NDR- and LATS-related kinases are distributed similar to the human homologs. While the sizes of NdrA and NdrB are comparable to human NDR1 (54.1 kDa) and NDR2 (53.9 kDa), *Dictyostelium* Lats1 and Lats2 are significantly larger, corresponding to human LATS1 (126.9 kDa) and LATS2 (120.1 kDa). Renaming the *Dictyostelium* LATS-related kinases became apparent, because phenotypic characterization and sequence analysis suggest a closer relation of NdrC to mammalian LATS2. Based on the results obtained in this study, NdrC and NdrD were renamed to Lats2 and Lats1.

The group classification of *Dictyostelium* NDR/LATS kinases was performed by sequence alignments with the conserved domains of NDR/LATS of other organisms (Hergovich et al., 2006) (Figures 6, 25, 32). *Dictyostelium* NDR/LATS kinases are specified by an N-terminal regulatory domain, suggesting the binding of Mob1 proteins (Hirabayashi et al., 2008), and an auto-inhibitory segment, which is part of an AGC kinase specific insert in
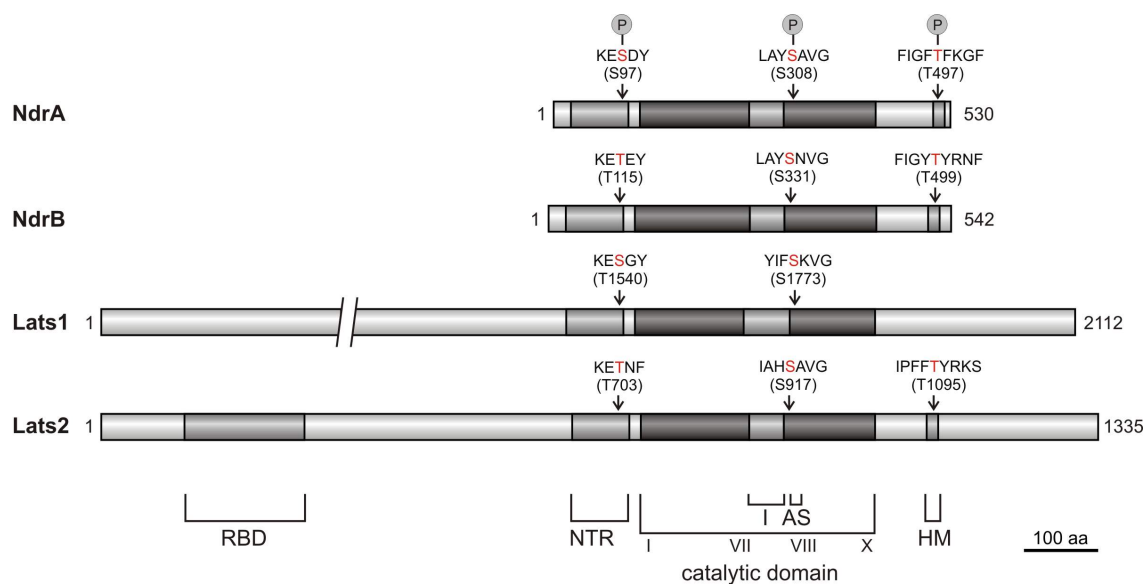
Figure 5: Domain structure of the *Dictyostelium* NDR/LATS kinases

Common features of NDR/LATS kinases comprise an N-terminal regulatory domain (NTR) mediating Mob1 binding, the catalytic domain harboring an insert (I) containg the autoinhibitory sequence and a specific activation site (AS), and a C-terminal hydrophobic motif (HM). Activity is regulated by auto-phosphorylation of a positively charged activation segment (AS) in the kinase domain. A threonine residue embedded in the conserved hydrophobic motif at the C-terminus serves as a putative target for Ste20 kinases. Those domains are all represented in NdrA, NdrB, Lats1 and Lats2 except for a phosphorylation site embedded in the hydrophobic motif of Lats1. In addition, this study revealed the presence of a Ras binding domain in Lats2.

the catalytic kinase domain (Figure 5). The further domain structure of NDR/LATS kinases is characterized by the general features of AGC kinases, comprising a central catalytic domain, containing insert and activation sequence, as well as consensus sequences harboring certain conserved serine/threonine residues that have been described to serve as Ste20 kinase phosphorylation sites in man and fly (Figure 5). Binding of Mob1 coactivators to the N-terminal regulatory domain is required for the release from autoinhibition via the auto-inhibitory sequence by enforcing autophosphorylation at the activation segment. The activation segment harbors a conserved serine, which was reported to act as a target for autophosphorylation and triggering the activity of NDR/LATS kinases (Hergovich et al., 2005). The AGC kinase-specific hydrophobic motif is characterized by the highly conserved consensus sequence F_X_X_Y/F_T_Y/F_K/R, and recognized by Ste20-like kinases that enhance kinase activity by phosphorylation of the embedded threonine (Hergovich et al., 2006). These conserved motifs are shared by all four *Dictyostelium* NDR/LATS kinases. Yet the hydrophobic motif of *Dictyostelium* Lats1 does not carry the predicted phosphorylation site, it is questionable whether its mode of activation is similar to the other NDR/LATS kinases. The NDR/LATS kinases of *Dictyostelium* have not been subject of investigation in any study so far. All the data presented here are resulting from the cellular and molecular analysis of these kinases in the course of this thesis.

The functional characterization of NdrA, which represents a member of the NDR-related kinases of *Dictyostelium,* is topic of Chapter 3.2, followed by the description of NdrB, the second *Dictyostelium* NDR-related kinase in Chapter 3.3. The analysis of the *Dictyostelium* LATS-related kinase Lats2 is topic of Chapter 3.4. Lats1 was no subject of this study.

3.2 The NDR-related kinase NdrA of *Dictyostelium*

3.2.1 NdrA compared to NDR kinases from other organisms

The *ndrA* gene of *Dictyostelium* encodes a protein kinase of 530 amino acid residues (61 kDa). The highest identities within the catalytic domain of NdrA are found with Trc of *Drosophila melanogaster*, human NDR1 and NDR2, *Dictyostelium* NdrB, *Caenorhabditis elegans* Sax1, *Schizosaccharomyces pombe* Orb6, *Neurospora crassa* Cot1 and *Saccharomyces cerevisiae* Cbk1 (Figure 6A). Identities were determined using BLASTp (Altschul et al., 1990). The central catalytic domain of NdrA (amino acid residues 112 to
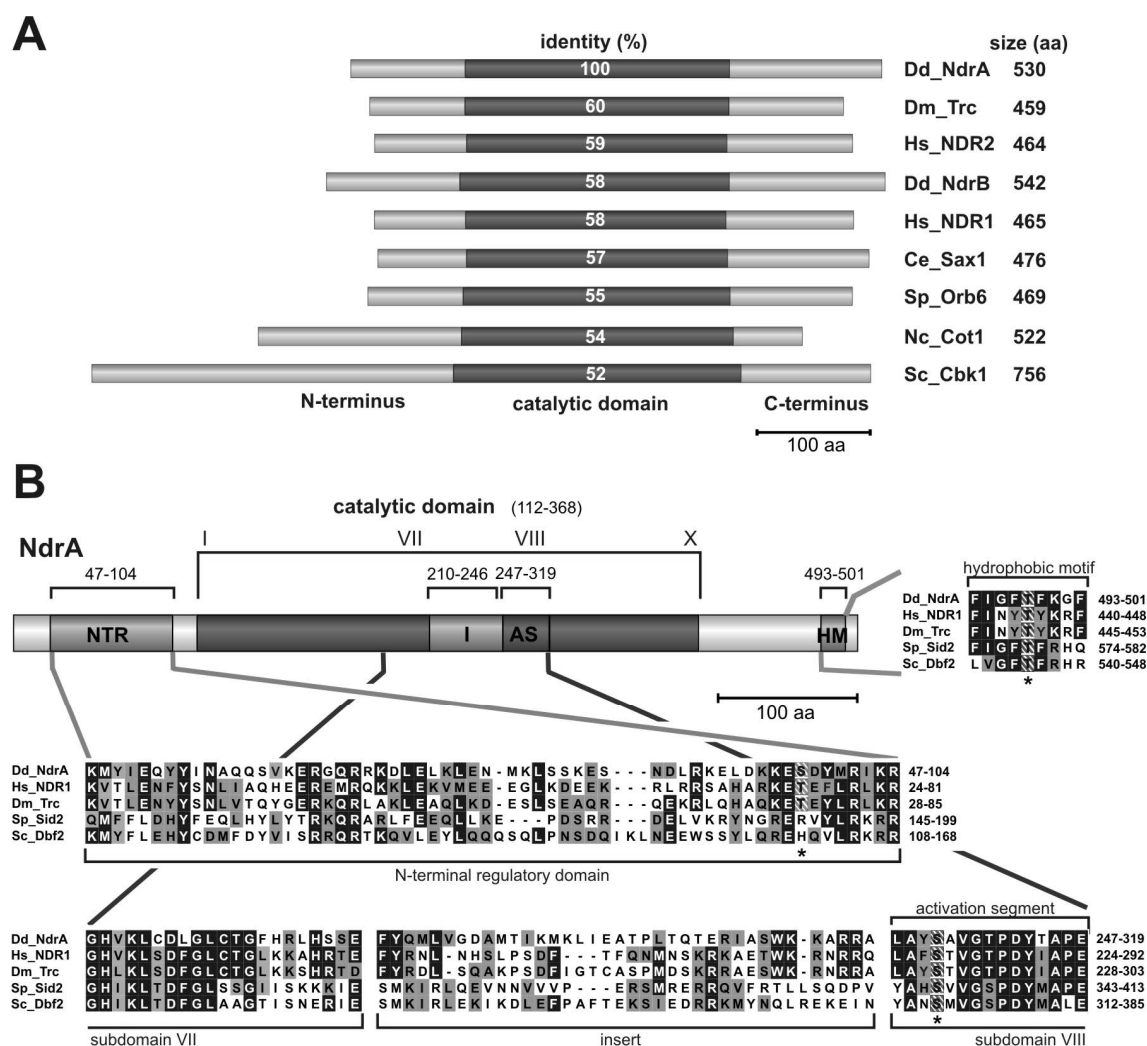
**Figure 6:** *Dictyostelium* **NdrA in comparison to other NDR/LATS kinases**

(**A**) Comparison of the catalytic domain of *Dictyostelium* NdrA with the catalytic domains of *D. melanogaster* Trc, *H. sapiens* NDR1 and 2, *Dictyostelium* NdrB, *C. elegans* Sax1, *S. pombe* Orb6 , *N. crassa* Cot1 and *S. cerevisiae* Cbk1. Numbers indicate percent identity within the catalytic domains compared to the NdrA catalytic domain determined by BLASTp. (**B**) Identification of NDR-kinase specific sequence signatures in NdrA. The N-terminal regulatory domain (NTR) contains a putative Mob1-binding site. The catalytic domain harbors between subdomain VII and VIII an insert that is followed by an activation segment (AS). The C-terminus carries a hydrophobic motif (HM). The domains are indicated by boxes in the NDR scheme. Identical amino acid residues are highlighted in black and conserved residues in grey. Potential phosphorylation sites are marked as hatched residues and are highlighted by asterisks.

406) contains an AGC-kinase specific insert (amino acid residues 268 to 304) between subdomains VII and VIII of the catalytic domain and an activation segment (AS) (amino acid residues 305 to 319). The conserved sequence within subdomain VIII of the catalytic domain (Figure 6B), harbors a serine, S308, which most probably is target for

autophosphorylation and triggers NDR/LATS kinase activity. Outside the catalytic domain the sequence of NdrA is characterized by specific features also present in the other NDR/LATS kinases. NdrA has an N-terminal regulatory region (amino acid residues 47 to 104) that may bind Mob1 proteins, which were reported to be required for the activation of NDR/LATS kinases. Additionally, the C-terminus harbors a hydrophobic motif (amino acid residues 493 to 501) with threonine T497, serving as a putative Ste20-like kinase phosphorylation site (Figure 6B).

3.2.2 Generation of NdrA-null mutants

In order to analyze the function of NdrA, mutant cells lacking NdrA were generated by transformation of AX2 wild-type cells with a gene replacement construct (Figure 7A). By
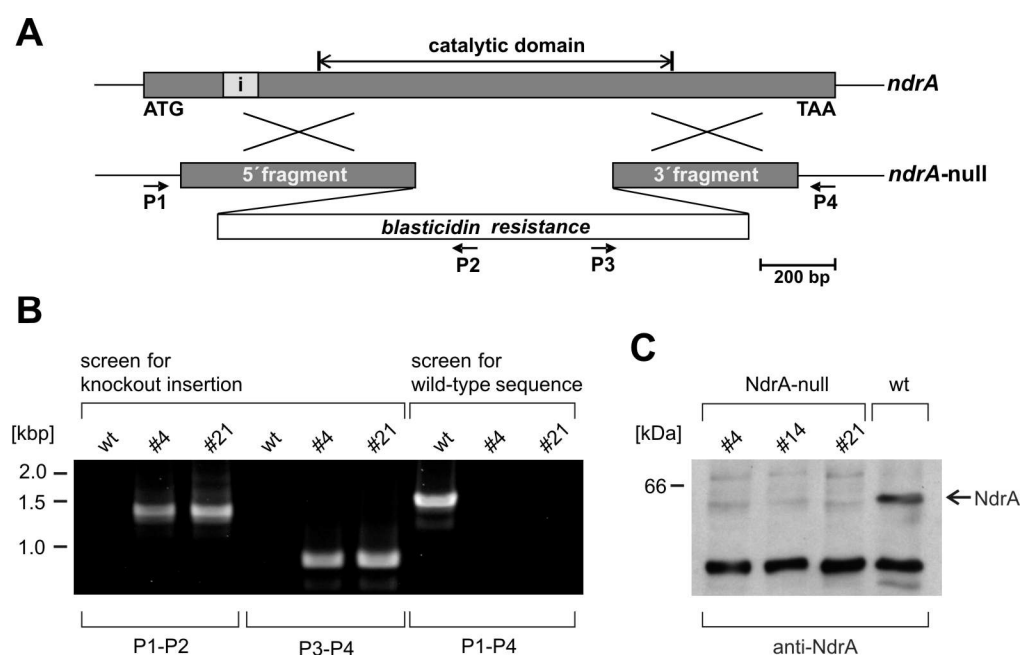
Figure 7: Generation of NdrA-null mutants

(**A**) An N- and a C-terminal fragment of the *ndrA* gene were amplified by PCR from genomic DNA and linked with the blasticidin-S-resistance cassette. This construct was used to transform wild-type cells. (**B**) Genomic DNA purified from blasticidin-S-resistant clones (#4, 21) or from wild-type (wt) was tested by PCR for insertion of the blasticidin cassette or the wild-type gene using the primer combinations indicated by arrows in (A). Expected sizes of PCR fragments are 1.4 kbp for primers P1-P2, 0.9 kbp for P3-P4 and 1.7 kbp for P1-P4. (**C**) Confirmation of the gene-knockout by Western blot analysis. Lysates from wild-type (right lane) and three independent NdrA-mutants (#4, 14, 21) were separated by SDS-PAGE, blotted and probed with anti-NdrA antibodies. In lysates prepared from wild-type, endogenous NdrA is detected at 61 kDa, while this band is absent in the mutant strains. An unspecified band, recognized by the anti-NdrA antibody served as internal loading control.

homologous recombination the core region of the *ndrA* gene encoding the kinase domain was replaced by an inverted blasticidin-S resistance cassette (Faix et al., 2004). Thus, translation of the *ndrA*-mRNA should terminate between kinase subdomains VIA and VIB. Disruption mutants were identified first by PCR (Figure 7B) and subsequently by Western blot analysis (Figure 7C). Three independent NdrA-null clones were generated by this approach, which were used for further studies.

To determine the expression levels of NdrA and to test the intracellular localization of NdrA, a polyclonal antibody against recombinant NdrA was generated. The antibody had been raised against NdrA by injection of a rabbit with recombinant NdrA, comprising amino acid residues 1-110 tagged to GST. Cell lysates of wild-type and NdrA-knockout cells were tested by Western blot analysis employing the anti-NdrA antibody, confirming the absence of NdrA in *Dictyostelium* cells, transformed with a gene replacement construct (Figure 7C). An additional band can be observed which is due to unspecified binding of the anti-NdrA antibody.

3.2.3 Development of NdrA-null cells is normal

As a consequence of deprivation of nutrients, *Dictyostelium* cells start to aggregate and form multicellular assemblies, called mounds. These mounds are able to further differentiate into motile slugs that move towards a light source. Both forms, mounds and slugs then form fruiting bodies, consisting of a basal plate and a stalk carrying a spore head on top. Investigation of the differentiation of NdrA-mutant cells revealed that NdrA-null cells develop indistinguishably from wild-type cells up to the formation of fruiting bodies within 24 h (Figure 8A).

In order to examine the expression of NdrA during the different developmental stages, cell lysates of NdrA-mutant cells were prepared every three hours and were subjected to Western blot analysis using anti-NdrA antibodies. NdrA was detected at all developmental stages with a slight increase during aggregation (Figure 8B). The slight increase during the aggregation stage (t = 6-12 h) is consistent with the expression data of *ndrA*-mRNA available from dictyExpress (www.ailab.si/dictyexpress) (Rot et al., 2009).

The ability of slugs to perform phototaxis was determined by measuring the covered distances of slugs from either wild-type or NdrA-null cells moving towards a light source (Figure 9A). The diagram indicates that average distances of phototactic slugs of wild-type and NdrA-null cells (n = 6) are comparable (Figure 9B).
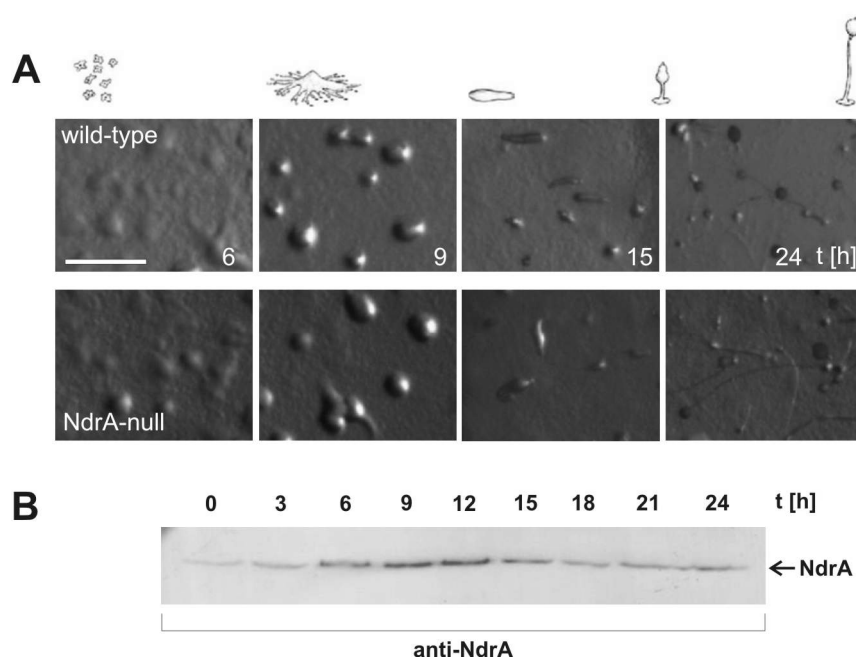
Figure 8: Development of NdrA-null cells

(**A**) Wild-type and NdrA-null were recorded during different stages of development on phosphate agar plates. NdrA-null cells develop indistinguishably from wild-type. The formation of loose and tight aggregates (6 hours and 9 hours), slugs (15 hours) and mature fruiting bodies (24 hours) are depicted. (**B**) NdrA is detected throughout the developmental life cycle of *Dictyostelium*. Protein corresponding to $2x10^5$ cells per lane was loaded, separated by SDS-PAGE and analyzed by Western blotting with antibodies directed against NdrA. The NdrA kinase is present at all stages with a moderate increase during the aggregation stage. Bar = 1 cm.
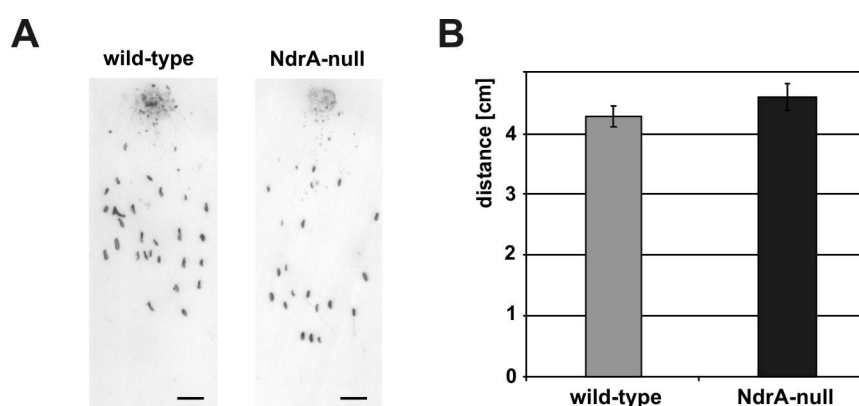
Figure 9: Phototaxis of NdrA-null cells

(**A**) NdrA-null cells show normal phototaxis. Slugs of wild-type or NdrA-null mutants on phosphate agar phototax towards a light source. (**B**) Phototaxis was quantified by measuring the distance of slug migration on phosphate agar towards a light source for wild-type and NdrA-null cells. Bars = 1 cm.

3.2.4 *Dictyostelium* cells lacking NdrA exhibit reduced growth rates

Growth of NdrA-null cells in shaken suspension culture and on bacterial lawns was investigated. To determine the growth rates for the different growth conditions, either the increase in cell number in shaking culture or diameters of *Dictyostelium* plaques on lawns of *Klebsiella aerogenes* were measured for NdrA-null in comparison to wild-type cells. While growth of NdrA-null cells compared to wild-type cells (n = 4, corresponding to 3 independent experiments) in suspension culture was only slightly decreased (Figure 10A), growth on a solid substrate with bacteria (n = 2, corresponding to 3 independent experiments) as food source was delayed (Figure 10B).
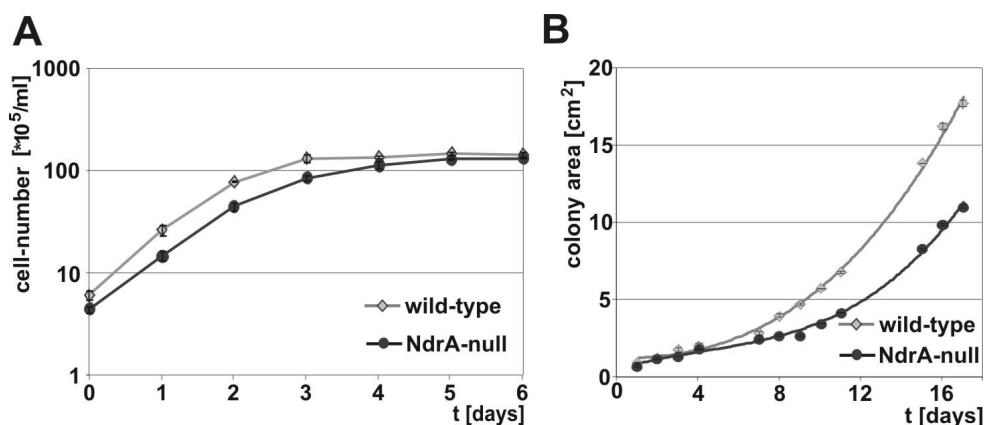
Figure 10: Deletion of NdrA affects growth on bacteria

(**A**) Growth rates of wild-type and NdrA-null cells in nutrient medium under shaking conditions. Axenic growth of NdrA-null cells is similar to wild-type. (**B**) Growth of wild-type and NdrA-null cells on lawns of non-pathogenic *K. aerogenes*. The diameters of *Dictyostelium* plaques were measured and colony sizes were determined.

3.2.5 NdrA is required for efficient phagocytosis

Growth of *Dictyostelium* cells in suspension culture depends on the uptake of nutrients via pinocytosis and macropinocytosis of the liquid medium (Hacker et al., 1997), growth on bacteria as a food source involves phagocytosis. To further investigate the route of ingestion of larger particles, the rates of phagocytosis were determined for NdrA-null cells in comparison to wild-type. Rates of phagocytic uptake were followed by feeding the cells with TRITC-labeled yeast and determining the increase in fluorescence of *Dictyostelium*
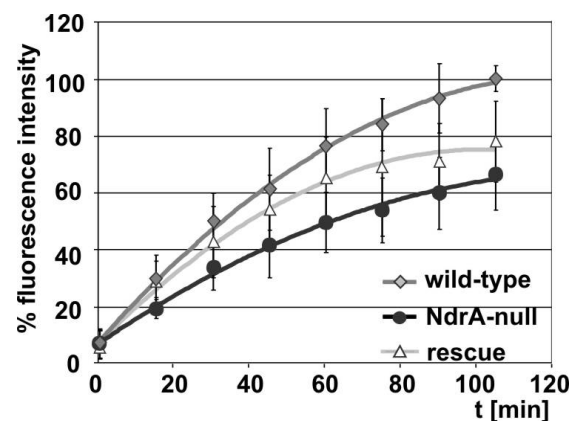
Figure 11: NdrA is required for efficient phagocytosis

Determination of phagocytosis rates in wild-type, NdrA-null and NdrA-null cells expressing GFP-NdrA. Cells were incubated with heat-killed, TRITC-labeled yeast cells and uptake was determined by measuring fluorescence at 574 nm at the indicated time points to determine phagocytosis rates.

cells at distinct time points (Figure 11). The rates of pinocytosis were determined by measuring the growth rates of NdrA-null cells in liquid medium compared to the ones of wild-type. The rates of phagocytosis were significantly reduced in cells lacking NdrA (n = 10) in comparison to wild-type cells (n = 10) indicating that NdrA is required for normal phagocytosis. Expression of GFP-NdrA in NdrA-null cells (n = 7) rescued the defect in phagocytosis partially (Figure 11). The lack of full recovery may be due to varying expression levels of GFP-NdrA in individual cells.

To investigate phagocytosis in more detail, wild-type and NdrA-null cells expressing LimEΔ-GFP were used to record the uptake of TRITC-labeled yeast cells. LimEΔ-GFP is a marker for filamentous actin (Bretschneider et al., 2004) and can be used for the visualization of phagocytic cup formation in living cells (Bretschneider et al., 2004; Clarke et al., 2006). The time needed from adhesion until complete engulfment of the yeast and closure of the phagocytic cup was measured for wild-type (n = 6) and NdrA-null cells (n = 6) (Figure 12A, B). On average, NdrA-mutant cells required 1.6-times longer for the uptake of yeast particles than wild-type cells (Figure 12C).

In order to determine the localization of NdrA during different routes of food uptake, NdrA-null cells expressing GFP-NdrA were recorded by confocal laser scanning microscopy. Analysis of the localization of GFP-NdrA during phagocytic uptake of TRITC-labeled yeast or macropinocytosis of TRITC-labeled dextran revealed that NdrA is not enriched at the sites of ingestion. Unlike a number of other proteins that have been shown to be
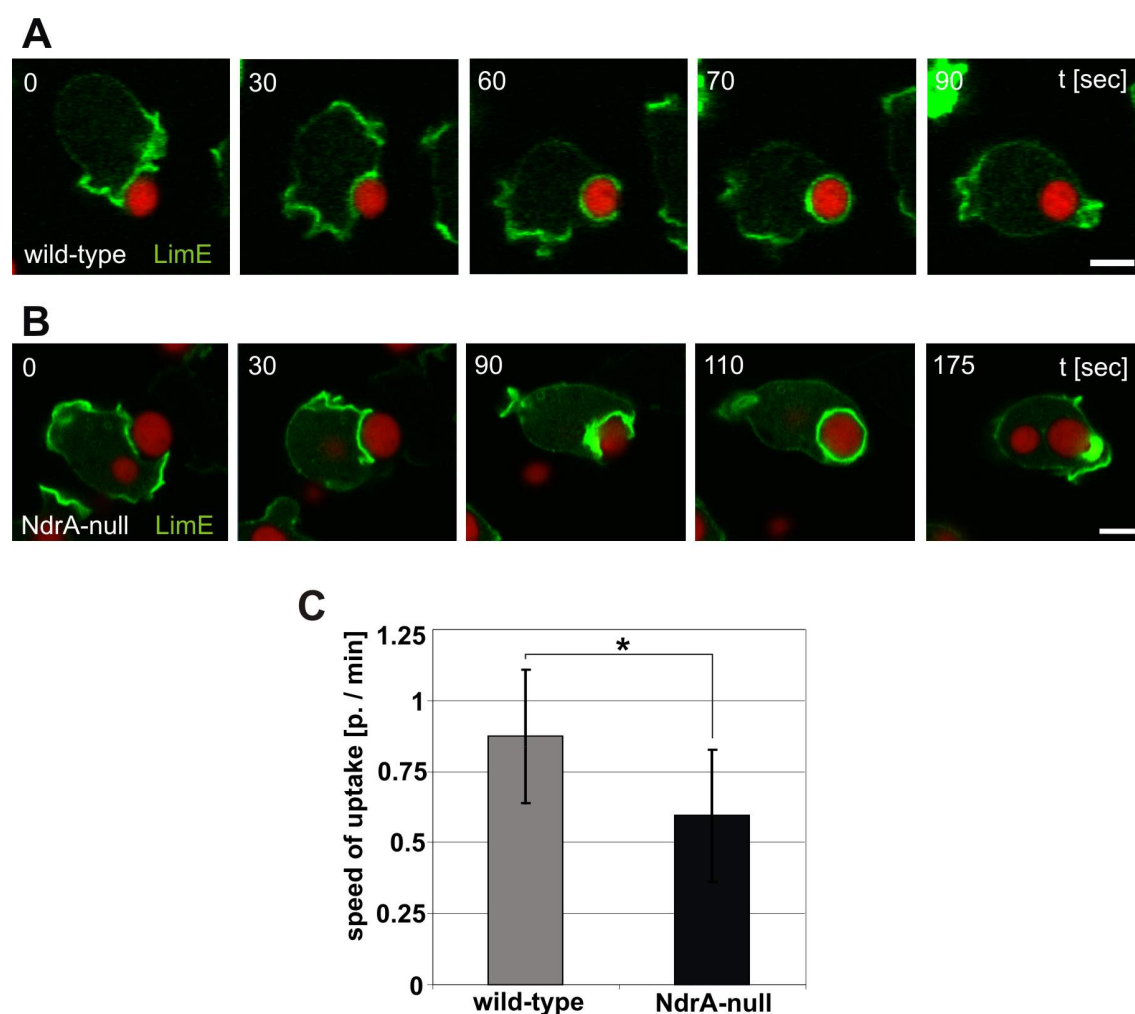
Figure 12: Retarded formation of phagocytic cups in NdrA-null cells

Live-cell recordings of wild-type (**A**) and NdrA-null (**B**) cells phagocytosing TRITC-labeled yeast cells (red). Wild-type and NdrA-null cells were expressing LimEΔ-GFP (Bretschneider et al., 2004; Clarke et al., 2006), a marker for filamentous actin (green) and used here to visualize and follow the formation of phagocytic cups from adhesion (t = 0 sec) to complete engulfment of the yeast. Time is indicated in seconds. (**C**) Average time required for uptake of a yeast cell determined by evaluating live-cell recordings as described in (A) and (B); significance was determined by a t-test. Bars = 5 μm.

required for efficient phagocytosis or macropinocytosis like for instance actin-regulating proteins (Konzok et al., 1999; Maniak et al., 1995), the localization of GFP-NdrA to the phagocytic cup or macropinosomes is apparently not required for its role in promoting phagocytosis (Figure 13A, B). It can not be completely excluded that a minor fraction of NdrA relocalizes to the phagocytic cup.
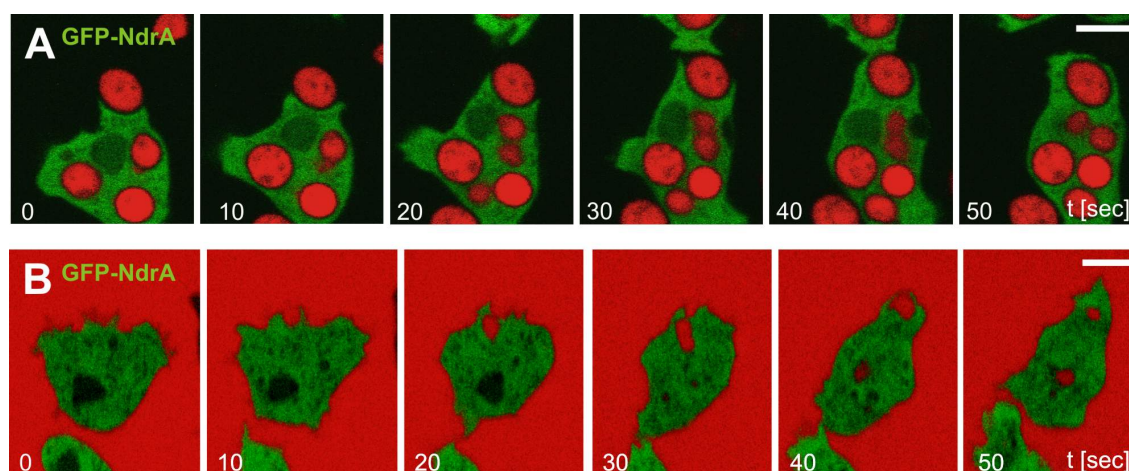
Figure 13: Localization of NdrA during phagocytosis and macropinocytosis

(**A**) *Dictyostelium* wild-type cells expressing GFP-NdrA (green) were incubated with TRITC-labeled yeast (red) cells to record phagocytosis, or (**B**) with TRITC-dextran (red) to record macropinocytosis. Time points are indicated in seconds. Bars = 5 µm.

3.2.6 NdrA localizes to the centrosome

Live-cell microscopy of interphase wild-type cells expressing GFP-NdrA revealed an enrichment of NdrA to the centrosome (Figure 14A). The localization of GFP-NdrA to the centrosome was confirmed by immunolabeling of GFP-NdrA-expressing cells with an antibody directed against an established centrosomal marker, CP224 (Gräf et al., 2000) (Figure 14B, C). Further analysis of the centrosomal colocalization of GFP-NdrA and CP224 by deconvolution of three-dimensional stacks confirmed that both labels completely coincided (Figure 14D, E). The generated anti-NdrA polyclonal antibodies (Chapter 3.2.2) were unsuitable for immunolabeling of fixed cells.

Next, isolated centrosomes that were prepared from wild-type and GFP-NdrA expressing cells were analyzed. NdrA was detected in purified centrosome fractions by immunostaining using antibodies against NdrA and co-localized with the centrosomal marker CP224 that was also visualized by immunostaining (Figure 15A). For centrosomes prepared from GFP-NdrA expressing *Dictyostelium* cells, colocalization of GFP-NdrA and CP224 was confirmed by immunostaining of CP224 (Figure 15B). Probing of centrosome fractions prepared from GFP-NdrA expressing wild-type cells by Western blotting using anti-NdrA antibodies revealed endogenous NdrA as well as GFP-NdrA (Figure 15C). Expression levels of wild-type and NdrA-null cells expressing GFP-tagged NdrA were tested by Western blot analysis using anti-NdrA antibodies (Figure 16). The levels of GFP-
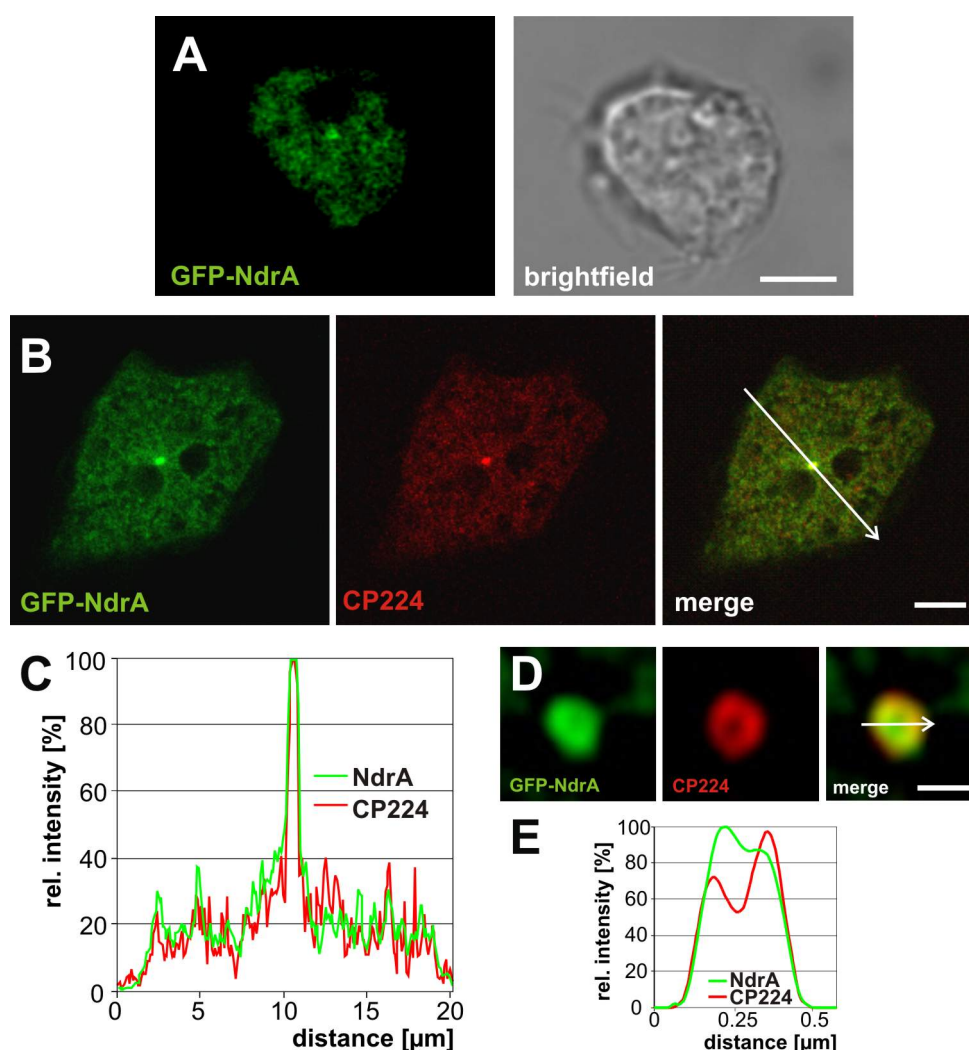
Figure 14: NdrA is enriched at centrosomes

(**A**) Confocal recording of living wild-type cells expressing GFP-NdrA shows an enrichment of GFP-NdrA at centrosomes during interphase. The GFP-fluorescence is shown on the left, the brightfield image on the right. Bar = 5 µm. (**B**) Confocal imaging of fixed wild-type cells expressing GFP-NdrA (green) indirectly immunolabeled with antibodies against a centrosomal marker, CP224 (red). Colocalization of GFP-NdrA with CP224 is depicted in the merged image. Bar = 5 µm (**C**) Scans determining the relative fluorescence of the green and red channel along the arrow depicted in (B) confirm the colocalization of GFP-NdrA and CP224. (**D**) Centrosome from GFP-NdrA expressing NdrA-null cell. The image was recorded by laser scanning microscopy and Z-slices were subjected to deconvolution. (**E**) Colocalization of GFP-NdrA and CP224 is confirmed by scans of the recording shown in (D) plotted for relative fluorescence intensities. Bar = 0.5 µm.

NdrA in wild-type and NdrA-null cells were only slightly increased compared to endogenous NdrA, and similar to the phosphomimetic variants of GFP-NdrA expressed in NdrA-null cells, GFP-NdrA-T497E and GFP-NdrA-T497A.
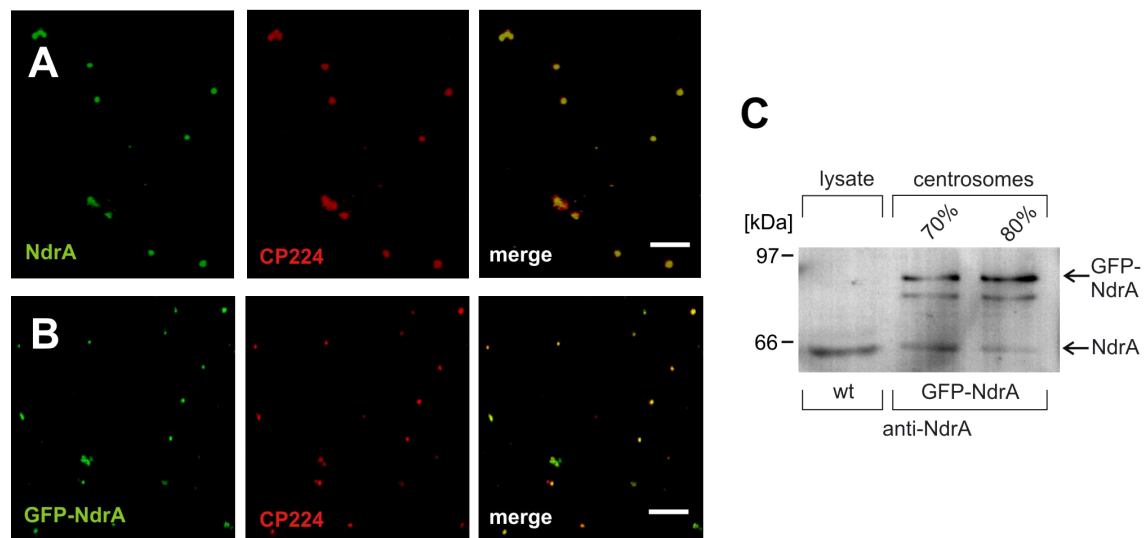
Figure 15: NdrA co-purifies with centrosomes prepared from *Dictyostelium* cells

Centrosomes were purified from (**A**) wild-type lysates and (**B**) lysates of GFP-NdrA-expressing cells, fixed, and immunostained with monoclonal anti-CP224 antibodies (red). Centrosomes prepared from wild-type cells (A) were co-stained with polyclonal antibodies against NdrA (green). (**C**) Fractions of centrosome preparations from GFP-NdrA expressing cells were separated by SDS-PAGE and subjected to Western blot analysis using polyclonal anti-NdrA antibodies. Bar = 5 µm.

3.2.7   Localization of NdrA during the cell cycle

The localization of NdrA was monitored during different stages of the cell cycle of NdrA-null and wild-type cells, both expressing GFP-NdrA. To visualize cell-cycle specific stages, wild-type and NdrA-null cells were immunostained for α-tubulin to visualize the mitotic spindle. In interphase, GFP-tagged NdrA was enriched at centrosomes (Figure 17A, B, upper row). This localization changed at the onset of mitosis. In prophase, the spindle was enwrapped by a cloud of GFP-NdrA (Figure 17A, B, middle-row). At later stages, NdrA was not detected any more at the spindle or its vicinity (Figure 17A, B, lower row).

The human kinases NDR1/2 are activated by upstream phosphorylation via the Ste20 family kinase MST3 at the highly conserved hydrophobic motif (Stegert et al., 2005). To investigate whether the localization of NdrA is influenced by phosphorylation within the hydrophobic motif, two GFP-NdrA variants carrying mutations in the hydrophobic motif (T497E and T497A) were tested for their localization. Mutation of threonine to glutamic acid (T497E) in the hydrophobic motif of *Dictyostelium* NdrA mimicks a phosphorylated residue and thereby activation; changing threonine to alanine (T497A) prevents activation. Expression levels of the GFP-NdrA-T497E and -T497A were determined by Western
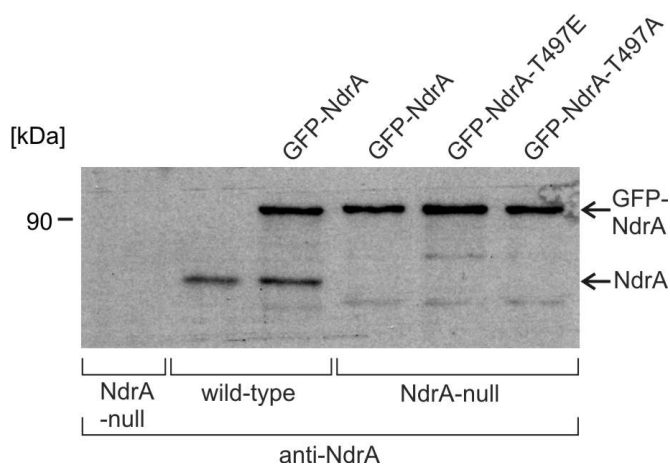
Figure 16: NdrA expression levels

Lysates prepared from wild-type or NdrA-null cells expressing either GFP-NdrA or GFP-NdrA variants were separated by SDS-PAGE, subjected to Western blot analysis, and NdrA or GFP-NdrA were detected using NdrA-specific polyclonal antibodies. In addition, lysates of wild-type or NdrA-mutant cells were loaded.

blotting using anti-NdrA antibodies (Figure 16). The localization of both mutant GFP-NdrA constructs was indistinguishable from that of GFP-NdrA, suggesting that the activation state is dispensable for the recruitment of NdrA (Figure 17C, D).

For human NDR1 it has been shown that it is involved in the regulation of centrosome duplication (Hergovich et al., 2007). Whether *Dictyostelium* NdrA affects the number of nuclei per cell, or the distribution of centrosomes was investigated by determining the number of nuclei and centrosomes per cell for fixed preparations of NdrA-null (n = 221) and wild-type cells (n = 241). For this purpose cells were stained with DAPI for the visualization of nuclei and immunostained with monoclonal antibodies against α-tubulin as a marker for centrosomes. The analysis showed that NdrA-null cells are mostly mononucleate with the centrosome connected to the nucleus and thus indistinguishable from wild-type (Figure 18A, B), indicating that NdrA is not involved in the regulation of mitosis through centrosomal functions.
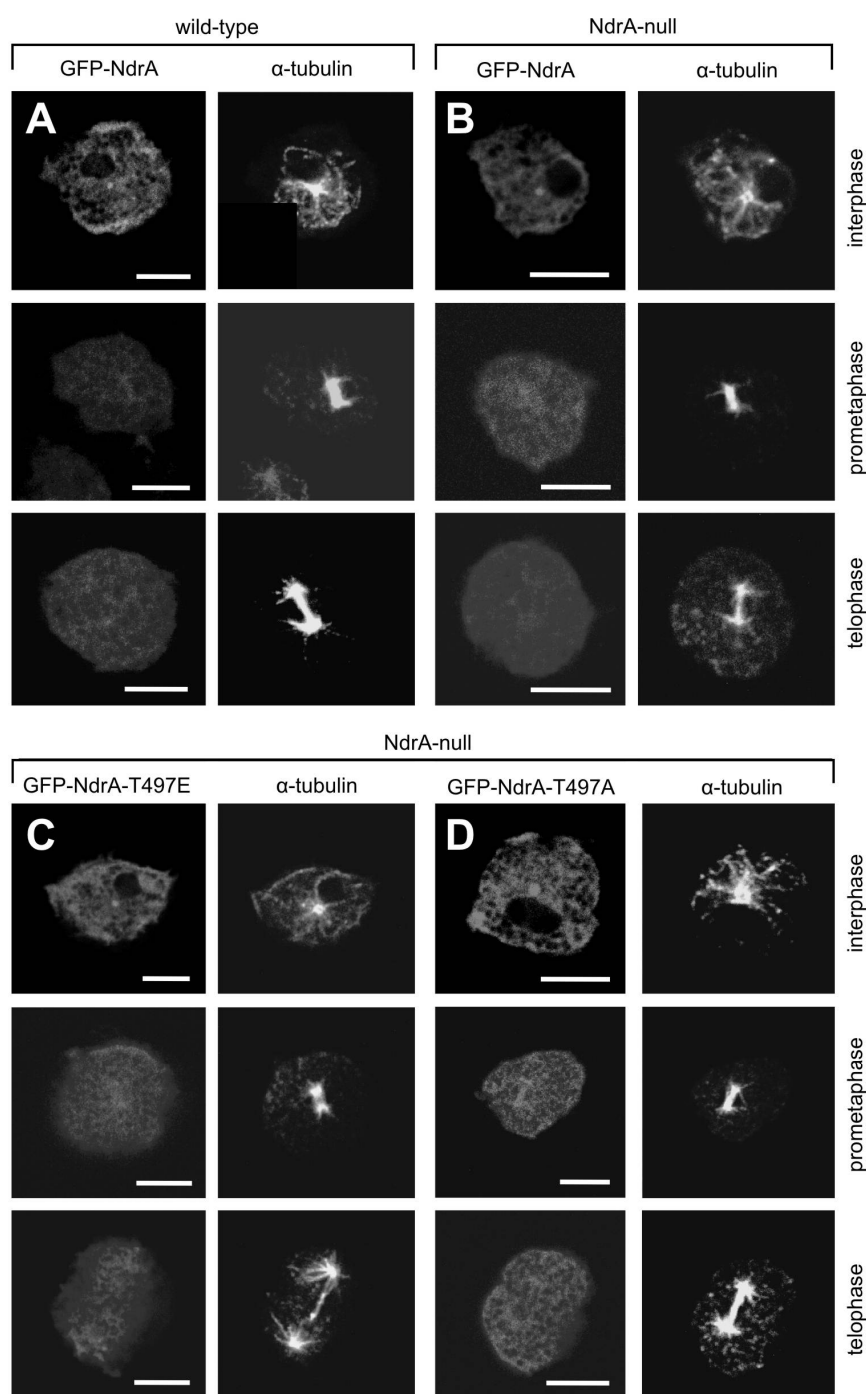
Figure 17: NdrA detaches from the mitotic spindle

Wild-type cells expressing GFP-NdrA (**A**) and NdrA-null cells expressing GFP-NdrA (**B**), GFP-NdrA-T497E (**C**) or GFP-NdrA-T497A (**D**) were fixed and stained with antibodies against α-tubulin. Interphase and mitotic stages of these cell lines were recorded by microscopy. Fluorescence of GFP is shown in the left, immunofluorescence labeling of α-tubulin in the right panels. In interphase, GFP-tagged NdrA or phosphomimetic GFP-NdrA variants are enriched at centrosomes (upper row). In prometaphase, GFP-fluorescence of NdrA is detected only weakly in the periphery of the mitotic spindle (middle row). At later stages of mitosis, none of the GFP-NdrA variants are associated with the mitotic apparatus (lower row). Bars = 5 µm.
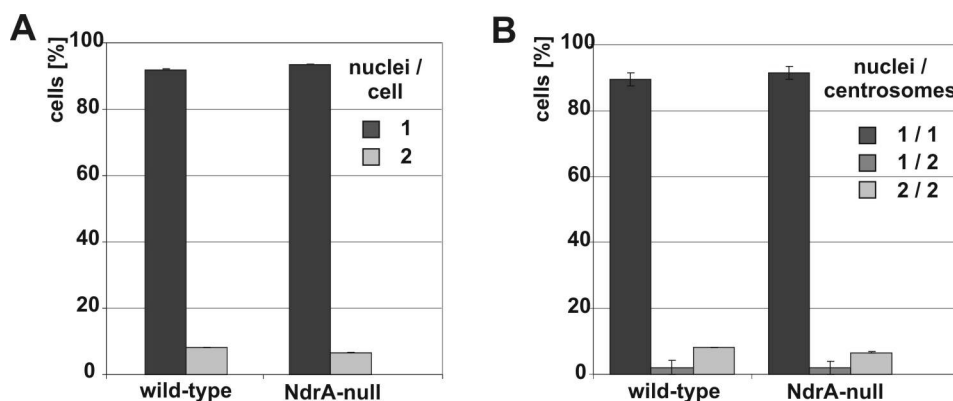
Figure 18: Cytokinesis of NdrA-null cells is normal

The number of nuclei and centrosomes was determined by counting DAPI-stained nuclei in fixed cell preparations and centrosomes immunolabeled by anti-α-tubulin antibodies of wild-type and NdrA-mutant cells. (**A**) In cells cultivated in liquid medium on plates, 92% of the wild-type and 93% of the NdrA-mutant cells were mononucleate. (**B**) Centrosome integrity was determined by analyzing the number of nuclei and centrosomes per cell of wild-type and NdrA-null mutants.

3.2.8 NdrA interacts with Mob1 coactivators

Several studies have shown that the activity and biological function of NDR kinases requires activation by Mob1 proteins (Bichsel et al., 2004; He et al., 2005; Hergovich et al., 2005; Hou et al., 2000). The genome of *Dictyostelium* encodes three Mob1 proteins, MobA (DDB_G0278907, 214 amino acid residues), MobB (DDB_G0292758, 217 amino acid residues) and MobC (DDB_G0293706, 217 amino acid residues). The *Dictyostelium* Mob1 proteins are sharing a high degree of sequence identities. MobA and MobB are more closely related to each other and more distant from MobC (Figure 19A, B). Gene expression profiling (Rot et al., 2009) indicated that MobA and MobB are similarly expressed with an increase during the early aggregation stage, while MobC is expressed only at very low levels throughout the developmental cycle of *Dictyostelium*. Therefore binding of Mob1 coactivators MobA and MobB to the highly conserved N-terminal regulatory domain of NdrA was tested by performing *in vitro* pull-down assays. GST-MobA and GST-MobB were used together with lysates from GFP-NdrA or GFP-NdrA-T497E expressing cells (Figure 19C). Both, MobA and MobB interacted with GFP-NdrA and GFP-NdrA-T497E. In GFP-NdrA cell lysates, a double-band was detected that may either correspond to differently modified forms of NdrA or could result from degradation. In contrast, in GFP-NdrA-T497E lysates only the upper band was present.
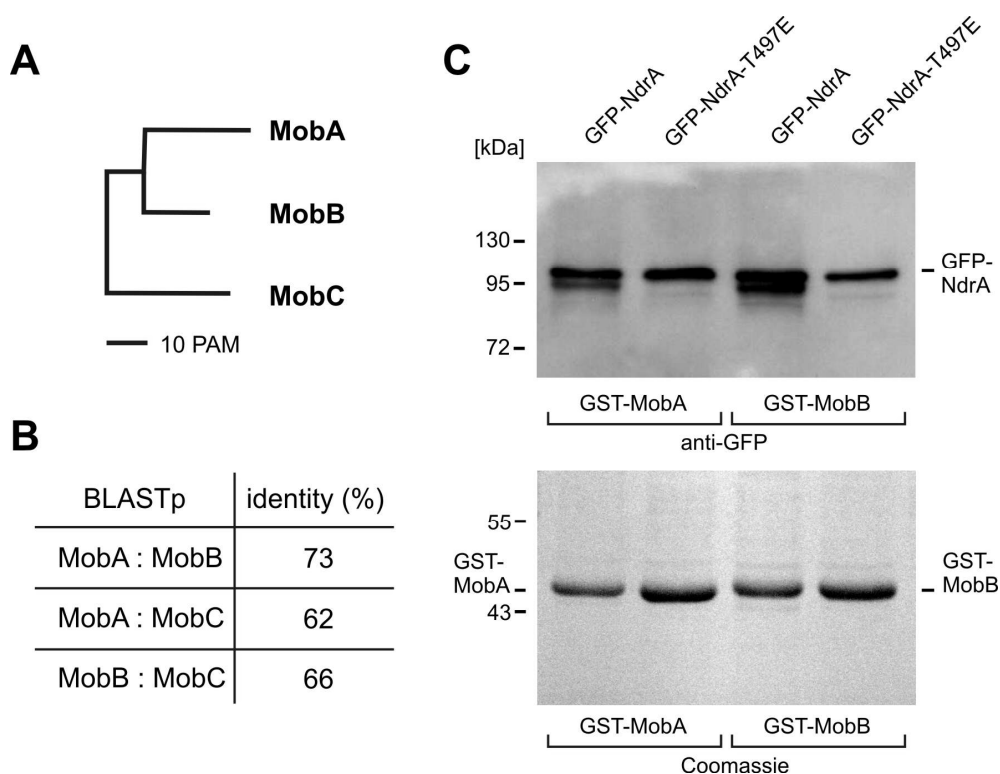
Figure 19: Mob1 proteins interact with NdrA

(**A**) Phylogeny of *Dictyostelium* Mob1 proteins. The tree was computed with MultAlin (http://bioinfo.genotoul.fr/multalin/multalin.html). PAM = percent accepted mutations. (**B**) Identities of the three homologs of the *Dictyostelium* Mob1-family of coactivators were determined by BLASTp analyses. (**C**) MobA and MobB were expressed as GST-fusion proteins and bound to glutathione-sepharose. The supernatants of pelleted lysates of wild-type cells expressing GFP-NdrA or its activated form GFP-NdrA-T497E were incubated with either GST-MobA- or GST-MobB-bound sepharose. After incubation, washed sepharose was boiled and the supernatant was separated by SDS-PAGE. The amounts of sepharose-bound GST-MobA and GST-MobB are shown by Coomassie staining. Western blot analysis using antibodies against GFP reveals that GFP-NdrA and GFP-NdrA-T497E are capable to bind to GST-MobA and GST-MobB.

The similar levels of binding for GFP-NdrA and GFP-NdrA-T497E to Mob1 suggest an interaction, independent of the phosphorylation state of the hydrophobic motif, unlike the reported influence of the phosphorylation state of the hydrophobic motif of NdrA on Mob1 binding (Hergovich et al., 2005).

In order to determine whether the Mob1 family proteins colocalize with NdrA, GFP-tagged MobA and MobB were expressed in *Dictyostelium* wild-type cells (Müller-Taubenberger et al., unpublished). Under-agar live-cell confocal laser scanning microscopy revealed centrosomal localization of GFP-tagged MobA as well as its presence in the cytosol. This localization is consistent with the cellular distribution determined for NdrA (Figure 20A). Unlike GFP-MobA, GFP-tagged MobB does not localize to the centrosome, and is found

throughout the cytoplasm (Figure 20B). Despite their capability to bind NdrA equally *in vitro*, the difference in localization of MobA and MobB suggests specific functions *in vivo* for MobA and MobB.
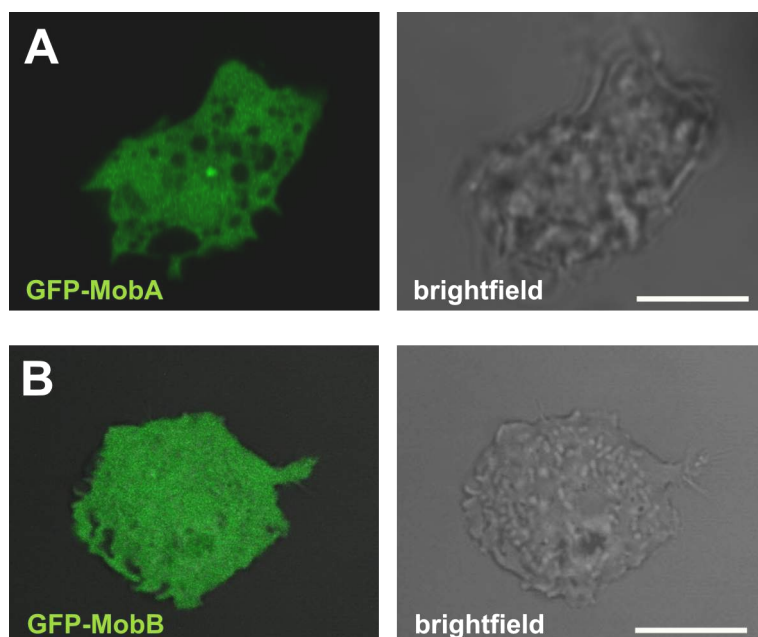
Figure 20: Localization of *Dictyostelium* Mob1 proteins

Confocal under-agar recordings of live GFP-MobA and GFP-MobB expressing wild-type cells. The GFP-fluorescence is shown on the left, the brightfield image on the right. (**A**) Fluorescence microscopy of cells expressing GFP-MobA shows an enrichment of GFP-MobA at centrosomes during interphase. (**B**) Imaging of GFP-MobB expressing cells reveals cytoplasmic localization of GFP-MobB. Bars = 5 µm.

3.2.9 Identification of EmpC as NdrA interactor

In an attempt to identify further potential interactors of NdrA, immunoprecipitation using anti-GFP specific nanobodies in combination with lysates prepared from cells overexpressing GFP-NdrA was employed. Using this approach followed by mass spectrometric analysis, several proteins were detected.

These include GFP-NdrA degradation products, hsc70 (DDB0191168), a heat shock protein commonly co-purified together with overexpressed protein, the elongation factor EF1a (DDB0191135), one of the most abundant proteins in *Dictyostelium* cells, and regularly found in interaction studies, as well as EmpC (DDB0215345) (Figure 21A, B).
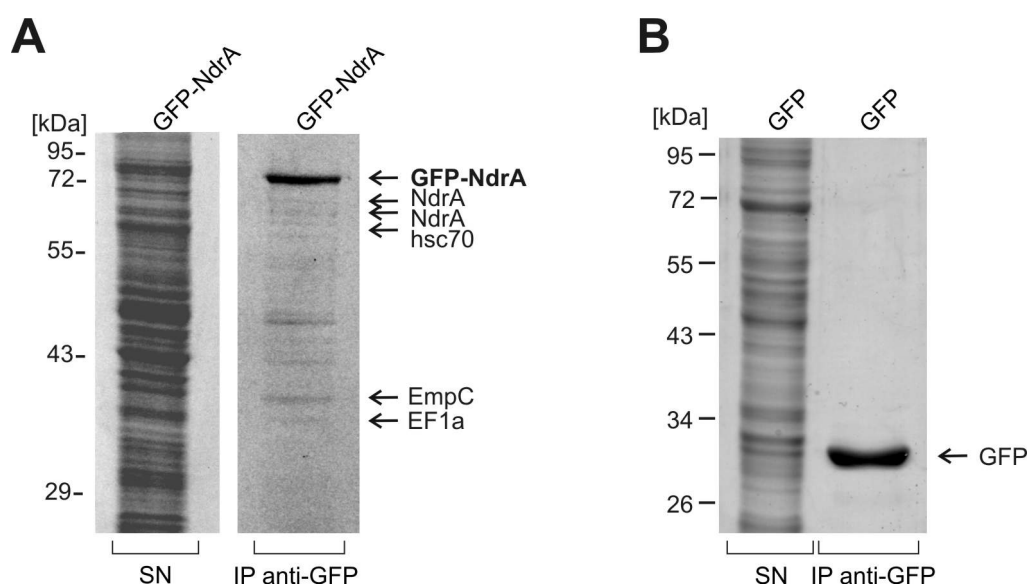
Figure 21: Identification of NdrA-interacting proteins

Immunoprecipitation of GFP-NdrA (A) or GFP (B) expressed in wild-type cells using a GFP-Trap kit. (**A**) Supernatants of pelleted lysates and immunoprecipitated proteins were separated by SDS-PAGE, stained with Coomassie Blue, and subsequently protein bands were cut out and analyzed by mass spectrometry. Identified proteins are indicated on the right. EmpC, a member of the emp24/gp25L/p24 family of cargoproteins was identified as interactor of GFP-NdrA. (**B**) As control GFP-expressing cells were used for immunoprecipitation.

EmpC is a transmembrane protein, implicated in trafficking between the Golgi network, the endoplasmic reticulum and the cell membrane and belongs to the emp24/gp25L/p24 family of proteins. According to the topology prediction, the major part of EmpC is localizing to the vesicle lumen; only the short C-terminus is exposed to the cytoplasm and is able to mediate interactions with other proteins (Figure 22A). To investigate the localization of EmpC, the protein was expressed in *Dictyostelium* cells as a C-terminally GFP-tagged fusion. The microscopic analysis of living cells showed that EmpC-GFP is enriched in a compartment close to the nucleus (Figure 22B); the expression level of EmpC-GFP was determined by Western blot analysis using anti-GFP antibodies (Figure 22C). By plotting the relative fluorescence of fixed preparations of EmpC-GFP expressing cells stained for DNA, the localization of EmpC-GFP to a vesicular compartment in the close proximity of the nucleus was confirmed (Figure 22D, E).

To investigate the localization of EmpC, observed by live-cell imaging of EmpC-GFP expressing cells in more detail, markers for centrosomes and recycling organels were tested for colocalization by immunostaining. Laser scanning microscopy of immunostained cells expressing EmpC-GFP with anti-CP224 antibodies to visualize the position of the
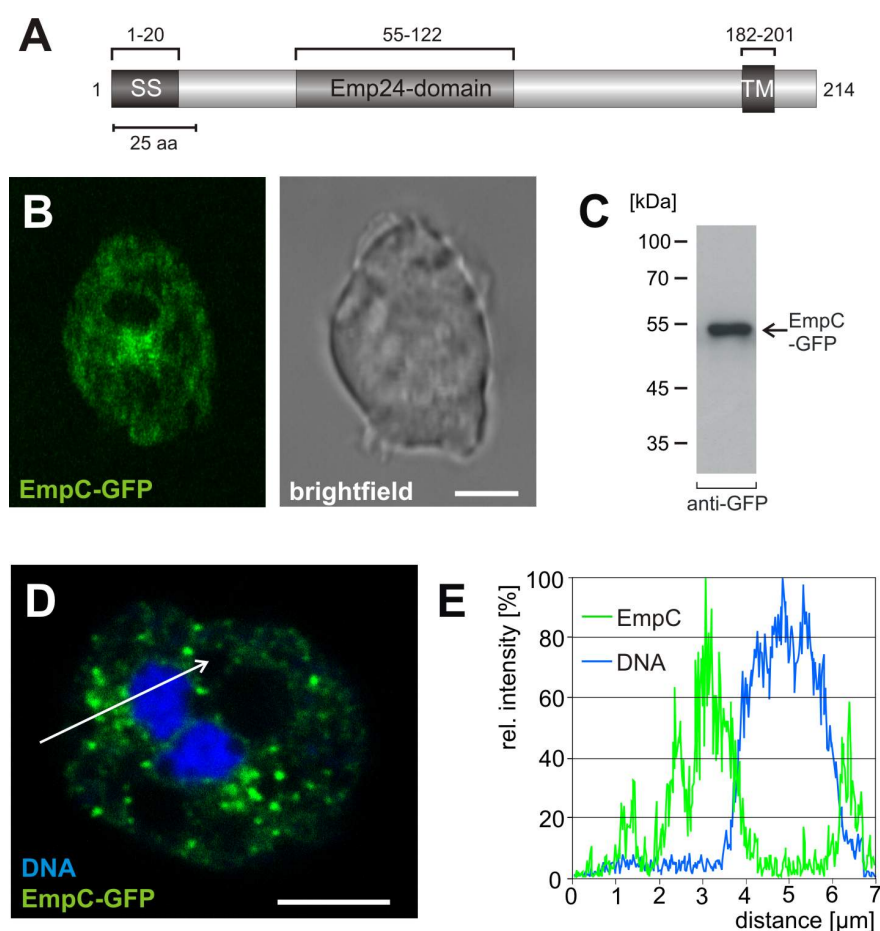
Figure 22: Analysis of the vesicular protein EmpC

(**A**) Schematic depiction of EmpC, highlighting the signal sequence (SS), the central Emp24-domain and the C-terminal transmembrane domain (TM). (**B**) The potential NdrA interactor EmpC was expressed as a C-terminally tagged GFP fusion protein in *Dictyostelium* cells. EmpC-GFP localizes adjacent to the nucleus and in close proximity to the centrosome. The image to the left shows the GFP-fluorescence in living cells, the right image the brightfield view. (**C**) Western blot analysis of lysates prepared from EmpC-GFP expressing cells using anti-GFP antibodies. (**D**) Wild-type cells expressing EmpC-GFP (green) were fixed and stained for DNA (blue). EmpC-GFP localizes in close proximity to the nucleus, also depicted by the scans in (**E**). Bars = 5 µm.

centrosome confirmed the localization of EmpC-GFP to a pericentrosomal region (Figure 23A) that could either correspond to the Golgi apparatus or to a endosomal recycling compartment, previously described for *Dictyostelium* (Charette et al., 2006). A marker specific for the latter compartment is the p25 protein, which is rapidly exchanged with an endocytic compartment that displays common characteristics with mammalian recycling endosomes, but is distinct from the Golgi apparatus. In addition, the vesicle component p23 was described (Ravanel et al., 2001). Whereas p25 is supposed to be involved in endosomal recycling, no functional analysis for p23 was performed. Immunostaining of

EmpC-GFP expressing cells with anti-p25 and anti-p23 antibodies revealed that though the EmpC-GFP and p25 label overlapped in the region around the centrosome, EmpC-GFP was found to localize to intracellular vesicles in contrast to p25 and was absent from the plasma membrane (Figure 23B). The staining for p23 revealed a strong pattern of localization to the plasma membrane and only weak enrichment at the pericentrosomal compartment. Apparently, EmpC seems to localize to a vesicular compartment, which is different to p25 or p23 specific compartments.
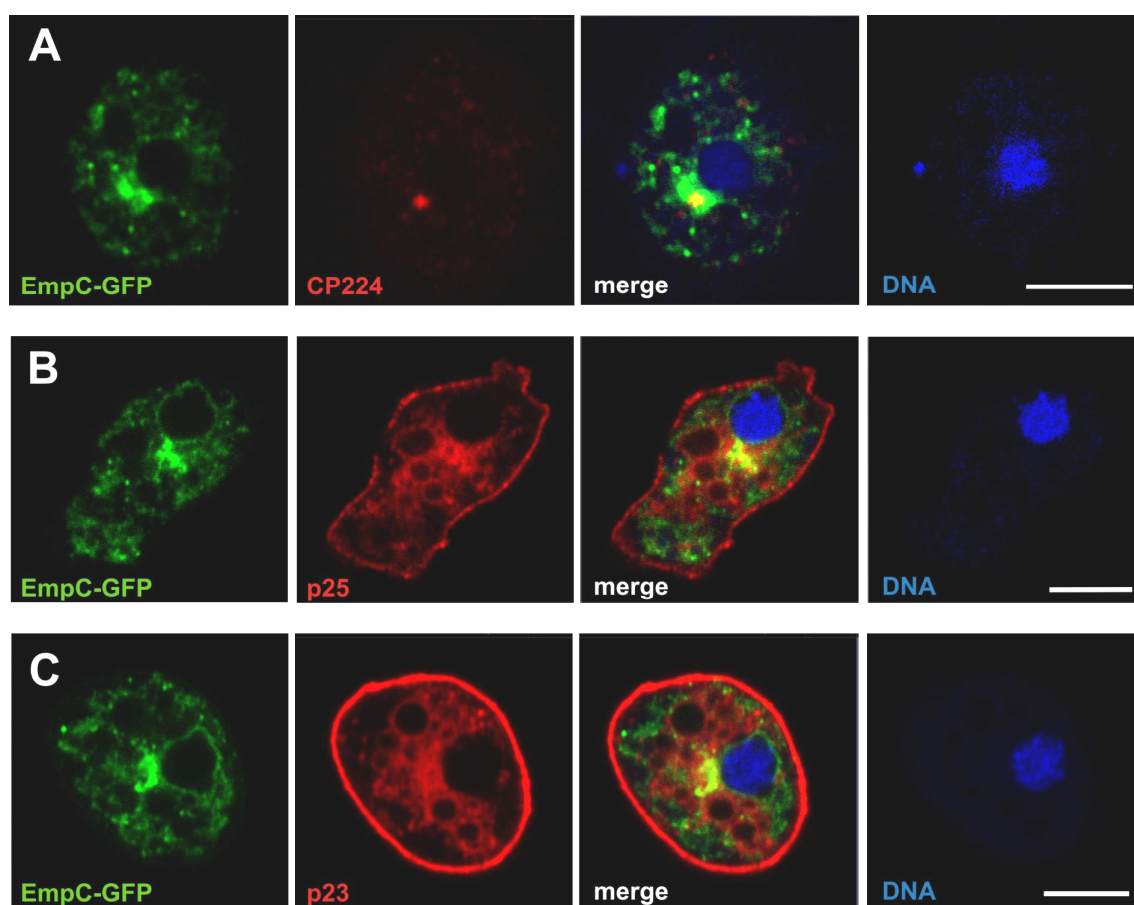
Figure 23: EmpC localizes to the pericentrosomal compartment

Wild-type cells expressing EmpC-GFP (green), were fixed and immunostained for the centrosome (A) or the pericentrosomal recycling compartment (B, C). (**A**) Immunostaining for CP224, a centrosomal marker, revealed that EmpC-GFP localizes to the vicinity of the centrosome. (**B**) The marker for the recycling compartment in the pericentrosomal region, p25 (Ravanel et al., 2001), only partially colocalizes with EmpC. (**C**) The membrane protein p23 colocalizes with GFP-EmpC in the pericentrosomal region, but is also highly abundant at the plasma membrane. Bars = 5 µm.

3.3 The NDR-related kinase NdrB of *Dictyostelium*

3.3.1 NdrB in comparison to NDR kinases from other organisms

The kinase NdrB, encoded by the *ndrB* gene of *Dictyostelium*, consists of 542 amino acid residues with a molecular mass of 63.6 kDa. The highest identities within the catalytic domain of NdrB are found with *Dictyostelium* NdrA, human NDR1 and NDR2, Trc of *D. melanogaster*, *C. elegans* Sax1, *S. pombe* Orb6, *S. cerevisiae* Cbk1 and Dbf2 as well as *S. pombe* Sid2 (Figure 24A). The amino acid sequence of NdrB, like NdrA, is characterized by typical sequence signatures of NDR/LATS kinases already described for NdrA (Chapter 3.2.1). Besides an AGC-kinase specific insert (amino acid residue 291 to 326) between subdomains VII and VIII of the NdrB catalytic domain (amino acid residues 130 to 391), subdomain VIII harbors an activation segment (amino acid residues 328 to 342), carrying a potential autophosphorylation site (S331) (Figure 24B). N-terminal of the catalytic domain, the N-terminal regulatory domain (amino acid residues 57 to 122) of NdrB serves as a putative target of Ste20-like kinase phosphorylation of T115. The N-terminal regulatory domain is a potential binding site for Mob1 proteins. At the C-terminus, a hydrophobic motif (amino acid residues 495 to 504), containing a potential phosphorylation site for upstream Ste20-like kinases, is located at T499 (Figure 24B).

3.3.2 NdrB localizes to the centrosome

In order to analyze the localization of NdrB, wild-type cells expressing GFP-NdrB were inspected by fluorescence microscopy. Live-cell imaging revealed the localization of NdrB to the centrosome (Figure 25A). By immunolabeling of GFP-NdrB-expressing cells with an antibody directed against α-tubulin for visualization of the centrosome, the enrichment of NdrB at the centrosome was confirmed (Figure 25A, B). The fluorescence intensities of the GFP-NdrB and α-tubulin signals were plotted in a fluorescence profile, showing an overlap of the NdrB signal with α-tubulin label. The GFP-NdrB expression levels compared to levels of GFP-NdrA expressed in wild-type cells were determined by Western blot analysis using anti-GFP antibodies. Thereby a moderate difference in the expression levels of GFP-tagged NdrA or NdrB was determined (Figure 29C).
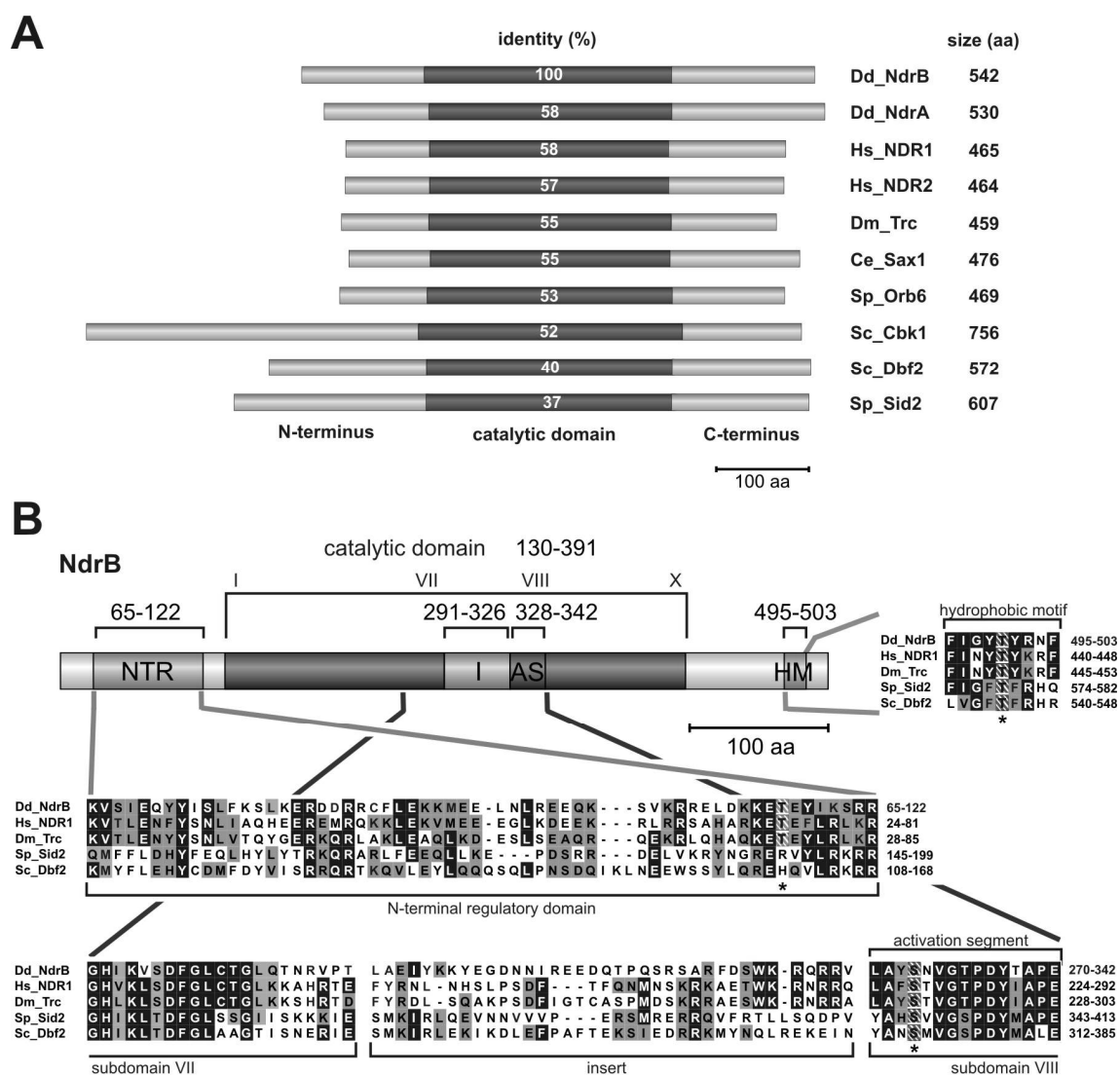
Figure 24: *Dictyostelium* **NdrB in comparison to other NDR/LATS kinases**

(**A**) Comparison of the catalytic domain of *Dictyostelium* NdrB with the catalytic domains of *Dictyostelium* NdrA, *H. sapiens* NDR1 and 2, *D. melanogaster* Trc, *C. elegans* Sax1, *S. pombe* Orb6 and Sid2, and *S. cerevisiae* Cbk1 and Dbf2. Numbers indicate percent identity within the catalytic domains compared to the NdrB catalytic domain and were determined by BLASTp. (**B**) Identification of NDR-kinase specific sequence signatures in NdrB. The N-terminal regulatory domain (NTR) contains a putative Mob1-binding site. Between subdomain VII and VIII the catalytic domain harbors an insert (I), followed by an activation segment (AS). The C-terminus contains a hydrophobic motif (HM). Domains are indicated by boxes in the NDR scheme. Identical amino acid residues are highlighted in black and conserved residues in grey. Potential phosphorylation sites are marked as hatched residues and are highlighted by asterisks.
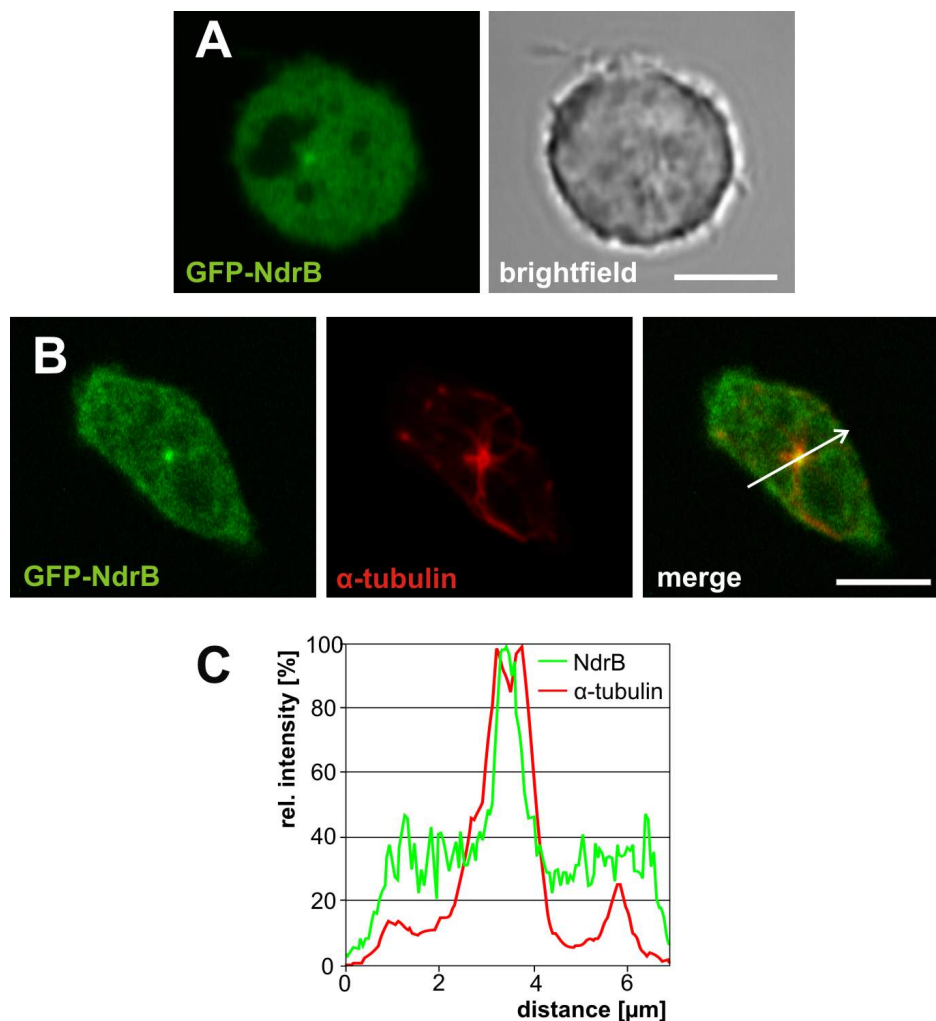
Figure 25: NdrB localizes to the centrosome

(**A**) Live-cell fluorescence microscopy of AX2 wild-type cells expressing GFP-tagged NdrB reveals an enrichment of GFP-NdrB at the centrosome. (**B**) Cells expressing GFP-NdrB were fixed with picric acid and immunostained using antibodies against α-tubulin. Laser scanning microscopy showed centrosomal as well as cytoplasmic localization of NdrB. (**C**) The colocalization of NdrB and α-tubulin is depicted by a fluorescence scan for green and red channels. Bar = 5 µm.

3.3.3 NdrB localizes to the mitotic spindle

The *Dictyostelium* NDR-related kinase NdrA localizes to a cloud-like structure around the spindle during early mitosis, however NdrA cannot be detected around the spindle or its vicinity during later mitotic stages (Chapter 3.2.7). Due to the centrosomal enrichment of NdrB, the localization of GFP-NdrB in the course of mitosis was recorded. Therefore, the localization of GFP-NdrB expressed in wild-type cells was determined by confocal laser scanning microscopy of fixed preparations, immunostained for α-tubulin using
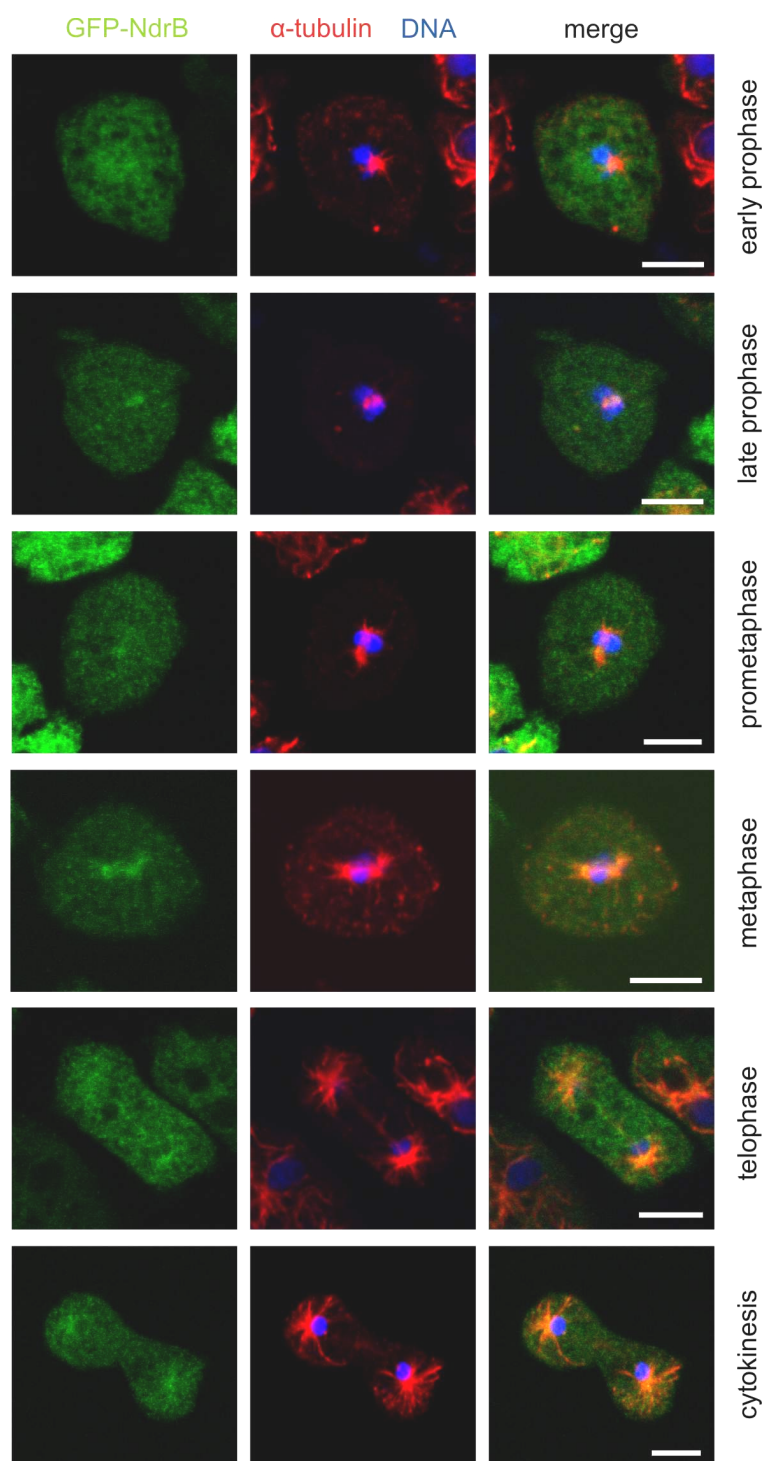
Figure 26: Localization of NdrB at the mitotic spindle

Wild-type cells expressing GFP-NdrB were fixed and stained with antibodies against α-tubulin. Interphase and mitotic stages were examined by confocal laser scanning microscopy. Fluorescence of GFP is shown in the left, immunofluorescence of α-tubulin labeling and TO-PRO-3 staining of DNA in the middle and merged images in the right panels. GFP-fluorescence of GFP-tagged NdrB, enriched at centrosomes in interphase, can be detected in the periphery of the mitotic spindle from prometaphase through metaphase to telophase. Bars = 5 µm.

monoclonal antibodies. The centrosomal localization of GFP-NdrB during interphase (Figure 25A, B) is changing during different stages of mitosis. GFP-NdrB forms a cloud-like formation in early prophase. However, from metaphase to telophase, NdrB was detected to be adjacent to the spindle as well as its vicinity (Figure 26). This finding is in contrast to the localization of NdrA during mitosis, which cannot be detected around the spindle in metaphase and later stages (Figure 17A, B), indicating different functions for both NDR kinases.

3.3.4 Identification of NdrB interacting proteins

In an attempt to identify potential interactors of NdrB, an immunoprecipation approach employing anti-GFP specific nanobodies in combination with lysates prepared from GFP-NdrB expressing cells was performed. Immunoprecipitated eluates were separated by SDS-PAGE, stained with Coomassie blue, and single bands were cut out from the gels and analyzed by mass spectrometry. By this approach, subunit B of the vacuolar ATPase (DDB0185207), the elongation factor EF1α (DDB0191135) and MobB (DDB0232217), a
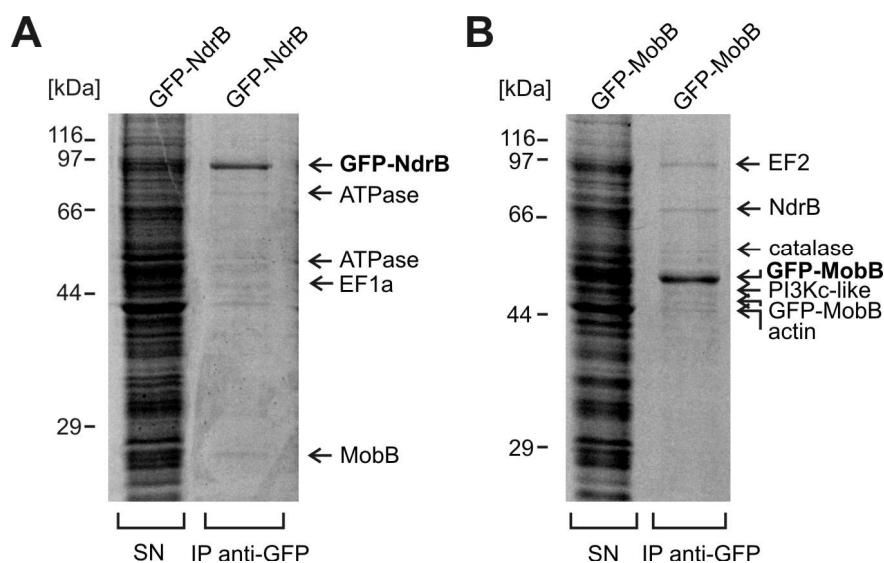
Figure 27: NdrB interacts with MobB

Immunoprecipitation of cell lysates from *Dictyostelium* cells expressing GFP-tagged NdrB was performed using nanobodies directed against GFP. The supernatants of pelleted lysates and eluates were separated by SDS-PAGE and stained with Coomassie blue. (**A**) By immunoprecipitation of GFP-NdrB, in addition to other binding proteins, MobB, a presumed coactivator of NDR/LATS kinases was enriched from whole cell lysate and identified by mass spectrometry. (**B**) Vice versa, by immunoprecipitation of GFP-MobB, NdrB is pulled down. Furthermore, a band revealed a possible interaction with a PI3Kc-like kinase (Hoeller and Kay, 2007) and several other interacting proteins.

member of the Mob1 family of activators, were identified (Figure 27A). Due to their high abundancy in *Dictyostelium* cells, the vacuolar ATPase subunits as well as the elongation factor EF1 were often detected as false positive binding proteins in immunoprecipitation experiments. Mob1 proteins bind the highly conserved N-terminal regulatory domains of NDR/LATS kinases and were reported to enhance kinase activity for mammalian NDR (Hergovich et al., 2005). Besides the binding of MobB to NdrB, pull-down experiments for NdrA revealed interaction with Mob1 proteins.

In order to confirm the interaction of GFP-NdrB with MobB, the anti-GFP nanobody immunoprecipitation approach was applied using lysates of GFP-MobB expressing cells. Thereby the binding of MobB to GFP-NdrB was confirmed.

By the immunoprecipitation experiment of GFP-MobB, the elongation factor EF2 (DDB0191363), a catalase subunit (DDB0185123), the phosphatidyinositol 3-kinase related protein kinase PI3Kc-like (DDB0238116) and actin were identified as putative binding proteins (Figure 27B). EF2 as well as subunits of the catalase and actin are highly abundant in *Dictyostelium* and known false positives. The functional interactor PI3Kc-like
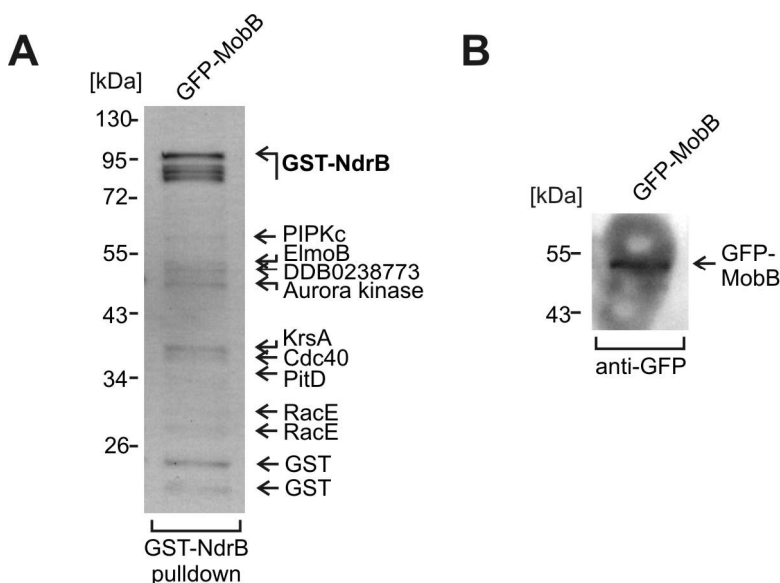
Figure 28: Identification of putative NdrB interaction partners

GST-pull-down of full-length recombinant GST-NdrB with lysate of wild-type cells expressing GFP-MobB. (**A**) Bound proteins were separated by SDS-PAGE, stained with Coomassie blue and bands of interest were cut out from the gel and analyzed by MALDI mass spectrometry. Proteins that were identified as NdrB-interactors are the Ste20-like kinase KrsA as well as the conserved NDR/LATS interactor AurK, PIPKc and PitD, required for phosphoinositol phosphate turnover, and the regulators of actin polymerization ElmoB and RacE as well as DDB0238773, a cyclin domain containing protein, and Cdc40. (**B**) Western blot analysis of the pull-down experiment shown in (A) with anti-GFP antibodies revealed binding of GFP-MobB to GST-NdrB.

kinase is a member of the phosphoinositide 3-kinase family, which was reported to be responsible for cell polarization by changing the composition of membrane pools of PIP_2 and PIP_3 (Hoeller and Kay, 2007).

To identify additional interactors of NdrB *in vitro*, recombinant GST-NdrB was used for pull-down assays. GST-NdrB coupled to glutathione sepharose was incubated with the supernatant of pelleted lysates of GFP-MobB expressing *Dictyostelium* cells. By Western blot analysis using antibodies against GFP, the interaction of GST-NdrB and GFP-MobB was detected (Figure 29B). This observed low binding rate compared to the high binding affinity of endogenous MobB to GFP-NdrB is probably caused by sterical interference of the GST- and GFP- tags of NdrB and MobB in this pull-down experiment. For control, lysate of wild-type cells was used with non-coupled glutathione sepharose, shown in (Figure 46).

Mass spectrometric analysis of Coomassie stained protein bands reveals binding of ElmoB (DDB0233921), an ELMO family member, as well as the Rho-GTPase RacE (DDB0214825) (Figure 28A). The ELMO family member ElmoA positively regulates actin polymerization through activation of the Rac small G proteins, e.g. during phagocytosis or cell migration (Isik et al., 2008).

Moreover, GST-NdrB is capable of binding PIPKc (phosphatidylinositol phosphate kinase 6, DDB0235161) as well as PitD (DDB0237592), a phosphoinositolphosphate transfer protein, suggesting an involvement of a NdrB/MobB complex in PIP_2/PIP_3 turnover. Furthermore, the *Dictyostelium* Aurora kinase AurK (DDB0216254) was found to co-precipitate GST-NdrB; human LATS2 was reported to be target of phosphorylation by Aurora-A (Toji et al., 2004). Besides the Aurora kinase, a cyclin domain containing protein (DDB0238773) and the regulator of cell cycle progression Cdc40 (DDB0233421) were pulled down by GST-NdrB. Additionally, the Ste20-like kinase KrsA (DDB0191170), implicated in stress response, was found to interact with GST-NdrB. The identification of these interactors by pull-down using GST-NdrB can be caused by the observed weak binding of GFP-MobB. Thus, the binding of NdrB to other interactors was enabled, suggesting an inhibitory function for MobB.

3.3.5 Generating antibodies against NdrB and MobB

In order to establish a tool for the detailed investigation of NdrB and MobB, polyclonal antibodies were generated by injecting rabbits with recombinant full length NdrB or MobB. The anti-NdrB polyclonal antibodies, generated against full-length NdrB in the course of
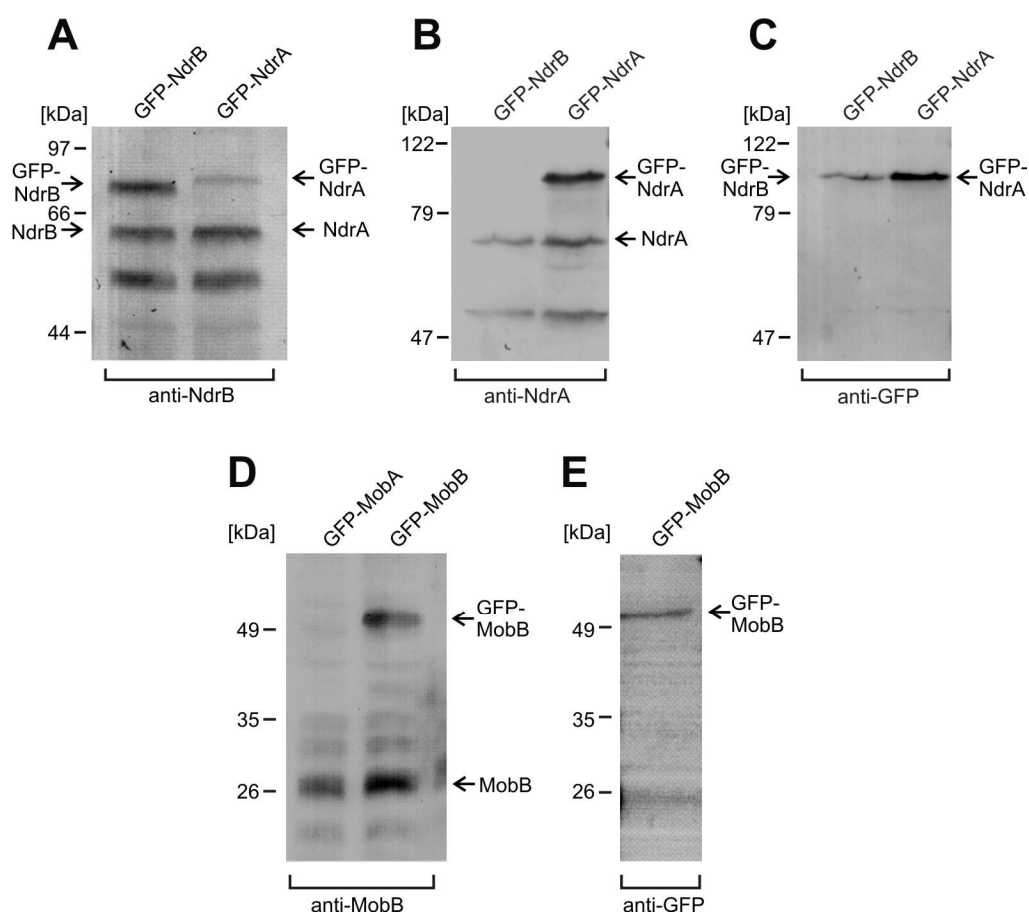
Figure 29: Generation of polyclonal antibodies against NdrB and MobB

(**A**) The antibody generated against recombinant GST-NdrB was tested by Western blot analysis using lysates of GFP-NdrB and GFP-NdrA expressing wild-type cells. The antibody generated against NdrB crossreacts with NdrA. (**B**) Lysates of GFP-NdrB and GFP-NdrA expressing cells were subjected to Western blot analysis using an antibody directed against NdrA. (**C**) For control, GFP-NdrB and GFP-NdrA lysates were used for Western blot analysis using a specific anti-GFP antibody. (**D**) A polyclonal antibody generated against MobB specifically recognizes overexpressed GFP-MobB and endogenous MobB. (**E**) Lysate of GFP-MobB expressing cells was probed using an antibody against GFP.

this study, crossreact with the NdrA kinase, and therefore were unsuitable for NdrB-specific analyses (Figure 29A, C), whereas the antibody generated against NdrA does not recognize GFP-NdrB (Figure 29B). The antibody generated against MobB specifically recognizes MobB (Figure 29D, E), thus offering the option of new approaches for the quantitative investigation of protein interactions or the functionality of MobB.

In an attempt to determine the role of NdrB, wild-type AX2 cells were transformed with a gene replacement construct for *ndrB* to generate an NdrB-knockout strain. By PCR analysis of single clones it became obvious that the genomic region on chromosome 5

harboring the *ndrB* gene was duplicated. In the course of this firstly undiscovered genomic alteration of the AX2-214 wild-type strain, the efforts of gene-replacement by a blasticidin-S resistance cassette were not successful. High-resolution genomic analysis (Bloomfield et al., 2008) revealed that the alternative wild-type strains AX3 and AX4 which were isolated independent of AX2 are most likely not carrying this particular genomic duplication. In order to screen for positive *ndrB* gene replacement, a specific antibody will be of high interest.

3.4 The LATS-related kinase Lats2 of *Dictyostelium*

3.4.1 Lats2 compared with LATS kinases from other organisms

The AGC protein kinase Lats2 (NdrC, DDB0219984) comprises 1335 amino acid residues (149 kDa). The highest identities of the catalytic domain of Lats2 from *Dictyostelium* with other LATS kinases were found with *Dictyostelium* Lats1, *D. melanogaster* Warts, and human LATS2 and LATS1 (Figure 30A). An N-terminal regulatory domain (NTR, amino acid residues 645-710) carries a conserved phosphorylation site at position T703. The catalytic kinase domain (subdomains I-X, amino acid residues 718-1019) contains an AGC-kinase specific insert (amino acid residues 867-913) with the autoinhibitory sequence, an activation segment (amino acid residues 914-928), harboring a putative phosphorylation site at position S917. At the C-terminus, a conserved sequence element, the hydrophobic motif (HM, amino acid residues 1092-1099), is found with a putative phosphorylation site at position T1095 (Figure 30B). This motif might be involved in the activation of Lats2.

By a two-hybrid screen for putative interactors of Ras GTPases, the laboratory of Prof. Gerald Weeks (UBC, Vancouver, Canada) has determined that Ras is binding Lats2 (Weeks and Bolourani, unpublished). It was found that in addition to the general features of NDR/LATS kinases, Lats2 harbors a Ras binding domain (RBD; amino acid residues 107-248). This Ras binding domain was further investigated in the course of this study (Figure 30B).

3.4.2 Generation of Lats2-null mutants

In order to characterize the function of Lats2, the *ndrC* gene (DDB_G0284839), coding for Lats2, was knocked out by homologous recombination with a construct carrying a
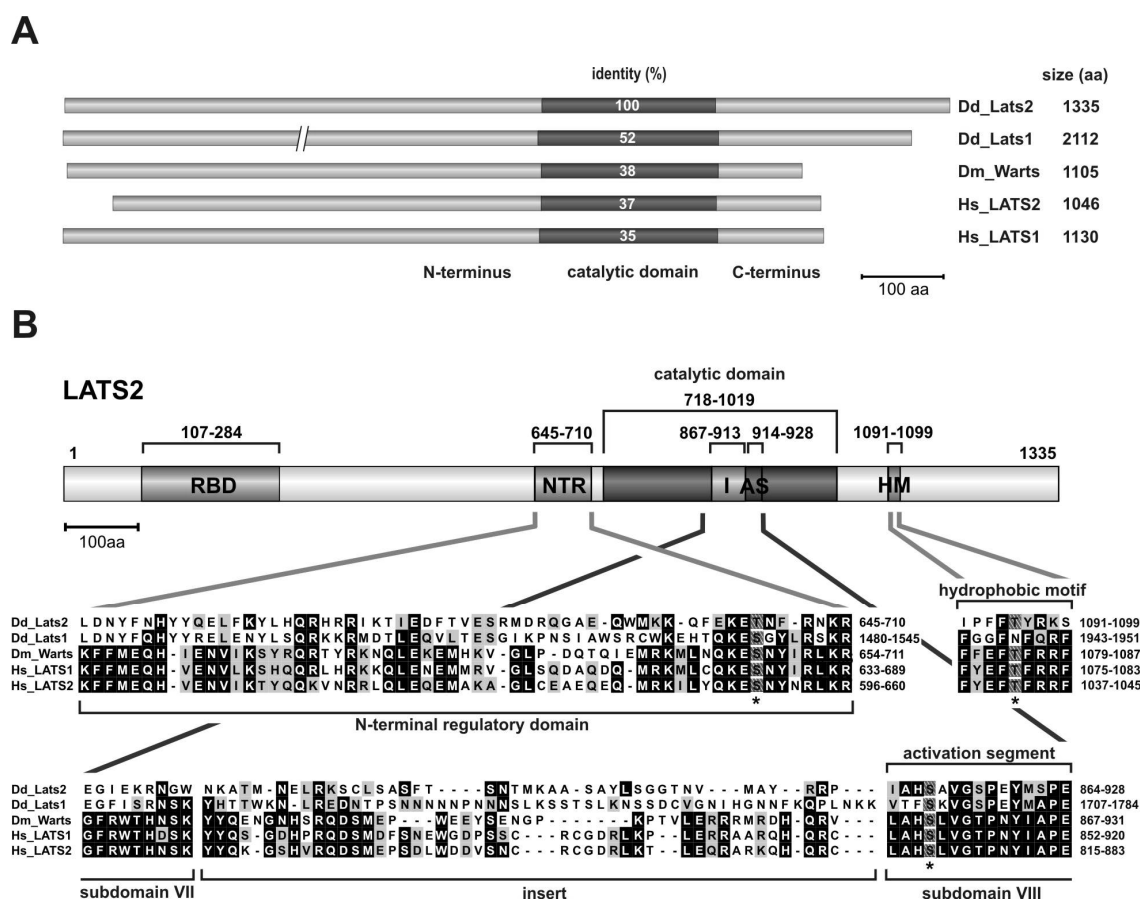
Figure 30: Domain structure of the *Dictyostelium* Lats2 kinase

(**A**) Comparison of the catalytic domain of *Dictyostelium* Lats2 with the catalytic domains of *Dictyostelium* Lats1, *D. melanogaster* Warts, *H. sapiens* LATS2 and LATS1. Numbers indicate percent identity within the catalytic domains compared to the Lats2 catalytic domain determined by BLASTp. (**B**) Domain organization of Lats2. The following domains were identified: a Ras binding domain (RBD amino acid residues 107-248), an N-terminal regulatory domain (amino acid residues 650-710, phosphorylation site T703), a catalytic domain (amino acid residues 718-1019, subdomains I-X) with a specific insert (amino acid residues 867-913) and an activation segment (amino acid residues 914-928, regulatory phosphorylation site S917) as well as a hydrophobic motif (amino acid residues 1092-1099, phosphorylation site T1095). Potential phosphorylation sites are marked as hatched residues and are highlighted by asterisks.

blasticidin-S resistance cassette (Faix et al., 2004). Insertion of the resistance cassette was tested by PCR using genomic DNA isolated from two independent blasticidin-S resistant clones and a wild-type control. Sequence-specific oligonucleotides were applied as primers to test for the wild-type gene (P1 and P3), resulting in a 1.7 kbp PCR-product. Insertion of the resistance cassette by homologous recombination into the *ndrC* gene resulted in a PCR-product of 1.2 kbp (P1 and P2) (Figure 31A, B). Two independent clones of Lats2-null cells were isolated and clone I was used for further studies. Lats2-null

cells grown at low cell density on solid surface were inspected by phase contrast microscopy and showed highly increased cell sizes compared to wild-type (Figure 31C), thus indicating a role for Lats2 in cytokinesis. The phenotype was investigated further by determining the effect on growth, development and cell division.
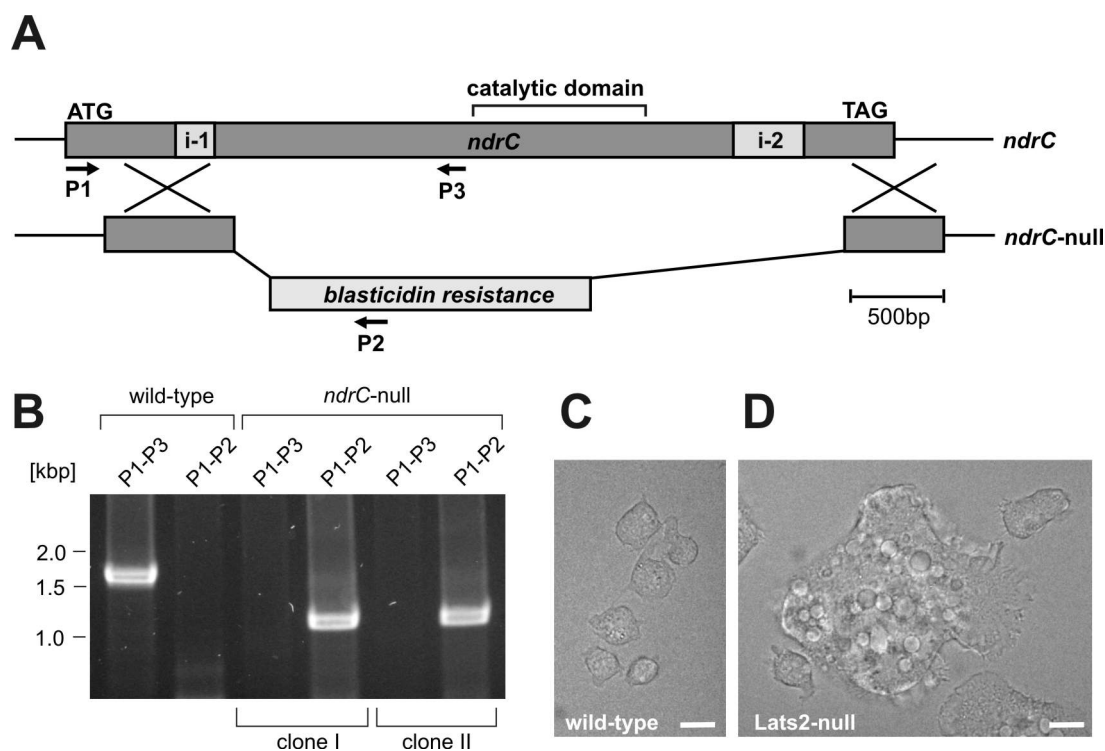
Figure 31: Generation of Lats2-null mutants

(**A**) Gene replacement of *ndrC* (DDB0219984), coding for Lats2. A construct comprising the blasticidin-S-resistance cassette linked with an N- and a C-terminal fragment of the *ndrC* gene was used for the transformation of wild-type cells. (**B**) Insertion of the *bsr*-cassette into the *ndrC* gene was tested by PCR with the primer combinations depicted in (A) using genomic DNA purified from blasticidin-S-resistant clones (clone I and II) or from wild-type. The expected sizes of PCR fragments are 1.7 kbp for primers P1-P3 (wild-type *ndrC* gene) and 1.2 kbp for P1-P2 (knockout). *Dictyostelium* wild-type (**C**) and Lats2-null cells (**D**) were analyzed by phase contrast microscopy. Lats2-null cells are much larger than wild-type. Bars = 10 µm.

3.4.3   Growth and development of Lats2-null cells

In order to examine the Lats2 gene-knockout with respect to cell growth, generation times in shaking culture with nutrient medium (n = 8) as well as *Dictyostelium* plaque sizes on lawns of *K. aerogenes* were measured for Lats2-null cells in comparison to wild-type (n = 6). The growth rates determined for Lats2-null cells were indistinguishable from those of wild-type cells for both growth conditions, shaking culture as well as on bacterial lawns
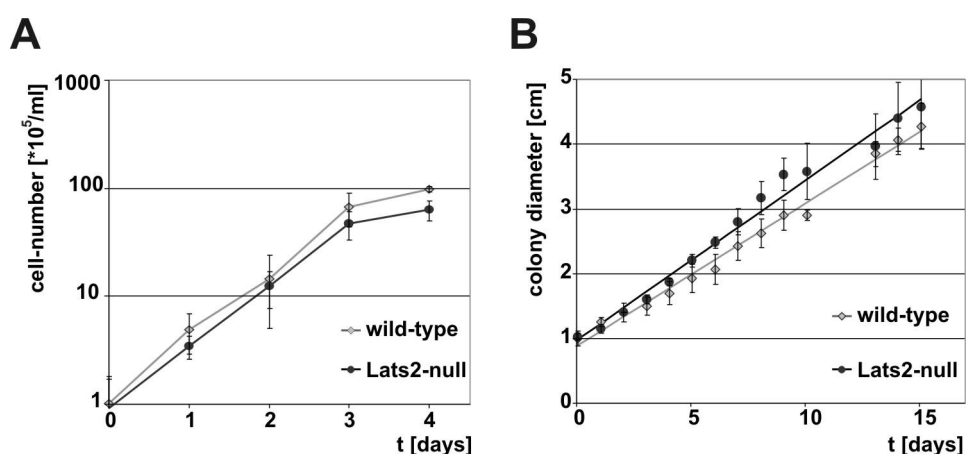
Figure 32: Growth rates of Lats2-null cells compared to wild-type

(**A**) Cell numbers of Lats2-null and wild-type cultures grown in nutrient medium under shaking conditions were measured every 24 h. (**B**) Diameters of wild-type and Lats2-null colonies grown on bacterial lawns of non-pathogenic *K. aerogenes*.
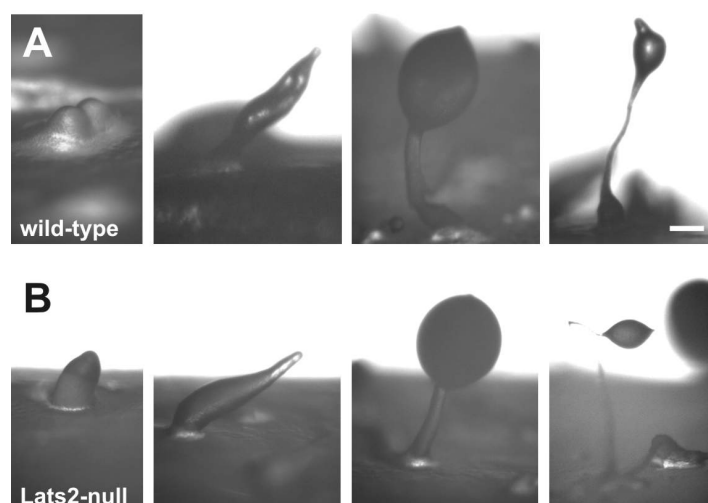
**Figure 33: Development of Lats2-null cells**

Wild-type (**A**) and Lats2-null (**B**) were recorded at different stages of development on lawns of *K. aerogenes* on SM plates. Lats2-null cells develop indistinguishably from wild-type. Representative developmental stages like the formation of tight aggregates, slugs, spore heads and mature fruiting bodies are depicted. Bar = 0.1 cm.

(Figure 32A, B). Gene expression profiling indicated that Lats2 is expressed at very low levels throughout the developmental cycle of *Dictyostelium* (Rot et al., 2009), indicating a role for *Dictyostelium* Lats2 not only in cytokinesis but also in development. Different

stages of *Dictyostelium* development were recorded of cells forming colonies on *K. aerogenes*. It was revealed that the differentiation of Lats2-null cells from aggregation to the formation of multicellular clusters and slug-like aggregates, which then form fruiting bodies is indistinguishable from wild-type (Figure 33).

3.4.4 Lats2 controls efficient cell division

To investigate the effect of the observed increased cell size of Lats2-null cell cultures on the number of nuclei and cytoskeletal markers, Lats2-null cells were observed by confocal
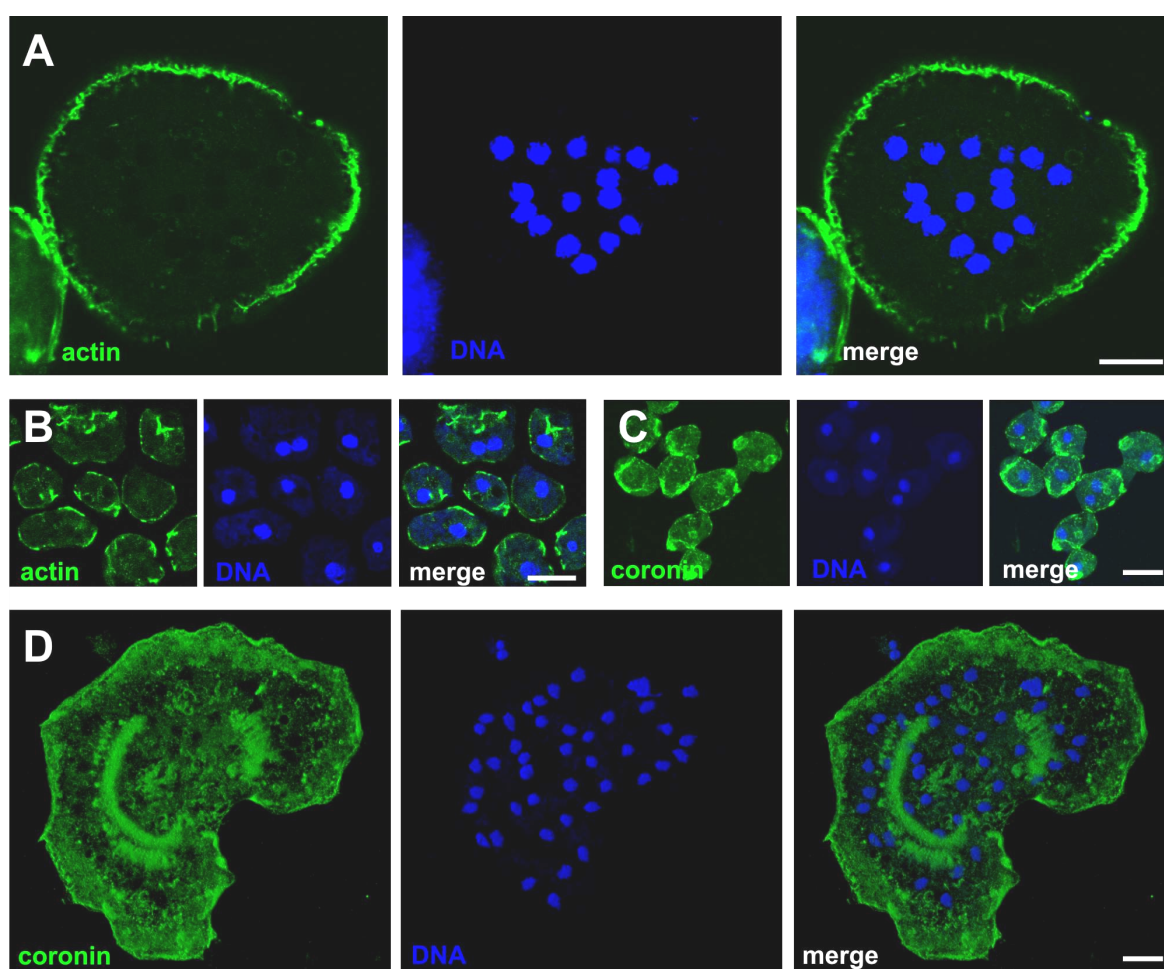
Figure 34: Lats2-null cells are multinucleated

Cells were fixed with ice-cold methanol and stained for actin using FITC-labelled phalloidin, or immunostained with polyclonal antibodies against coronin, shown in the left panels, and TO-PRO-3 for DNA in the middle panels. Merged images are shown on the right. (**A**) Fixed Lats2-null cell stained with FITC-Phalloidin for actin shows cortical localization of actin. (**B**) Fixed wild-type cell stained with FITC-Phalloidin for actin and TO-PRO-3 for DNA. (**C**) Recording of fixed wild-type cells stained with monoclonal antibodies against coronin. (**D**) Fixed Lats2-null cell immunostained for coronin. Bars = 10 µm.
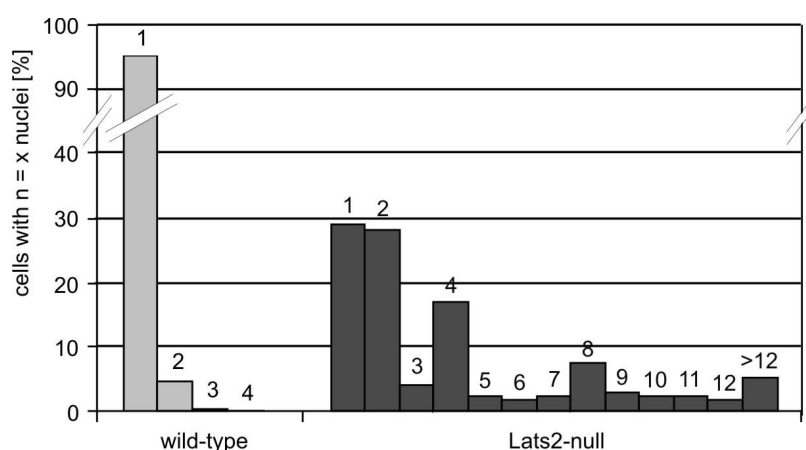
Figure 35: Lats2-null cells are multinucleate

The histogram shows the percentage of cells carrying the indicated numbers of nuclei. Cells were fixed and stained with DAPI to determine the numbers of nuclei per cell for wild-type and Lats2-null cells grown on coverslips.

laser scanning microscopy. Fixed preparations of wild-type and Lats2-null cells were grown on coverslips and stained with TO-PRO-3 for visualization of nuclei and with FITC-coupled phalloidin for the actin cytoskeleton or by immunostaining using antibodies directed against the cytoskeletal marker coronin (Figure 34A-D). Lats2-null cells are characterized by a highly increased number of nuclei. Lats2-null cells stained with FITC-coupled phalloidin, or immunolabeled using monoclonal anti-coronin antibodies, exhibited a normal localization of actin at the cell cortex when compared to wild-type (Figure 34A-D).

To quantify the multinucleate phenotype of Lats2-null cells, the numbers of nuclei per cell were determined for cell cultures grown on coverslips. DAPI-stained preparations of wild-type and Lats2-null cells were analyzed by fluorescence microscopy (Figure 35). In wild-type, 94.9% of cells are mononucleate (n = 529), whereas in Lats2-null cells the portion of mononucleate cells comprises 28.7% (n = 178).

Live-cell recordings of Lats2-null cells show hindered cell divisions, leaving putative daughter cells connected due to omitted separation (Figure 36). This observation suggests a mechanism of cell division by traction-mediated cytofission rather than cytokinesis, resulting in enlarged multinucleate cells.
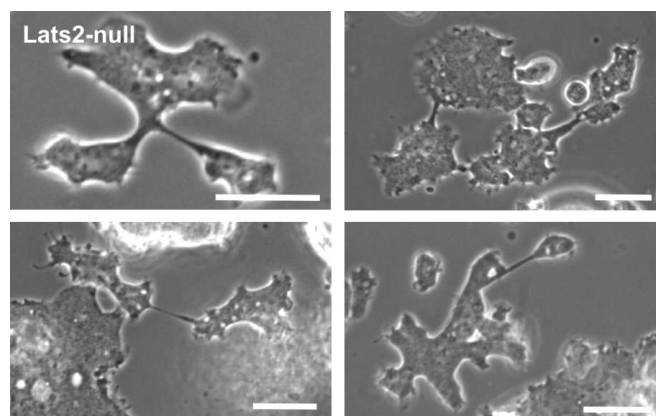
Figure 36: Lats2-null cells divide by traction-mediated cytofission

Live-cell recordings of Lats2-null cells during traction-mediated cytofission of cells, grown on coverslips. Bars = 10 µm.

3.4.5 Lats2-null cells have aberrant numbers of centrosomes

The human LATS homologs were reported to control cell proliferation as well as mitotic exit (Bothos et al., 2005; Li et al., 2003) and human NDR kinases have been described to be regulators of centrosome duplication (Hergovich et al., 2007). Therefore, it was investigated, whether the observed multinucleate phenotype of *Dictyostelium* cells lacking Lats2 is connected to changes in the distribution of centrosomes. Wild-type and Lats2-null cells grown on solid surfaces were fixed and immunostained with anti-α-tubulin antibodies as marker for centrosomes, and stained for DNA using TO-PRO-3 (Figure 37A-C). Wild-type cells are mononucleated and one centrosome is connected to the nucleus. In contrast, additional supernumerous centrosomes were observed in multinucleate Lats2-null cells. Unlike normal centrosomes (Figure 37D) which are permanently connected to the nucleus, a connection of supernumerary centrosomes to nuclei was not observed (Figure 37A-C).

For the detailed analysis of the integrity of nucleus-centrosome connections, the number of nuclei and centrosomes per cell was determined for fixed preparations of Lats2-null and wild-type cells. Cells grown on coverslips were immunostained using monoclonal antibodies against the centrosomal marker α-tubulin and stained for DNA using DAPI. The ratio of centrosomes and nuclei is depicted in a histogram (Figure 38), revealing that more than 19% of Lats2-null cells (n = 123) carry more than one centrosome per nucleus, whereas only 1% of the wild-type controls (n = 158) were aberrant.
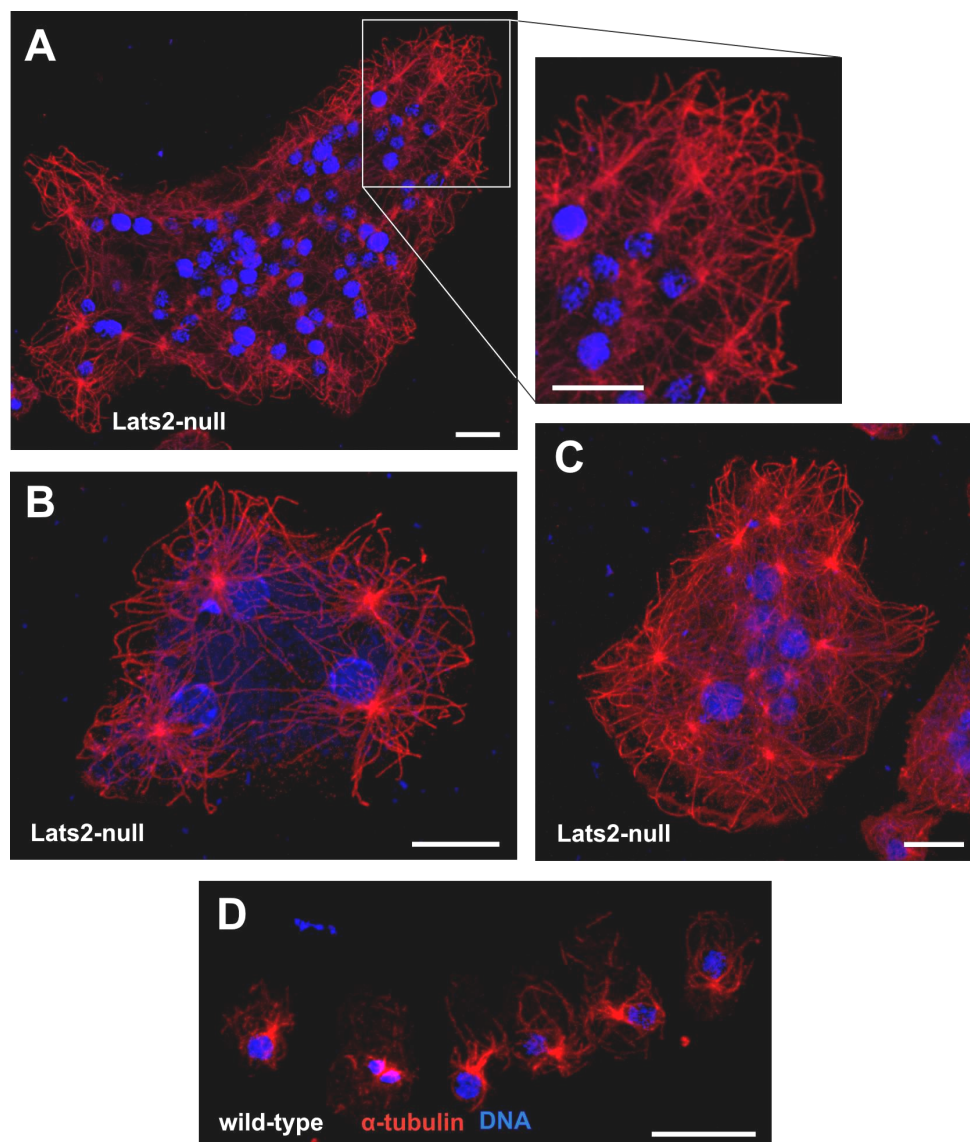
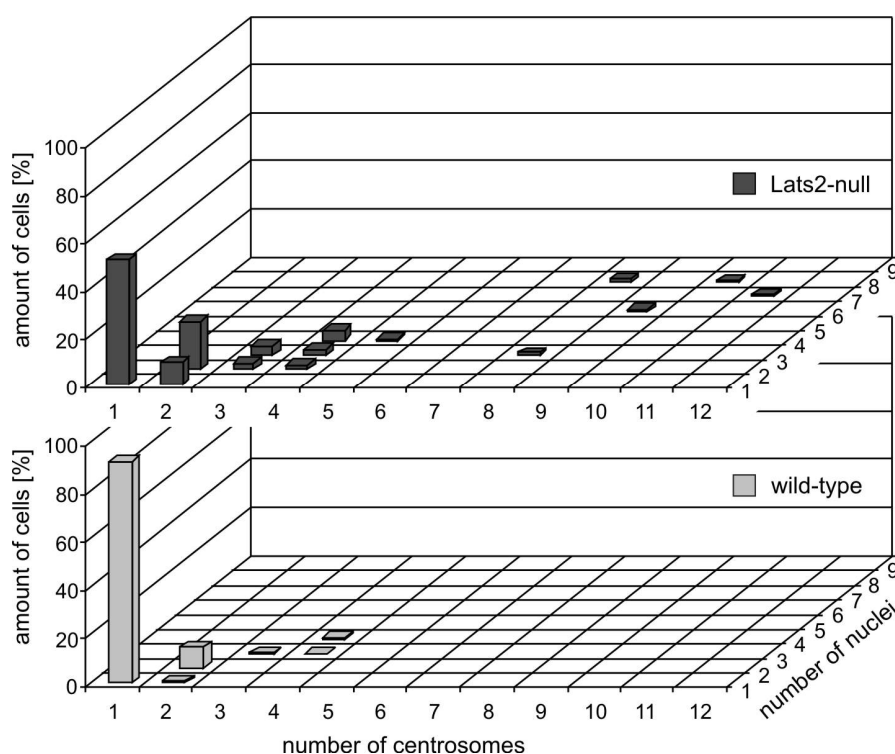**Figure 37: Centrosomal aberrations in Lats2-null cells**

Wild-type and Lats2-null cells were fixed and stained with antibodies against α-tubulin as a marker for centrosomes and TO-PRO-3 for DNA to visualize nuclei. Interphase stages were recorded by confocal laser scanning microscopy. (**A**,**B**) Lats2-null cells have multiple nuclei and supernumerous centrosomes, which are not connected to nuclei. (**C**) Besides an aberrant number of centrosomes, enlarged nuclei are observed. (**D**) In wild-type cells the centrosome is attached to the nucleus. Bars = 10 µm.

3.4.6 Effect of aberrant centrosomes on mitosis

Efficient mitosis requires the duplication of the centrosome and formation of a mitotic spindle. In-between the daughter centrosomes, the chromosomes align in the equatorial disc followed by separation of the sister chromatids and their transfer to the spindle poles.

Figure 38: Aberrant numbers of centrosomes in Lats2-null cells

Interphase stages of fixed cells were stained with antibodies against α-tubulin as a marker for centrosomes and DAPI for DNA to visualize the nuclei and were recorded by fluorescence microscopy. Histogram depicting the aberrant percentage of centrosomes in multinucleated Lats2-null cells and the wild-type control.

To investigate the presence of mitotic spindles in multinucleate cells as well as the effect of excess centrosomes on mitosis, Lats2-null cells were fixed and stained using antibodies against α-tubulin for visualization of mitotic spindles and TO-PRO-3 for chromosomal DNA. By confocal laser scanning microscopy, mitotic spindles were recorded spacially in Lats2-null (Figure 39A-E) and wild-type cells (Figure 39F, G).

Concerted mitosis was observed in Lats2-null cells carrying a single or multiple spindles (Figure 39A-C), according to the mitosis in wild-type cells carrying one or two spindles (Figure 39F, G). It is shown that cells with even as well as uneven distributions of spindles go through mitosis in a concerted manner. Moreover, excess centrosomes do not have an effect on accomplishing mitosis. The unattached supernumerous centrosomes are not forming independent spindles (Figure 39D, E), thus, a direct effect of an increased ratio of centrosomes per nuclei could not be observed.
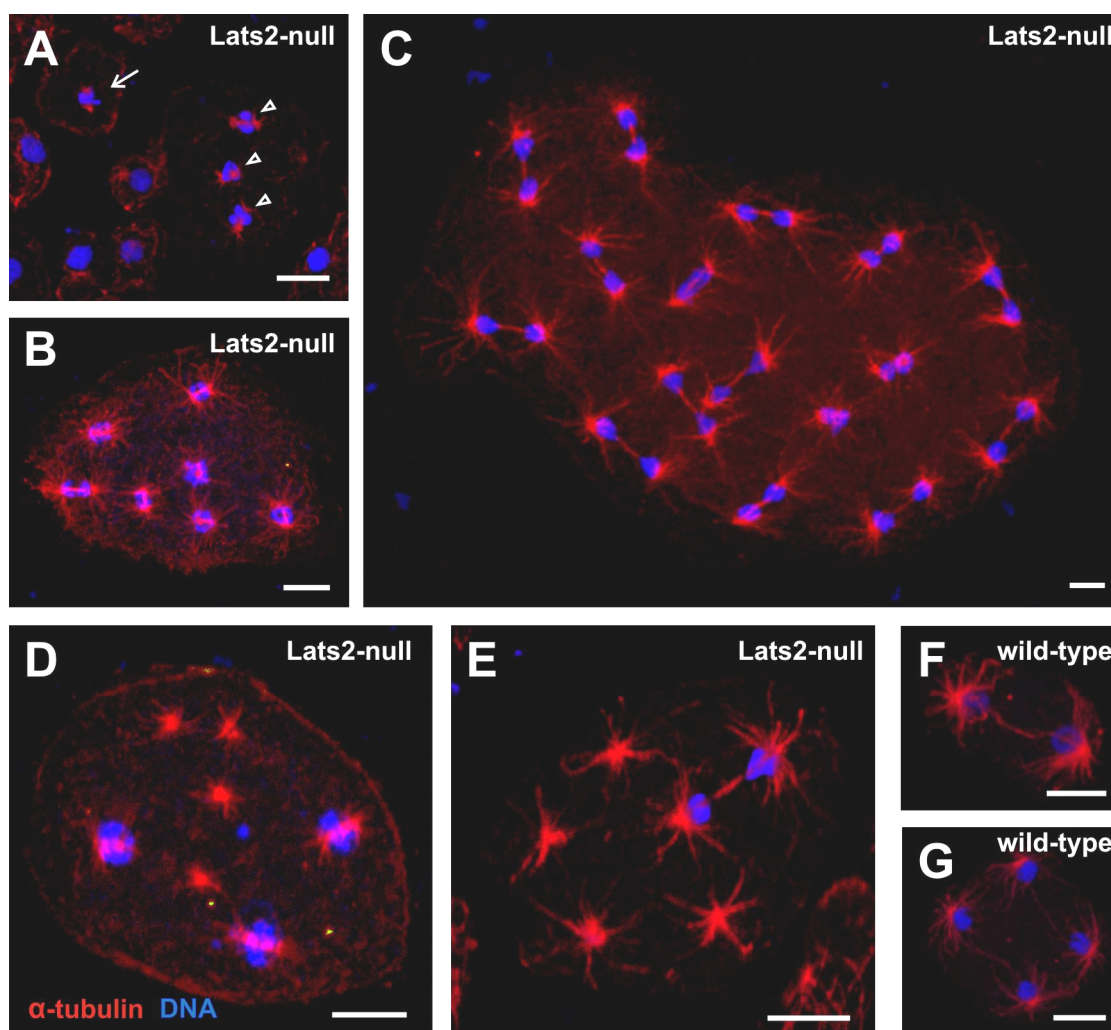
**Figure 39: Multinucleated Lats2-null cells during mitosis**

Lats2-null and wild-type cells were fixed and stained with monoclonal antibodies against anti-α-tubulin to visualize mitotic spindles, and TO-PRO-3 for DNA. (**A**-**C**) Recordings of Lats2-null cells by confocal laser scanning microscopy, carrying 1 (Arrow in A), 3 (Arrowheads in A), 7 (B), or 16 (C) mitotic spindles. The formation of spindles and mitosis occurs in a concerted manner. (**D**,**E**) Confocal images showing enlarged Lats2-null cells carrying aberrant numbers of centrosomes. The accomplishment of mitosis is not affected in cells carrying excess numbers of centrosomes. (**F**,**G**) Formation of mitotic spindles in wild-type cells carrying one or two spindles. Bars = 5 µm.

3.4.7 Identification of Ras GTPases as Lats2 interactors

In an approach to identify novel interactors of small GTPases of the Ras family, the laboratory of Prof. Gerald Weeks (UBC, Vancouver, Canada) used different *Dictyostelium* Ras GTPases as bait in yeast-two-hybrid screens. By this approach Lats2 was identified as a strong interactor of RasG (DDB0201663) and Rap1 (DDB0216229). The Ras binding domain RBD of Lats2 was mapped genetically between amino acid residues 107 and 284,

and represented the shortest fragment of Lats2 that was able to interact with Ras GTPases in yeast-two-hybrid assays (Figure 40A). The sequence of the newly identified Lats2 RBD does not share significant identities with other Ras binding domains. For investigating the interaction in detail, the Ras binding domain RBD of Lats2 was amplified by PCR and cloned into a GST-expression vector.

The 22.3 kDa Ras GTPase RasB (DDB0201661) encoded by *rasB* (DDB_G0292998), and the 21.3 kDa RasG encoded by *rasG* (DDB_G0293434) were amplified from cDNA and tagged with GFP for expression in *Dictyostelium* cells. Pull-down assays were performed using GST-Lats2-RBD bound sepharose with lysates of *Dictyostelium* cells expressing GFP-tagged RasB and RasG. Lysates as well as eluates and controls were
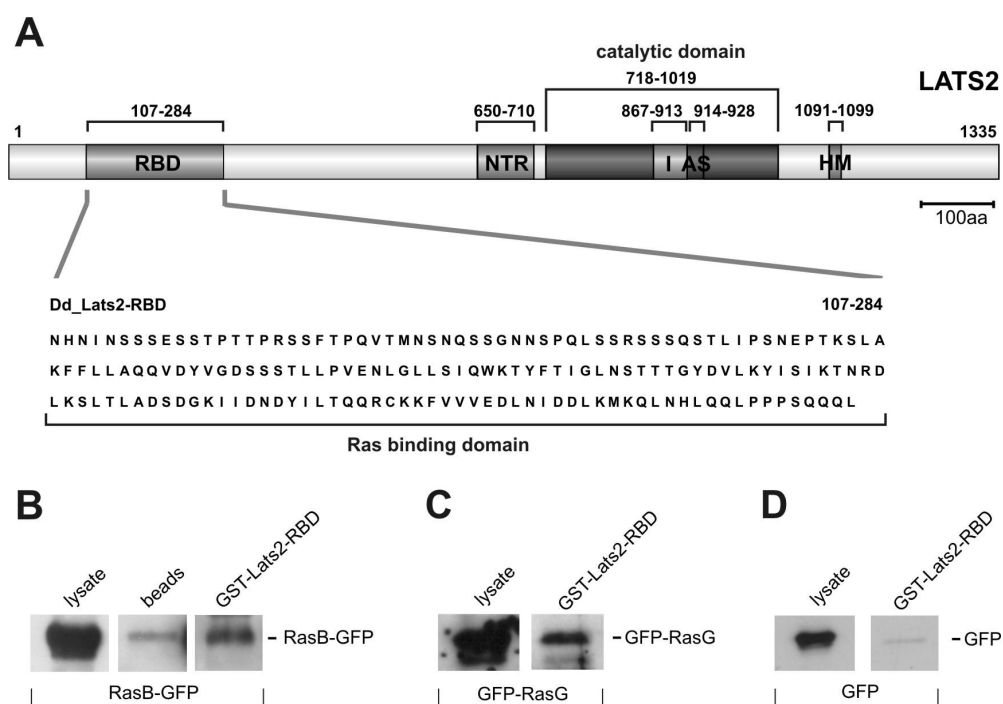
Figure 40: Binding of GFP-tagged Ras to the Lats2-RBD

Analysis of binding of GFP-tagged RasB and RasG to the Lats2-RBD. (**A**) Sequence of the Ras binding domain of Lats2 determined by yeast-two-hybrid assays. (B-D) The RBD of Lats2 was expressed as GST-fusion protein and bound to glutathione-sepharose. The supernatant of pelleted lysates of wild-type cells expressing RasB-GFP, GFP-RasG or the control GFP were incubated with GST-Lats2-RBD-bound sepharose. (**B**) Eluates were separated by SDS-PAGE. Western blot analysis using anti-GFP antibodies reveals that RasB binds the RBD of Lats2 *in vitro*. The lysate is shown on the left. For control, beads without GST-protein were used (middle lane). (**C**) GFP-tagged RasG expressed in wild-type cells interacts with the GST-Lats2-RBD. The levels of bound RasG were detected by Western-blotting using anti-GFP antibodies. (**D**) For control, lysate of GFP expressing wild-type cells was pulled down with GST-Lats2-RBD. For both experiments (C, D), lysates are shown on the left, eluates on the right.

separated by SDS gel electrophoresis and subjected to Western-blot analysis using monoclonal antibodies directed against GFP. RasB tagged with GFP was found to interact with the Lats2-RBD (Figure 40B) and the interaction of GFP-RasG with the GST-Lats2-RBD was also shown (Figure 40C). As control, *Dictyostelium* cells expressing GFP were incubated with GST-Lats2-RBD coupled sepharose (Figure 40D). The finding that Lats2 interacts with GFP-tagged Ras GTPases was confirmed by pull-down assays performed by the laboratory of Prof. Weeks using lysates of wild-type cells with the GST-Lats2-RBD. Bound Ras was detected by Western blot analysis using specific polyclonal antibodies directed against RasB, RasG and Rap1 (Daniel et al., 1994; Khosla et al., 2000; Seastone et al., 1999). Thereby the interaction of the Lats2-RBD with RasB and RasG was confirmed by an independent approach and the interaction with Rap1 (21.0 kDa) found by the yeast-two-hybrid assay was confirmed (Figure 41A, first lane).

3.4.8 Increased levels of GTP-bound Ras in the absence of Lats2

The question whether Lats2 is involved in the regulation of Ras GTPases was addressed by investigation of the levels of activated RasB, RasG and Rap1 in Lats2-null cells. Therefore the amount of GTP-bound Ras GTPases was determined for wild-type and Lats2-null cells by applying an indirect reporter assay using the RBD of *S. pombe* Byr2 (Kae et al., 2004). Only GTP-bound Ras is able to bind the Byr2-RBD, thus the amount of Ras detected in Byr2-RBD pull-down experiments represents the amount of activated Ras in the cell lysate. The eluates of pull-down experiments were subjected to Western blot analysis applying specific polyclonal antibodies for RasB, RasG and Rap1. In the absence of Lats2, the levels of activated RasB and RasG are increased compared to wild-type cells, whereas the amount of activated Rap1 is not affected (Figure 41A, lanes 2-5). Since the levels of activated RasB and RasG were elevated in Lats2-null cells, it was investigated whether the expression of constitutively activated RasB or the deletion of RasG affects the amounts of activated endogenous RasB, RasG or Rap1. The levels of RasB, RasG and Rap1 were determined by binding to the RBD of *S. pombe* Byr2 in pull-down assays and eluates were analyzed Western blot analysis performed in the laboratory of Prof. Weeks. The levels of activated GTP-bound RasB were observed to be highly increased in RasG-null cells. Corresponding, the amount of activated GTP-RasG is elevated in wild-type cells expressing GFP-RasB or constitutively active GFP-RasB-G12T, whereas the levels of Rap1 did not change significantly for the tested cell lines (Figure 41B).
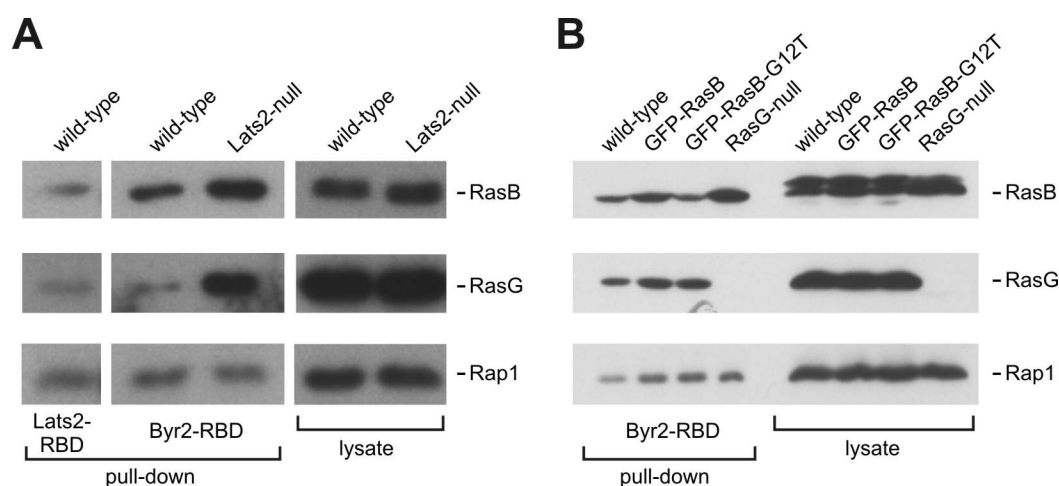
Figure 41: Levels of activated Ras proteins in wild-type, Lats2-null and Ras mutant strains

Analysis of the binding of GTP-bound Ras to the RBD of Lats2 and the levels of activated Ras in different cell-lines. Pull-down assays using the GST-tagged RBD of Lats2 or *S. pombe* Byr2 coupled glutathione-sepharose with lysates of *Dictyostelium* cells were separated by SDS gel-electrophoresis and were subjected to Western blot analysis using specific antibodies against RasB, RasG, or Rap1. For control, lysates are shown. (**A**) Ras binding of the GST-tagged Lats2-RBD was tested for lysates of wild-type cells (first lane). The binding of RasB, RasG and Rap1 from lysates of wild-type and Lats2-null cells to the GST-tagged Byr2-RBD is shown (lanes 2 and 3). As control, the levels of RasB, RasG and Rap1 in lyates of wild-type and Lats2-null cells are shown. (**B**) The levels of activated RasB, RasG and Rap1, binding the Byr2-RBD, were determined for wild-type cells, wild-type cells expressing GFP-RasB or GFP-RasB-G12T and RasG-null cells.

3.4.9 RasB and RasG localize to the cell cortex

In order to determine whether the state of activation has an influence on the localization of *Dictyostelium* Ras GTPases, the localization of GFP-tagged Ras proteins was observed. *Dictyostelium* RasG (Sasaki et al., 2004) and Rap1 were reported to localize to the cell cortex (Jeon et al., 2007). Addressing the question, where the Lats2-interactor RasB is localizing in living *Dictyostelium* cells, the localization of the GFP-tagged Ras GTPases RasB and RasG was observed by live-cell microscopy. Live-cell laser scanning microscopy of wild-type cells expressing GFP-RasB revealed that GFP-RasB localizes to the cell-cortex (Figure 42A). Wild-type AX2 cells expressing GFP-RasG also localized to the cell-cortex (Figure 42B). The expression of GFP-RasB or GFP-RasG does not cause obvious phenotypic changes in wild-type.

The next step was to observe the localization of activated RasB and RasG. Therefore an amino acid exchange of the conserved amino acid residue 12 from glycine to threonine was performed for RasB and RasG. These constitutively active forms are unable to
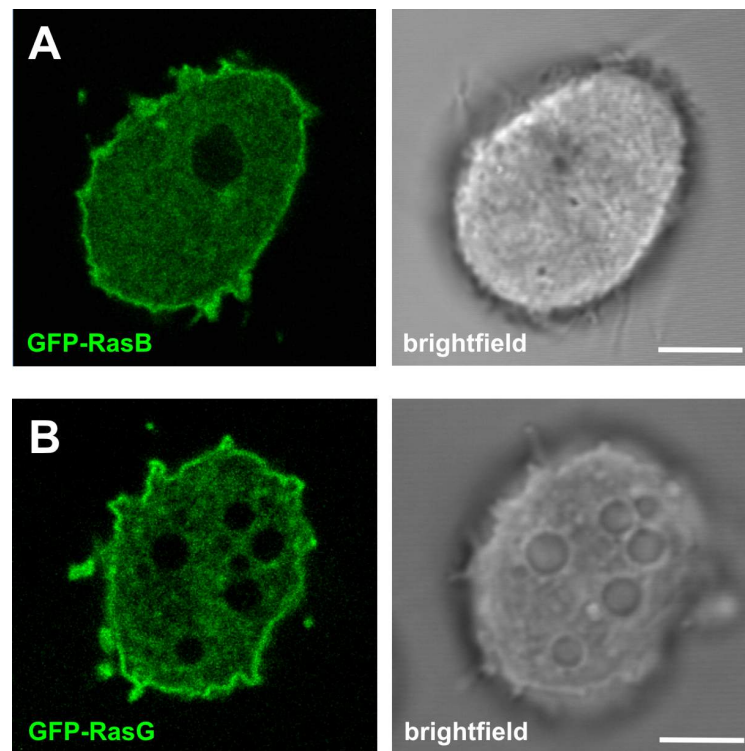
Figure 42: Localization of GFP-RasB and GFP-RasG

Confocal live-cell recordings of GFP-tagged RasB (**A**) and RasG (**B**) expressing *Dictyostelium* cells. The GFP-fluorescence is shown on the left, brightfield on the right. GFP-RasB and GFP-RasG localize to the cell-cortex. Bars = 5 μm.

hydrolyze GTP to GDP. It was observed that GFP-RasB-G12T expressed in wild-type cells localizes to the plasma-membrane (Figure 43A) and exhibits a phenotype of large multinucleated cells, probably caused by a severe cytokinesis/mitosis defect, similar to the findings reported for the overexpression of RasB-G12T (Sutherland et al., 2001). Moreover, expression of GFP-RasB-G12T causes an increased number of filopodia. Traction-mediated cytofission was observed frequently as described for Lats2-null cells (Figure 43B). The GFP-tagged activated form GFP-RasG-G12T also localizes to the plasma-membrane of wild-type cells (Figure 43C). Whereas expression of GFP-RasB-G12T caused the formation of larger cells, GFP-RasG-G12T expression did not affect cell size.
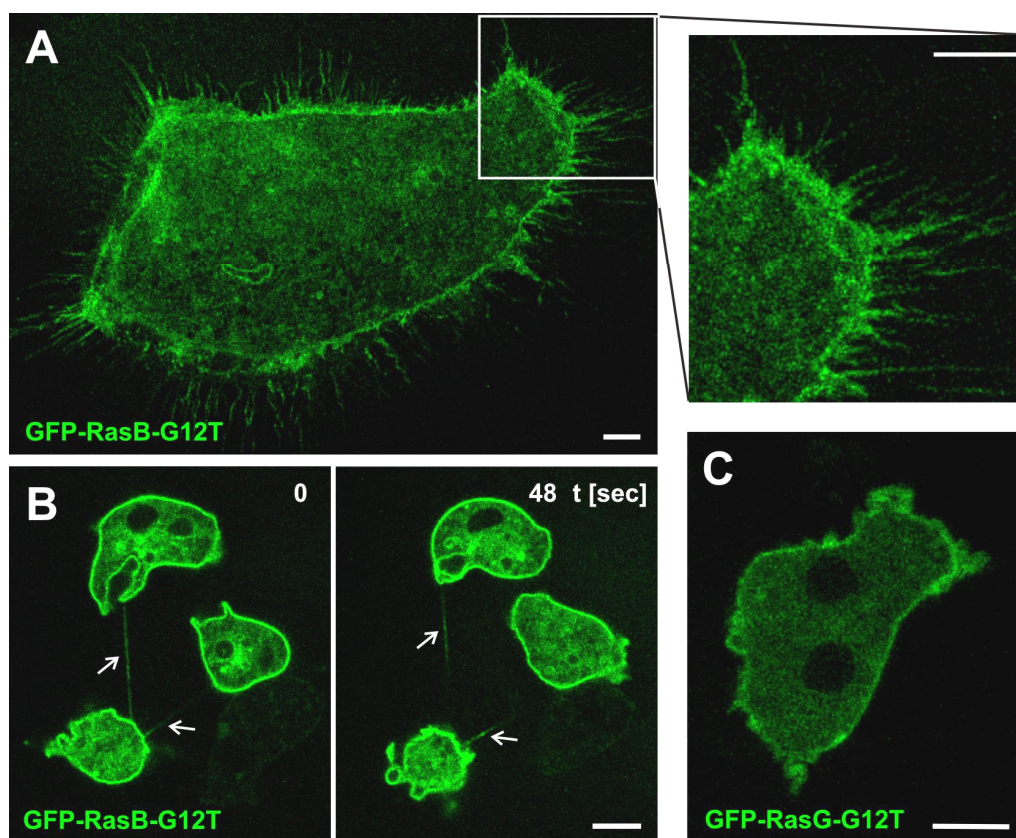
Figure 43: Localization of the activated forms of RasB and RasG

Live-cell imaging of *Dictyostelium* cells expressing GFP-tagged constitutively active RasB and RasG. (**A**) Recording of a GFP-RasB-G12T expressing *Dictyostelium* cell. As shown for GFP-RasB, constitutively active RasB also localizes to the cell-cortex. Moreover, it causes large cells as well as elongated filopodia, shown in the enlarged inset on the right. (**B**) Recording of GFP-RasB-G12T cells performing cytofission; arrows indicate cytoplasmic bridges. (**C**) GFP-RasG-G12T is enriched at the cortex of wild-type cells. The expression of constitutively activated RasG does not affect cell size. Bars = 5 µm.

3.4.10 Localization of Lats2-domains

To investigate whether the patterns of localization of Lats2 and its interactors RasB and RasG coincide, the localization of subdomains of Lats2 was studied. Attempts to clone the full-length *ndrC* gene were not successful, which can probably be explained by rejection of the ligated construct by *E. coli* due to the nucleotide composition of the *ndrC* coding sequence. Therefore the regions covering amino acid residues 2-300 harboring the Ras binding domain RBD and amino acid residues 435-1335 comprising the N-terminal regulatory domain, the catalytic domain as well as the hydrophobic motif were amplified by PCR and tagged to GFP as depicted in a model of constructs (Figure 44A). Wild-type
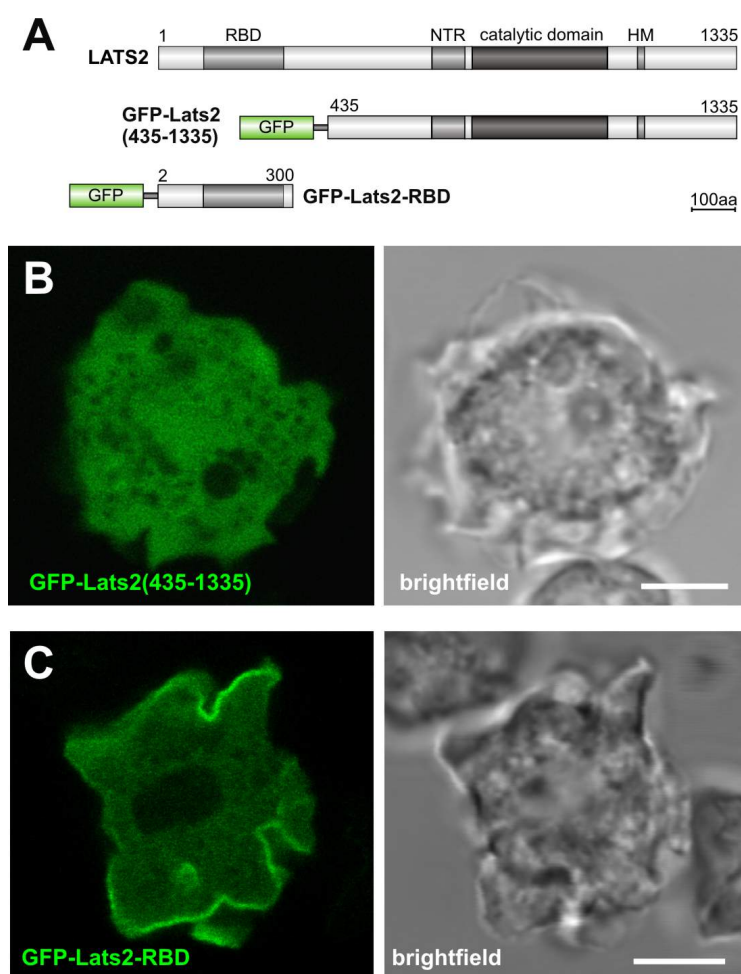
Figure 44: Localization of domains of Lats2

(**A**) Schematic view of the GFP-tagged fragments of amino acid residues 2-300 and 435-1335 of Lats2 expressed in *Dictyostelium* cells. (**B**) Confocal recording of living wild-type cells expressing GFP-Lats2(435-1335), comprising the catalytic domain and lacking the N-terminal RBD, reveals an overall cytoplasmic localization. GFP-fluorescence is shown in the left, brightfield in the right image. (**C**) Live-cell imaging reveals that the GFP-tagged Lats2-RBD localizes to the cell cortex of *Dictyostelium* cells. Bars = 5 µm.

cells were transformed with constructs for the expression of the GFP-Lats2-RBD and GFP-Lats2(435-1335). Expression of GFP-tagged Lats2(435-1335) lacking the Ras binding domain revealed exclusively cytoplasmic localization, analyzed by live-cell confocal laser scanning microscopy (Figure 44B). Live-cell analysis of GFP-Lats2-RBD expressing *Dictyostelium* cells showed the localization of the Lats2 Ras binding domain to the cell-cortex (Figure 44C). The recruitment of GFP-Lats2-RBD is probably caused by Ras GTPases, localizing to the plasma-membrane. The separate expressions of GFP-Lats2-RBD and GFP-Lats2(435-1335) do not cause phenotypic changes.

3.4.11 Lats2 interacts with the RasGAP NF1

With the aim of identifying further interactors of Lats2, pull-down assays using the GST-tagged Lats2-RBD were performed. Lysate of wild-type cells was incubated together with GST-Lats2-RBD coupled glutathione-sepharose in presence of the protein crosslinker DSP. Eluates were separated by SDS gel-electrophoresis, and specific colloidal stained bands were cut out and analyzed by MALDI mass spectrometry. Peptides corresponding to the RasGAP NF1 (DDB0233763), the elongation factor EF1b (DDB0191174) and GST (DDB0305661, DDB0305662) were detected (Figure 47A). For control glutathione-sepharose without coupled GST-Lats2-RBD was used (Figure 45B). The binding of EF1b is a common artefact of protein binding assays using *Dictyostelium* lysate, and the presence of GST can be explained by binding to the unsaturated glutathione-sepharose, as observed in the control (Figure 45B).
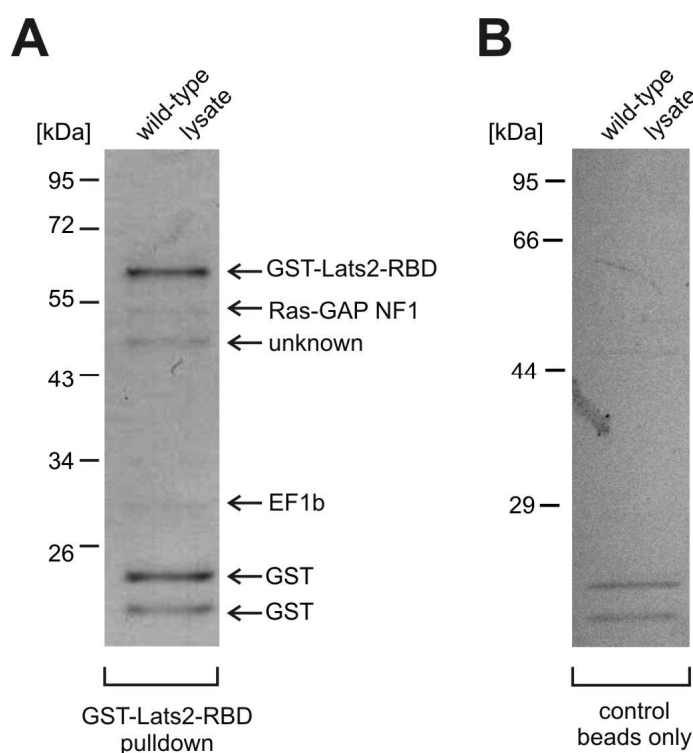
Figure 45: Identification of putative Lats2 interactors

Pull-down experiment employing GST-Lats2-RBD to identify potential interactors. Eluates of the GST-Lats2-RBD coupled to glutathione-sepharose, incubated with wild-type lysate were separated by SDS-PAGE, stained with Coomassie and analyzed by MALDI mass spectrometry. Identified proteins are indicated on the right. (**A**) Proteins interacting with purified GST-Lats2-RBD fusion protein. Lats2 interacts with the endogenous Ras GTPase activating protein (Ras-GAP) NF1. (**B**) Pull-down of glutathione-sepharose with wild-type cell lysate.

The identified peptides which represent the 104.0 kDa RasGAP NF1 cover a region from amino acid residues 54 to 532. This region has a predicted molecular mass of 53.1 kDa, corresponding to the size of the colloidal stained band analyzed by mass spectrometry. Neurofibromin1 (NF1; *nfaA*), the *Dictyostelium* homolog of human neurofibromin1, a Ras GTPase activating protein is involved in the regulation of cytokinesis. Loss of *Dictyostelium* NF1 results in enlarged multinucleate cells (Zhang et al., 2008).

4 Discussion

NDR/LATS kinases are important signaling components involved in the regulation of cell cycle progression and morphology (Hergovich et al., 2006). The major goal of this study was the characterization of NDR/LATS kinases in *Dictyostelium*. The genome of *Dictyostelium* encodes four NDR family kinases (NdrA, NdrB, Lats1 and Lats2). Two of which correspond to the NDR-related kinases (NdrA and NdrB), the two others (Lats1 and Lats2) were considered as LATS-related. This classification corresponds to the one described for human NDR/LATS kinases and only few organisms besides were described to have a similar distribution of NDR/LATS kinases as mammals. While *D. melanogaster* comprises one LATS-related kinase (Warts) and a single NDR-related homolog, Trc, the NDR/LATS kinases of the yeasts can not be specified as NDR- or LATS-related. The phylogeny of NDR/LATS kinases in *Dictyostelium* is not well established yet and will be subject to change within the next years.

Dictyostelium NdrA/B, Lats1 and 2 share all characteristic features specific for NDR/LATS kinases including a Mob1-binding site in the N-terminal region, a conserved activation sequence within the catalytic domain, and a conserved phosphorylation site within the C-terminal hydrophobic motif; Lats1 does not share the regulatory phosphorylation site within the hydrophobic motif. One result of this study is that besides these conserved features characteristic for NDR/LATS kinases, Lats2 was shown to harbor a Ras binding domain.

4.1 NdrA is controlling efficient phagocytosis

The characterization of the NdrA kinase in *Dictyostelium* revealed that this NDR-related kinase is involved in regulating the uptake of particles by phagocytosis and localizes to centrosomes in interphase cells but detaches during mitosis.

The human kinases NDR1 and 2 were shown to play a role in centrosome duplication and their depletion caused failures in centrosome integrity (Hergovich et al., 2007). The analysis of the NdrA-null mutant revealed that NdrA, though localizing to centrosomes, is neither involved in centrosome stability nor in cytokinesis in *Dictyostelium*. NdrA is also not required for the development from the single cell to the multicellular stage. The detailed analysis of NdrA-deficient cells revealed that NdrA is triggering proper

phagocytosis. Cells lacking NdrA are impaired in growth on bacteria and show a reduced phagocytosis rate in combination with a retarded engulfment of large particles while fluid phase uptake is similar to wild-type. The formation of a phagocytic cup requires cytoskeletal rearrangements that have been studied in detail in *Dictyostelium* (Janssen and Schleicher, 2001; Konzok et al., 1999; Maniak et al., 1995) as well as membrane remodeling at the phagocytic cup. Furthermore, lipid vesicle trafficking towards the sites of phagocytic uptake provides supplies of membrane (Swanson, 2008). One possible explanation for the observed deficiencies of NdrA-mutant cells in phagocytosis could be that for the engulfment of larger particles like yeast cells, membrane constituents supplied by endocytic vesicles that fuse at sites of phagocytic cup formation are required for efficient internalization. Such a mechanism has been suggested already earlier based on the observation that marked changes occur in the membrane composition prior to the completion of phagocytosis, which was also dependent on the size of particles being ingested (Lee et al., 2007). The membrane of a phagocytic cup is extensively remodeled during the internalization of large but not small particles (Lee et al., 2007; Swanson, 2008). The source of the extra membrane is most likely contributed by intracellular compartments, either recycling endosomes (Bajno et al., 2000; Czibener et al., 2006) or the endoplasmic reticulum (Gagnon et al., 2002). Disturbances of the supply via endomembranes would result in decreased rates of uptake and prolonged internalization times. This mechanistic view would be in agreement with the observed phenotype of NdrA-null cells, an impairment of phagocytosis while pinocytosis is essentially unaffected.

Members of the NDR/LATS kinase family from yeast to human bind Mob1 coactivators which were reported to enhance kinase activity. The *in vitro* analysis of Mob1 binding revealed an interaction of NdrA with MobA and MobB. This interaction is independent of phosphorylation by upstream Ste20-like kinases, and the binding of MobA and MobB to NdrA and to the phosphomimetic mutant NdrA-T497E was comparable. In accordance with these findings is that the gene expression profiles (Rot et al., 2009) observed for NdrA, MobA and MobB are similar. MobC is expressed only at very low levels and therefore was not included in the initial characterization of Mob1 protein binding activity.

NdrA localizes to centrosomes, and thus it is tempting to speculate that NdrA acts through activation of a downstream component, not at the site of phagocytic cup formation but in vicinity to centrosomes. Proteomic analyses of *Dictyostelium* phagosomes (Gotthardt et al., 2006) did not identify NdrA as centrosomal protein. One possible downstream effector could be EmpC or another protein forming a complex with EmpC. The identification of

EmpC as a potential target of NdrA also suggests a possible link to endocytic transport. EmpC as a member of the emp24/gp25/p24 family is a late endocytic intermediate component and involved in trafficking between the endoplasmic reticulum and the Golgi apparatus (Blum et al., 1996). In this study it was shown that *Dictyostelium* EmpC-GFP localizes to a compartment in the pericentrosomal region. The pericentrosomal compartment could correspond to either the Golgi apparatus or an endocytic compartment with features reminiscent of recycling endosomes that has been described earlier for *Dictyostelium* (Charette et al., 2006). However, co-localization experiments showed that the EmpC-containing structures are different from the recycling endosomes characterized by p25. Thus it is more likely that EmpC-GFP-labeled structures are related to the Golgi apparatus and shuttling vesicles. Immunofluorescence deconvolution analysis showed that NdrA localizes to the corona of centrosomes. At the onset of mitosis the centrosomal corona dissociates (Gräf et al., 2004); this is accompanied by the dispersal of the Golgi apparatus and may provide an explanation for the absence of NdrA at mitotic spindle poles.

Based on the findings resulting from the phenotypic analysis of NdrA-null cells and the potential link to vesicle trafficking, a hypothetical model for the function of NdrA is
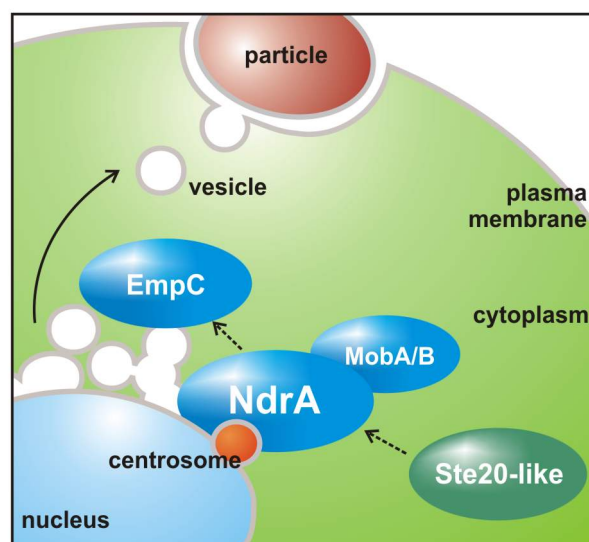
Figure 46: Hypothetical model for the function of NdrA

NdrA localizes to the centrosome and is thought to be activated by an upstream Ste20-like kinase. Probably, the activity of NdrA is regulated by binding to a Mob1 protein (MobA/B). NdrA directly or indirectly regulates EmpC, which is involved in the formation of transport vesicles and vesicular trafficking. These vesicles are supposed to shuttle towards the plasma membrane providing a reservoir of membrane constituents and thus assist in the formation of phagocytic cups.

proposed (Figure 46). NdrA localizes to the corona of centrosomes and thus in close proximity to the Golgi apparatus. NdrA interacts with a Mob1 protein (MobA/B) and is likely to be activated by an upstream Ste20-like kinase. Most likely NdrA activates EmpC in the pericentrosomal region either directly, or indirectly through another member of the EmpC-containing complex, which is essential for the formation of transport vesicles. These vesicles are supposed to shuttle towards the plasma membrane providing a reservoir of membrane constituents and thus assist the formation of phagocytic cups.

In *S. cerevisiae* NDR/LATS kinases are involved in regulating secretion or cell growth by the so-called RAM (regulation of Ace2 activity and cellular morphogenesis) signaling network involving the NDR/LATS kinase Cbk1 (Dohrmann et al., 1996; Jansen et al., 2006). Cbk1 regulates growth via Golgi-dependent secretion by interfering with Sec2 and Sec4, two regulators of secretion (Kurischko et al., 2008). Moreover, mutants lacking the NDR/LATS kinase COT1 of *N. crassa* also exhibit growth defects and altered cell wall composition (Ziv et al., 2009).

In conclusion, the results obtained in the course of this study suggest that NdrA regulates phagocytosis through triggering processes that involve endosomal compartments or the Golgi apparatus that supply membranous material required for forming the phagocytic cup. NdrA is closely related to the NDR/LATS group kinases Cbk1 and COT1, which were shown previously to have also a role in secretion. Although these kinases act through specific interactions, the underlying mechanisms that regulate endocytic trafficking seem to be closely related.

4.2 The centrosomal kinase NdrB

The characterization of the NDR-related kinase NdrB in *Dictyostelium* revealed its distinct localization to the centrosome and the strong interaction of NdrB with MobB, a member of the Mob1 family of coactivators. NdrB is the closest homolog of NdrA and comprises all features that are characteristic for NDR/LATS kinases. GFP-NdrB is enriched at the centrosome during interphase. NdrB was found to be associated with the spindle throughout mitosis from prophase to telophase and is present at the spindle poles in cytokinesis. This is in contrast to the NdrA kinase that dissociates from the spindle during mitosis. Similar to NdrB, the human kinases NDR1 and 2 were detected at the spindle poles in the course of mitosis (Hergovich et al., 2007).

Centrosomes of *Dictyostelium* consist of a layered core structure, surrounded by the corona which nucleates microtubules (Schulz et al., 2009). The duplication of centrosomes is controlled by the Aurora kinase AurK, the Polo like kinase Plk1 (Li et al., 2008) and the NIMA-related kinase Nek2 (Gräf, 2002). A number of potential interactors of NdrB were described in the course of this study. NdrB was found to co-precipitate with the Aurora kinase AurK, which was described as a regulator of mitosis and functions at the spindle pole as well as the equatorial region (Li et al., 2008). Interestingly, the human NDR/LATS kinase LATS2 was also reported to be directly phosphorylated by Aurora-A (Toji et al., 2004). In addition to AurK, a regulator of cell cycle progression, Cdc40, and a cyclin domain containing protein (DDB0238773) precipitated together with NdrB, emhasizing a putative role of NdrB in the course of the cell cycle. However, proteomics analysis of highly abundant structural components of *Dictyostelium* centrosomes (Reinders et al., 2006) revealed that NdrA and NdrB are not present in the centrosomal core structure, indicating that both NDR/LATS kinases are rather centrosome associated proteins than structural constituents.

Members of the Mob1 family of coactivators are implicated in the regulation of NDR/LATS kinases (Hergovich et al., 2005). The strong interaction of NdrB with one of three Mob1 homologs in *Dictyostelium,* MobB, indicates the presence of a rather stable NdrB-MobB complex. In contrast, the affinity for Mob1 proteins bound to NdrA is much lower, as NdrA-Mob1 interactions could only be shown *in vitro*. Thus, it is very likely that Mob1 proteins have different binding preferencies for NDR/LATS kinases. Moreover, the described centrosomal enrichment of *Dictyostelium* MobA, and the cytoplasmic localization of MobB suggest spatial differences in the regulatory roles of Mob1 proteins. Very recent analyses uncovered a negative role for Mob2, a member of the human MOB family in the regulation of human NDR kinases (Kohler et al., 2010).

Both, NdrB and MobB were shown to coprecipitate with members of the PIPKc kinases (phosphatidylinositol phosphate kinases). The interaction with PI3Kc kinases suggests an involvement of the NdrB-MobB complex in processes requiring phosphoinositide phoshate turnover. In addition, pull-down experiments revealed that the Rho-GTPase RacE is a putative interactor of NdrB. NdrB is also capable of binding ElmoB, an ELMO family member. Activation of Rac small G proteins was reported to be mediated by ELMO family members during processes requiring remodeling of the actin cytoskeleton (Isik et al., 2008).

Another protein identified to interact with NdrB is the putative upstream activator KrsA, a *Dictyostelium* homolog of the human Ste20-like kinases MST1 and 2 (Arasada et al., 2006) that were reported to phosphorylate NDR/LATS kinases. In man, MST1 controls centrosome duplication by regulating NDR kinase activity (Hergovich et al., 2009). Due to the different interactors of NdrB and different binding affinities of NDR-related kinases and Mob1 proteins in *Dictyostelium*, highly complex regulatory mechanisms can be predicted that require more detailed investigation in the future.

Several attempts to generate NdrB knockout mutants in order to study the functional implications of NdrB were unsuccessful. In the course of this study it became clear that this inability was due to a duplication of the genomic region harboring the *ndrB* gene on chromosome 5 of the *Dictyostelium* AX2 wild-type strain that was used. DNA microarray analysis indicated that the *Dictyostelium* strains AX3 and AX4 are most likely not carrying this particular genomic duplication (Bloomfield et al., 2008) and should be used for the generation of an NdrB-null cells.

A model based on the findings resulting from the analysis of the localization and the interaction partners of NdrB is proposed (Figure 47) and serves as a basis for further
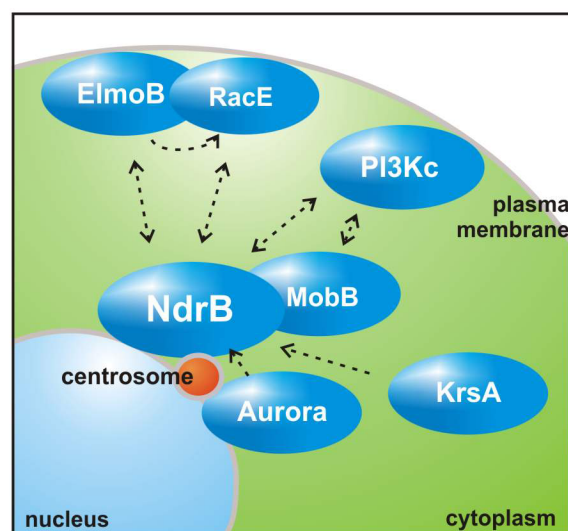
Figure 47: Model of putative NdrB interactions

The centrosomal kinase NdrB is bound to its coactivator MobB. NdrB is activated by the putative upstream regulators KrsA and/or the Aurora kinase. Due to the interaction of NdrB and MobB with the phosphoinositol phosphate kinases, the involvement of an NdrB/MobB complex in PI3Kc signaling is suggested. Putative targets of a signaling cascade could involve a regulator of actin dynamics like RacE and an ELMO family protein, suggesting a role of NdrB in the regulation of cytoskeletal processes.

studies. This model suggests that activation of the centrosomal kinase NdrB bound to its coactivator MobB is mediated by the putative upstream regulators like KrsA and/or the centrosomal Aurora kinase, a core component of mitosis signaling. Both, the interactions of NdrB and MobB with PI3Kc kinases, implicated in phospholipid turnover, as well as the binding of NdrB to the cytoskeletal regulator RacE and its putative activator ElmoB, suggest a role for NdrB in cell shape remodeling.

4.3 Regulation of cell division by Lats2 and Ras

The investigation of Lats2 revealed its essential role in the regulation of cytokinesis. Cells lacking Lats2 have a severe defect in division resulting in multinucleated cells and aberrant numbers of centrosomes. Data obtained in the course of this study proof that in addition to the conserved domains specifying NDR/LATS kinases, Lats2 carries a Ras binding domain RBD. This finding links the regulatory functions of the tumor suppressor homolog Lats2 to the growth promoting activities of the Ras oncogene homologs.

Lats2-null mutant cells are larger than wild-type and carry aberrant numbers of centrosomes. Mitosis of Lats2-null cells occurs in a concerted manner; moreover the presence of excess centrosomes does not affect the proceeding of mitosis. The distribution of nuclei, present in Lats2-null cells, peaks at numbers of 1, 2, 4 and 8 (Figure 35), which supports the observation of concerted mitosis in Lats2-null cells. These observations lead to the conclusion that Lats2 is not involved in the regulation of mitosis. Hence, Lats2 rather acts downstream of mitosis, than is involved in the regulation of mitosis.

In mammals aberrant numbers of nuclei and centrosomes are one of the major causes for tumorigenesis (Nigg, 2006). LATS tumor suppressors in human are responsible for the suppression of cellular alterations causing tumors (Hergovich and Hemmings, 2009). Similar phenotypes were observed for LATS2 knockout-mice (McPherson et al., 2004; Yabuta et al., 2007) or depletion of human NDR1/2 (Hergovich et al., 2008; Hergovich et al., 2007). The cell division defect caused by depletion of mammalian LATS1 was interpreted as disruption of the signaling cascade towards cytokinesis (Yang et al., 2004) and human LATS2 was shown to inhibit the G1/S transition (Li et al., 2003). Whereas loss of LATS2 severely affects the control of nuclear division, human LATS1 was reported to act as mitotic exit network kinase (Bothos et al., 2005) being responsible for the regulation

of the G2/M-arrest (Yang et al., 2001). Moreover, the *Drosophila* LATS-homolog Warts is implicated in the regulation of mitotic progression (Iida et al., 2004).

The interaction of *Dictyostelium* Lats2 with members of the Ras family of GTPases was revealed by yeast-two-hybrid experiments that were performed previously in the laboratory of Prof. Gerald Weeks (Weeks and Bolourani, unpublished). A Ras binding domain RBD was found to be located at the N-terminus of Lats2. Ras GTPases are monomeric proteins that act as molecular switches, changing between a GDP-bound inactive and a GTP-bound activated state. Guanine-nucleotide-exchange factors (GEFs) catalyze the exchange of GDP for GTP, thereby activating the GTPase. Inactivation of GTPases is regulated by GTPase activating proteins (GAPs) that stimulate the hydrolysis of bound GTP to GDP (Mitin et al., 2005). The region of Lats2 mapped for Ras binding is close to the N-terminus of Lats2 and comprises 177 amino acid residues. The investigation of the Ras binding capacity of the Lats2-RBD *in vitro* revealed an interaction with RasB, RasG and Rap1.

Deletion of Lats2 causes high levels of activated RasB and RasG, but not Rap1, indicating Lats2-dependent activation of RasB and RasG. Earlier investigations of *Dictyostelium* cells expressing constitutively active RasB (Sutherland et al., 2001) or lacking RasG (Tuxworth et al., 1997) revealed also multinucleate phenotypes, which were similar to the phenotype for Lats2-null cells. A similarity to the unchanged level of activated Rap1 in Lats2-null cells is that cell division was described not to be affected by loss or upregulation of Rap1 (Kang et al., 2002).

While the levels of activity for RasB and RasG were found to be elevated in Lats2-null cells, increased amounts of activated RasG were shown for *Dictyostelium* cells expressing constitutively active RasB. Vice versa, the level of activity of RasB is increased in RasG-null cells, suggesting an antagonistic tug-of-war mechanism for the activities of RasB and RasG. These observations are consistent with the observation that RasG-null cells exhibit increased levels of RasB protein (Khosla et al., 2000). RasB is activated by the RasGEF-Q, and its overexpression in the constitutively active form causes severe defects in cytokinesis (Mondal et al., 2008). Defects in cytokinesis also were observed before for the overexpression of constitutively activated RasB (Sutherland et al., 2001). In addition to the effect on cell division, Lats2-null cells exhibit enlarged nuclei, similar to the phenotypes of constitutively active RasB and RasGEF-Q. The loss of Lats2 does not affect the growth rates, as shown previously for the loss of RasG (Tuxworth et al., 1997) or the overexpression of constitutively active RasB (Sutherland et al., 2001). A possible

explanation for this effect could be mechanically assisted division of cells, known as traction-mediated cytofission, which may partially compensate for insufficient cytokinesis.

Mammalian Ras GTPases localize to membranous structures ranging from the cell-membrane to vesicular membranes, and endomembranes of the Golgi complex or the endoplasmic reticulum, and the association is mediated by farnesylation or palmitoylation (Hancock, 2003; Karnoub and Weinberg, 2008). Mammalian Ras is modified at a conserved C-terminal CAAX sequence. However, *Dictyostelium* Ras GTPases comprise only the conserved cysteine at the fourth from last C-terminal position. An interaction of small GTPases and members of the NDR/LATS kinases was already indicated in a previous study that showed indirectly, that the GTPase Cdc42 in *S. pombe* is responsible for recruiting the NDR/LATS kinase Orb6 to the plasma membrane (Das et al., 2009). In *Dictyostelium*, GFP-tagged RasB and RasG are recruited to the plasma membrane. By analyzing the role of Lats2-subdomains for the localization of Lats2 it turned out that the Ras binding domain is sufficient for membrane localization, whereas the protein lacking the RBD was enriched in the cytosol. Due to the membrane localization of *Dictyostelium* RasB, RasG and Rap1 (Jeon et al., 2007) and the *in vitro* interaction of the Lats2-RBD with RasB, RasG and Rap1, it is suggested that *in vivo* the RBD of Lats2 is recruited to the plasma membrane by members of the Ras family of GTPases.

The upregulation of RasB and RasG activity in the absence of Lats2 could either be caused by a RasGEF or a RasGAP, affecting both, RasB and RasG. In an attempt to determine interactors of Lats2 by pull-down experiments, the RasGAP NF1 was identified as a potential interactor of Lats2. NF1 in *Dictyostelium* is a close homolog of the human RasGAP Neurofibromin 1, also carrying the characteristic domain architecture harboring RasGAP, Sec14 and PH domains. Human NF1 has a central role in the regulation of Ras signaling (McGillicuddy et al., 2009). Inactivation of NF1 results in gliomagenesis, emphasizing its role as tumor suppressor. A recent study investigating the role of *Dictyostelium* NF1 in the regulation of Ras GTPases revealed its specific role for the regulation of RasB and RasG (Zhang et al., 2008). Deletion of NF1 coincides with decreased GTPase activity of RasB and RasG exclusively, causing highly prolonged activity of RasB and RasG upon stimulation, whereas RasC, RasD and Rap1 were unaffected by the loss of NF1 (Zhang et al., 2008). Moreover, deletion of NF1 in *Dictyostelium* exhibits severe defects in growth and cytokinesis. Whether the integrity of centrosome numbers of NF1-null cells is affected is unknown and of future interest. Whereas the RasGAP NF1 is implicated in the regulation of both, *Dictyostelium* RasB and
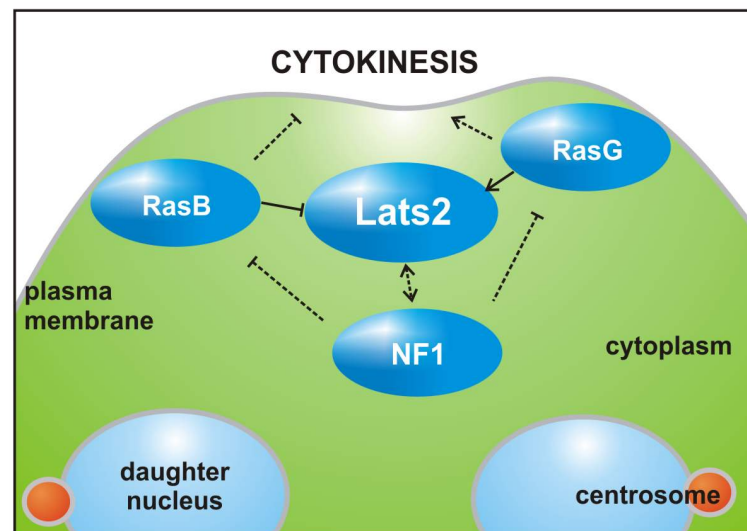
**Figure 48: Model for the regulation of cytokinesis by Lats2**

The model shows the putative regulation of cell division in *Dictyostelium* by the large tumor suppressor homolog Lats2. The activity of Lats2 is responsible for changing the state of activation of the key regulators RasB and RasG of the oncogenic class of Ras GTPases. Lats2 interacts with the Ras GTPase activating protein NF1 which inhibits the activity of RasB and RasG. It is assumed that RasB and RasG have antagonistic effects on Lats2 function as well as cytokinesis.

RasG, the RasGEFs for these Ras GTPases are different. RasB is specifically activated by RasGEF-Q (Mondal et al., 2008) and RasG by RasGEF-A (Sasaki et al., 2004). The specific regulation of the GTP exchange of RasB and RasG implicates a Lats2-dependent regulation of RasB- and RasG-activity by a common RasGAP as NF1. Recent analyses revealed that RasB can be linked to the function of myosin-II by enhancing myosin-II-phosphorylation through a myosin-II heavy chain kinase MHCK (Mondal et al., 2008). Deletion of myosin-II was shown to cause a severe defect in cell division (Manstein et al., 1989). Multinucleate cells were also described for the triple gene-knockout of the myosin-II upstream effectors MHCK-A/B/C (Yumura et al., 2005).

Based on the finding that cell division in *Dictyostelium* is regulated by the large tumor suppressor homolog Lats2, a hypothetical model for the regulation of Lats2 is proposed (Figure 48). The activity of Lats2 is influencing the levels of activation of the key regulators RasB and RasG of the oncogenic class of Ras GTPases. The role of Lats2 in the regulation of cytokinesis suggests a regulatory feedback loop together with the Ras GTPases RasB and RasG as well as the Ras GTPase activating protein NF1 which is implicated in having a role as tumor suppressor.

Lats2 is closely related to the human NDR/LATS group kinases LATS1 and LATS2, which were shown previously to be major regulators of cell division. It is tempting to speculate that the mammalian homologs of Lats2 are also regulated by Ras proteins and this will offer interesting aspects for future investigations.

A regulatory pathway similar to the *S. cerevisiae* "septation initiation network" and the *S. pombe* "mitotic exit network" has been described in *Dictyostelium* (Müller-Taubenberger, unpublished). At the end of these pathways in the two yeasts, NDR/LATS kinases are responsible for transducing the signal triggering cytokinesis to the cleavage site by yet undiscovered mechanisms. Due to the link from Lats2 to cytokinesis, one can speculate on regulation of cell division by a SIN-related pathway in *Dicyostelium* (Figure 49).The
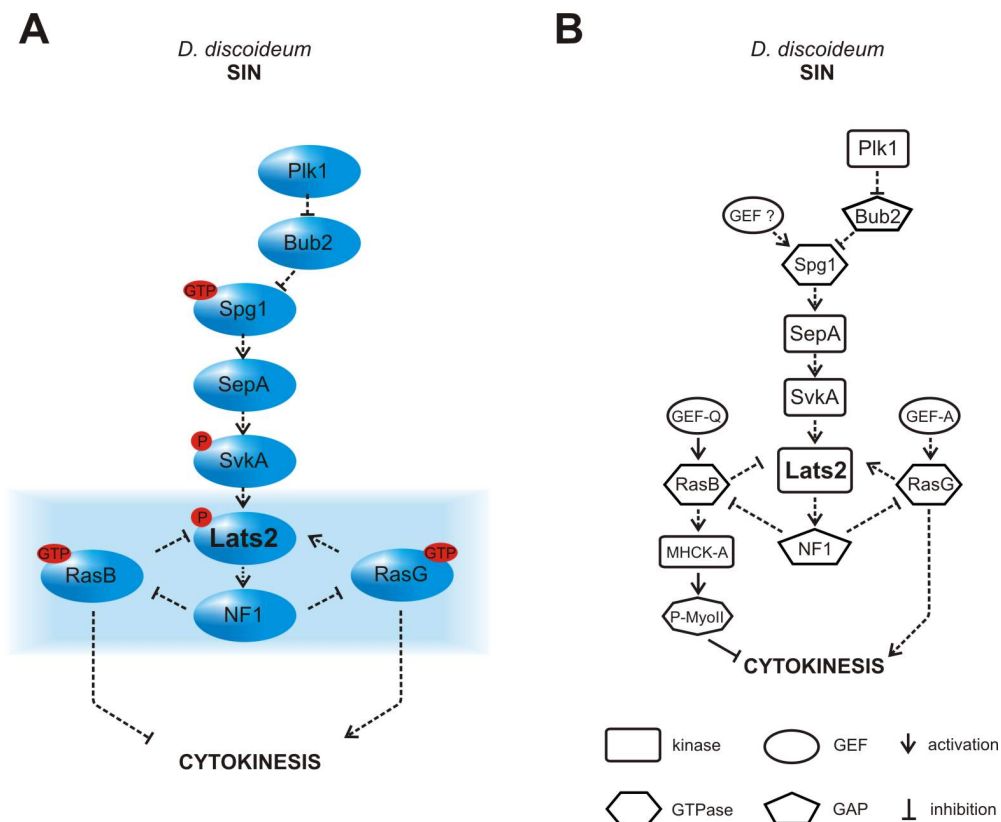
Figure 49: A SIN-related pathway in *Dictyostelium*

(**A**) The diagram shows the putative SIN-related signaling cascade in *Dictyostelium*. As in *S. cerevisiae* the Polo-like kinase Plk is supposed to trigger the GAP Bub2, which in turn regulates the activity of Spg1, its putative downstream GTPase (Müller-Taubenberger, unpublished). Spg1 is likely to be an effector of the kinase SepA. Knockout of SepA (Müller-Taubenberger et al., 2009) as well as the presumed downstream effector SvkA (Rohlfs et al., 2007) revealed a strong defect in cytokinesis as observed for Lats2-null cells. Cytokinesis is regulated by the Lats2-interactors RasB and RasG. (**B**) Depiction of a model for the regulation of cytokinesis for *Dictyostelium* showing the distinct roles of RasB and RasG (Mondal et al., 2008; Sasaki et al., 2004).

Ste20-like kinase SvkA has been investigated in detail and was shown to be crucial for cell division (Rohlfs et al., 2007). These observations suggest a downstream position of Lats2 due to its conserved Ste20-like kinase phosphorylation site. Regulation of cytokinesis by the Lats2-interators RasB and RasG indicates that Lats2 as well as the Ras GTPases RasB and RasG function at the end of the SIN signaling cascade.

5 References

Adeyinka, A., E. Emberley, Y. Niu, L. Snell, L.C. Murphy, H. Sowter, C.C. Wykoff, A.L. Harris, and P.H. Watson. 2002. Analysis of gene expression in ductal carcinoma in situ of the breast. *Clin Cancer Res*. 8:3788-95.

Altschul, S.F., W. Gish, W. Miller, E.W. Myers, and D.J. Lipman. 1990. Basic local alignment search tool. *J Mol Biol*. 215:403-10.

Arasada, R., H. Son, N. Ramalingam, L. Eichinger, M. Schleicher, and M. Rohlfs. 2006. Characterization of the Ste20-like kinase Krs1 of *Dictyostelium discoideum*. *Eur J Cell Biol*. 85:1059-68.

Avruch, J., R. Xavier, N. Bardeesy, X.F. Zhang, M. Praskova, D. Zhou, and F. Xia. 2009. Rassf family of tumor suppressor polypeptides. *J Biol Chem*. 284:11001-5.

Bajno, L., X.R. Peng, A.D. Schreiber, H.P. Moore, W.S. Trimble, and S. Grinstein. 2000. Focal exocytosis of VAMP3-containing vesicles at sites of phagosome formation. *J Cell Biol*. 149:697-706.

Bao, Y., K. Sumita, T. Kudo, K. Withanage, K. Nakagawa, M. Ikeda, K. Ohno, Y. Wang, and Y. Hata. 2009. Roles of mammalian sterile 20-like kinase 2-dependent phosphorylations of Mps one binder 1B in the activation of nuclear Dbf2-related kinases. *Genes Cells*. 14:1369-81.

Bardin, A.J., and A. Amon. 2001. Men and sin: what's the difference? *Nat Rev Mol Cell Biol*. 2:815-26.

Bichsel, S.J., R. Tamaskovic, M.R. Stegert, and B.A. Hemmings. 2004. Mechanism of activation of NDR (nuclear Dbf2-related) protein kinase by the hMOB1 protein. *J Biol Chem*. 279:35228-35.

Bloomfield, G., Y. Tanaka, J. Skelton, A. Ivens, and R.R. Kay. 2008. Widespread duplications in the genomes of laboratory stocks of *Dictyostelium discoideum*. *Genome Biol*. 9:R75.

Blum, R., P. Feick, M. Puype, J. Vandekerckhove, R. Klengel, W. Nastainczyk, and I. Schulz. 1996. Tmp21 and p24A, two type I proteins enriched in pancreatic microsomal membranes, are members of a protein family involved in vesicular trafficking. *J Biol Chem*. 271:17183-9.

Bothos, J., R.L. Tuttle, M. Ottey, F.C. Luca, and T.D. Halazonetis. 2005. Human LATS1 is a mitotic exit network kinase. *Cancer Res*. 65:6568-75.

Brefeld, O. 1869. *Dictyostelium mucoroides*. Ein neuer Organismus aus der Verwandtschaft der Myxomyceten. *Abhandlungen der Senckenbergischen Naturforschenden Gesellschaft*. 7:85-107.

Bretschneider, T., S. Diez, K. Anderson, J. Heuser, M. Clarke, A. Müller-Taubenberger, J. Köhler, and G. Gerisch. 2004. Dynamic actin patterns and Arp2/3 assembly at the substrate-attached surface of motile cells. *Curr Biol*. 14:1-10.

Chan, E.H., M. Nousiainen, R.B. Chalamalasetty, A. Schafer, E.A. Nigg, and H.H. Sillje. 2005. The Ste20-like kinase Mst2 activates the human large tumor suppressor kinase Lats1. *Oncogene*. 24:2076-86.

Charette, S.J., and P. Cosson. 2004. Preparation of genomic DNA from *Dictyostelium discoideum* for PCR analysis. *Biotechniques*. 36:574-5.

Charette, S.J., V. Mercanti, F. Letourneur, N. Bennett, and P. Cosson. 2006. A role for adaptor protein-3 complex in the organization of the endocytic pathway in *Dictyostelium*. *Traffic*. 7:1528-38.

Chisholm, R.L., P. Gaudet, E.M. Just, K.E. Pilcher, P. Fey, S.N. Merchant, and W.A. Kibbe. 2006. dictyBase, the model organism database for *Dictyostelium discoideum*. *Nucleic Acids Res*. 34:D423-7.

Clarke, M., L. Maddera, U. Engel, and G. Gerisch. 2010. Retrieval of the vacuolar H-ATPase from phagosomes revealed by live cell imaging. *PLoS One*. 5:e8585.

Clarke, M., A. Müller-Taubenberger, K.I. Anderson, U. Engel, and G. Gerisch. 2006. Mechanically induced actin-mediated rocketing of phagosomes. *Mol Biol Cell*. 17:4866-75.

Cornils, H., M.R. Stegert, A. Hergovich, D. Hynx, D. Schmitz, S. Dirnhofer, and B.A. Hemmings. 2010. Ablation of the kinase NDR1 predisposes mice to the development of T cell lymphoma. *Sci Signal*. 3:ra47.

Corpet, F. 1988. Multiple sequence alignment with hierarchical clustering. *Nucleic Acids Res*. 16:10881-90.

Czibener, C., N.M. Sherer, S.M. Becker, M. Pypaert, E. Hui, E.R. Chapman, W. Mothes, and N.W. Andrews. 2006. Ca2+ and synaptotagmin VII-dependent delivery of lysosomal membrane to nascent phagosomes. *J Cell Biol*. 174:997-1007.

Dagert, M., and S.D. Ehrlich. 1979. Prolonged incubation in calcium chloride improves the competence of *Escherichia coli* cells. *Gene*. 6:23-8.

Daniel, J., J. Bush, J. Cardelli, G.B. Spiegelman, and G. Weeks. 1994. Isolation of two novel ras genes in *Dictyostelium discoideum*; evidence for a complex, developmentally regulated ras gene subfamily. *Oncogene*. 9:501-8.

Das, M., D.J. Wiley, X. Chen, K. Shah, and F. Verde. 2009. The conserved NDR kinase Orb6 controls polarized cell growth by spatial regulation of the small GTPase Cdc42. *Curr Biol*. 19:1314-9.

de Hostos, E.L., B. Bradtke, F. Lottspeich, R. Guggenheim, and G. Gerisch. 1991. Coronin, an actin binding protein of *Dictyostelium discoideum* localized to cell surface projections, has sequence similarities to G protein beta subunits. *Embo J*. 10:4097-104.

de Hostos, E.L., C. Rehfuess, B. Bradtke, D.R. Waddell, R. Albrecht, J. Murphy, and G. Gerisch. 1993. *Dictyostelium* mutants lacking the cytoskeletal protein coronin are defective in cytokinesis and cell motility. *J Cell Biol*. 120:163-73.

Doherty, G.J., and H.T. McMahon. 2009. Mechanisms of endocytosis. *Annu Rev Biochem*. 78:857-902.

Dohrmann, P.R., W.P. Voth, and D.J. Stillman. 1996. Role of negative regulation in promoter specificity of the homologous transcriptional activators Ace2p and Swi5p. *Mol Cell Biol*. 16:1746-58.

Edgar, B.A. 2006. From cell structure to transcription: Hippo forges a new path. *Cell*. 124:267-73.

Effler, J.C., Y.S. Kee, J.M. Berk, M.N. Tran, P.A. Iglesias, and D.N. Robinson. 2006. Mitosis-specific mechanosensing and contractile-protein redistribution control cell shape. *Curr Biol*. 16:1962-7.

Eichinger, L., J.A. Pachebat, G. Glockner, M.A. Rajandream, R. Sucgang, M. Berriman, J. Song, R. Olsen, K. Szafranski, Q. Xu, B. Tunggal, S. Kummerfeld, M. Madera, B.A. Konfortov, F. Rivero, A.T. Bankier, R. Lehmann, N. Hamlin, R. Davies, P. Gaudet, P. Fey, K. Pilcher, G. Chen, D. Saunders, E. Sodergren, P. Davis, A. Kerhornou, X. Nie, N. Hall, C. Anjard, L. Hemphill, N. Bason, P. Farbrother, B. Desany, E. Just, T. Morio, R. Rost, C. Churcher, J. Cooper, S. Haydock, N. van Driessche, A. Cronin, I. Goodhead, D. Muzny, T. Mourier, A. Pain, M. Lu, D. Harper, R. Lindsay, H. Hauser, K. James, M. Quiles, M. Madan Babu, T. Saito, C. Buchrieser, A. Wardroper, M. Felder, M. Thangavelu, D. Johnson, A. Knights, H. Loulseged, K. Mungall, K. Oliver, C. Price, M.A. Quail, H. Urushihara, J. Hernandez, E. Rabbinowitsch, D. Steffen, M. Sanders, J. Ma, Y. Kohara, S. Sharp, M. Simmonds, S. Spiegler, A. Tivey, S. Sugano, B. White, D. Walker, J. Woodward, T. Winckler, Y. Tanaka, G. Shaulsky, M. Schleicher, G. Weinstock, A. Rosenthal, E.C. Cox, R.L. Chisholm, R. Gibbs, W.F. Loomis, M. Platzer, R.R. Kay, J. Williams, P.H. Dear, A.A. Noegel, B. Barrell, and A. Kuspa. 2005. The genome of the social amoeba *Dictyostelium discoideum*. *Nature*. 435:43-57.

Faix, J., L. Kreppel, G. Shaulsky, M. Schleicher, and A.R. Kimmel. 2004. A rapid and efficient method to generate multiple gene disruptions in *Dictyostelium discoideum* using a single selectable marker and the Cre-loxP system. *Nucleic Acids Res*. 32:e143.

Faix, J., M. Steinmetz, H. Boves, R.A. Kammerer, F. Lottspeich, U. Mintert, J. Murphy, A. Stock, U. Aebi, and G. Gerisch. 1996. Cortexillins, major determinants of cell shape and size, are actin-bundling proteins with a parallel coiled-coil tail. *Cell*. 86:631-42.

Gagnon, E., S. Duclos, C. Rondeau, E. Chevet, P.H. Cameron, O. Steele-Mortimer, J. Paiement, J.J. Bergeron, and M. Desjardins. 2002. Endoplasmic reticulum-mediated phagocytosis is a mechanism of entry into macrophages. *Cell*. 110:119-31.

Garin, J., R. Diez, S. Kieffer, J.F. Dermine, S. Duclos, E. Gagnon, R. Sadoul, C. Rondeau, and M. Desjardins. 2001. The phagosome proteome: insight into phagosome functions. *J Cell Biol*. 152:165-80.

Gerisch, G., J. Faix, J. Kohler, and A. Müller-Taubenberger. 2004. Actin-binding proteins required for reliable chromosome segregation in mitosis. *Cell Motil Cytoskeleton*. 57:18-25.

Gerisch, G., and A. Müller-Taubenberger. 2003. GFP-fusion proteins as fluorescent reporters to study organelle and cytoskeleton dynamics in chemotaxis and phagocytosis. *Methods Enzymol*. 361:320-37.

Glotzer, M. 1997. The mechanism and control of cytokinesis. *Curr Opin Cell Biol*. 9:815-23.

Glotzer, M. 2001. Animal cell cytokinesis. *Annu Rev Cell Dev Biol*. 17:351-86.

Goldberg, J.M., G. Manning, A. Liu, P. Fey, K.E. Pilcher, Y. Xu, and J.L. Smith. 2006. The *Dictyostelium* kinome - analysis of the protein kinases from a simple model organism. *PLoS Genet*. 2:e38.

Gotthardt, D., V. Blancheteau, A. Bosserhoff, T. Ruppert, M. Delorenzi, and T. Soldati. 2006. Proteomics fingerprinting of phagosome maturation and evidence for the role of a Galpha during uptake. *Mol Cell Proteomics*. 5:2228-43.

Gotthardt, D., H.J. Warnatz, O. Henschel, F. Bruckert, M. Schleicher, and T. Soldati. 2002. High-resolution dissection of phagosome maturation reveals distinct membrane trafficking phases. *Mol Biol Cell*. 13:3508-20.

Gräf, R. 2002. DdNek2, the first non-vertebrate homologue of human Nek2, is involved in the formation of microtubule-organizing centers. *J Cell Sci*. 115:1919-29.

Gräf, R., C. Daunderer, and M. Schliwa. 1999. Cell cycle-dependent localization of monoclonal antibodies raised against isolated *Dictyostelium centrosomes*. *Biol Cell*. 91:471-7.

Gräf, R., C. Daunderer, and M. Schliwa. 2000. *Dictyostelium* DdCP224 is a microtubule-associated protein and a permanent centrosomal resident involved in centrosome duplication. *J Cell Sci*. 113 (Pt 10):1747-58.

Gräf, R., C. Daunderer, and I. Schulz. 2004. Molecular and functional analysis of the *Dictyostelium* centrosome. *Int Rev Cytol*. 241:155-202.

Guerin, N.A., and D.A. Larochelle. 2002. A user's guide to restriction enzyme-mediated integration in *Dictyostelium*. *J Muscle Res Cell Motil*. 23:597-604.

Guertin, D.A., S. Trautmann, and D. McCollum. 2002. Cytokinesis in eukaryotes. *Microbiol Mol Biol Rev*. 66:155-78.

Hacker, U., R. Albrecht, and M. Maniak. 1997. Fluid-phase uptake by macropinocytosis in *Dictyostelium*. *J Cell Sci*. 110 (Pt 2):105-12.

Hancock, J.F. 2003. Ras proteins: different signals from different locations. *Nat Rev Mol Cell Biol*. 4:373-84.

Hanks, S.K., and T. Hunter. 1995. Protein kinases 6. The eukaryotic protein kinase superfamily: kinase (catalytic) domain structure and classification. *Faseb J*. 9:576-96.

He, Y., K. Emoto, X. Fang, N. Ren, X. Tian, Y.N. Jan, and P.N. Adler. 2005. *Drosophila* Mob family proteins interact with the related tricornered (Trc) and warts (Wts) kinases. *Mol Biol Cell*. 16:4139-52.

Hergovich, A., S.J. Bichsel, and B.A. Hemmings. 2005. Human NDR kinases are rapidly activated by MOB proteins through recruitment to the plasma membrane and phosphorylation. *Mol Cell Biol*. 25:8259-72.

Hergovich, A., H. Cornils, and B.A. Hemmings. 2008. Mammalian NDR protein kinases: from regulation to a role in centrosome duplication. *Biochim Biophys Acta*. 1784:3-15.

Hergovich, A., and B.A. Hemmings. 2009. Mammalian NDR/LATS protein kinases in hippo tumor suppressor signaling. *Biofactors*. 35:338-45.

Hergovich, A., R.S. Kohler, D. Schmitz, A. Vichalkovski, H. Cornils, and B.A. Hemmings. 2009. The MST1 and hMOB1 tumor suppressors control human centrosome duplication by regulating NDR kinase phosphorylation. *Curr Biol*. 19:1692-702.

Hergovich, A., S. Lamla, E.A. Nigg, and B.A. Hemmings. 2007. Centrosome-associated NDR kinase regulates centrosome duplication. *Mol Cell*. 25:625-34.

Hergovich, A., M.R. Stegert, D. Schmitz, and B.A. Hemmings. 2006. NDR kinases regulate essential cell processes from yeast to humans. *Nat Rev Mol Cell Biol*. 7:253-64.

Hirabayashi, S., K. Nakagawa, K. Sumita, S. Hidaka, T. Kawai, M. Ikeda, A. Kawata, K. Ohno, and Y. Hata. 2008. Threonine 74 of MOB1 is a putative key phosphorylation site by MST2 to form the scaffold to activate nuclear Dbf2-related kinase 1. *Oncogene*. 27:4281-92.

Hoeller, O., and R.R. Kay. 2007. Chemotaxis in the absence of PIP3 gradients. *Curr Biol*. 17:813-7.

Hou, M.C., D.A. Guertin, and D. McCollum. 2004. Initiation of cytokinesis is controlled through multiple modes of regulation of the Sid2p-Mob1p kinase complex. *Mol Cell Biol*. 24:3262-76.

Hou, M.C., J. Salek, and D. McCollum. 2000. Mob1p interacts with the Sid2p kinase and is required for cytokinesis in fission yeast. *Curr Biol*. 10:619-22.

Huang, J., S. Wu, J. Barrera, K. Matthews, and D. Pan. 2005. The Hippo signaling pathway coordinately regulates cell proliferation and apoptosis by inactivating Yorkie, the *Drosophila* Homolog of YAP. *Cell*. 122:421-34.

Huynh, K.K., J.G. Kay, J.L. Stow, and S. Grinstein. 2007. Fusion, fission, and secretion during phagocytosis. *Physiology (Bethesda)*. 22:366-72.

Iida, S., T. Hirota, T. Morisaki, T. Marumoto, T. Hara, S. Kuninaka, S. Honda, K. Kosai, M. Kawasuji, D.C. Pallas, and H. Saya. 2004. Tumor suppressor WARTS ensures genomic integrity by regulating both mitotic progression and G1 tetraploidy checkpoint function. *Oncogene*. 23:5266-74.

Isik, N., J.A. Brzostowski, and T. Jin. 2008. An Elmo-like protein associated with myosin II restricts spurious F-actin events to coordinate phagocytosis and chemotaxis. *Dev Cell*. 15:590-602.

Jansen, J.M., M.F. Barry, C.K. Yoo, and E.L. Weiss. 2006. Phosphoregulation of Cbk1 is critical for RAM network control of transcription and morphogenesis. *J Cell Biol*. 175:755-66.

Janssen, K.P., and M. Schleicher. 2001. *Dictyostelium discoideum*: a genetic model system for the study of professional phagocytes. Profilin, phosphoinositides and the lmp gene family in Dictyostelium. *Biochim Biophys Acta*. 1525:228-33.

Jeon, T.J., D.J. Lee, S. Merlot, G. Weeks, and R.A. Firtel. 2007. Rap1 controls cell adhesion and cell motility through the regulation of myosin II. *J Cell Biol*. 176:1021-33.

Kae, H., C.J. Lim, G.B. Spiegelman, and G. Weeks. 2004. Chemoattractant-induced Ras activation during *Dictyostelium* aggregation. *EMBO Rep*. 5:602-6.

Kaelin, W.G., Jr., W. Krek, W.R. Sellers, J.A. DeCaprio, F. Ajchenbaum, C.S. Fuchs, T. Chittenden, Y. Li, P.J. Farnham, M.A. Blanar, and et al. 1992. Expression cloning of a cDNA encoding a retinoblastoma-binding protein with E2F-like properties. *Cell*. 70:351-64.

Kang, R., H. Kae, H. Ip, G.B. Spiegelman, and G. Weeks. 2002. Evidence for a role for the *Dictyostelium* Rap1 in cell viability and the response to osmotic stress. *J Cell Sci*. 115:3675-82.

Karnoub, A.E., and R.A. Weinberg. 2008. Ras oncogenes: split personalities. *Nat Rev Mol Cell Biol*. 9:517-31.

Khosla, M., G.B. Spiegelman, R. Insall, and G. Weeks. 2000. Functional overlap of the *Dictyostelium* RasG, RasD and RasB proteins. *J Cell Sci*. 113 (Pt 8):1427-34.

Kohler, R.S., D. Schmitz, H. Cornils, B.A. Hemmings, and A. Hergovich. 2010. Differential NDR/LATS Interactions with the Human MOB Family Reveal a Negative Role for hMOB2 in the Regulation of Human NDR Kinases. *Mol Cell Biol*.

Konzok, A., I. Weber, E. Simmeth, U. Hacker, M. Maniak, and A. Müller-Taubenberger. 1999. DAip1, a *Dictyostelium* homologue of the yeast actin-interacting protein 1, is involved in endocytosis, cytokinesis, and motility. *J Cell Biol*. 146:453-64.

Kurischko, C., V.K. Kuravi, N. Wannissorn, P.A. Nazarov, M. Husain, C. Zhang, K.M. Shokat, J.M. McCaffery, and F.C. Luca. 2008. The yeast LATS/NDR kinase Cbk1 regulates growth via Golgi-dependent glycosylation and secretion. *Mol Biol Cell*. 19:5559-78.

Lee, W.L., D. Mason, A.D. Schreiber, and S. Grinstein. 2007. Quantitative analysis of membrane remodeling at the phagocytic cup. *Mol Biol Cell*. 18:2883-92.

Li, H., Q. Chen, M. Kaller, W. Nellen, R. Graf, and A. De Lozanne. 2008. *Dictyostelium* Aurora kinase has properties of both Aurora A and Aurora B kinases. *Eukaryot Cell*. 7:894-905.

Li, Y., J. Pei, H. Xia, H. Ke, H. Wang, and W. Tao. 2003. Lats2, a putative tumor suppressor, inhibits G1/S transition. *Oncogene*. 22:4398-405.

Lindmo, K., and H. Stenmark. 2006. Regulation of membrane traffic by phosphoinositide 3-kinases. *J Cell Sci*. 119:605-14.

Longin, A., C. Souchier, M. Ffrench, and P.A. Bryon. 1993. Comparison of anti-fading agents used in fluorescence microscopy: image analysis and laser confocal microscopy study. *J Histochem Cytochem*. 41:1833-40.

Mah, A.S., J. Jang, and R.J. Deshaies. 2001. Protein kinase Cdc15 activates the Dbf2-Mob1 kinase complex. *Proc Natl Acad Sci U S A*. 98:7325-30.

Maniak, M., R. Rauchenberger, R. Albrecht, J. Murphy, and G. Gerisch. 1995. Coronin involved in phagocytosis: dynamics of particle-induced relocalization visualized by a green fluorescent protein Tag. *Cell*. 83:915-24.

Manstein, D.J., M.A. Titus, A. De Lozanne, and J.A. Spudich. 1989. Gene replacement in *Dictyostelium*: generation of myosin null mutants. *Embo J*. 8:923-32.

McGillicuddy, L.T., J.A. Fromm, P.E. Hollstein, S. Kubek, R. Beroukhim, T. De Raedt, B.W. Johnson, S.M. Williams, P. Nghiemphu, L.M. Liau, T.F. Cloughesy, P.S. Mischel, A. Parret, J. Seiler, G. Moldenhauer, K. Scheffzek, A.O. Stemmer-Rachamimov, C.L. Sawyers, C. Brennan, L. Messiaen, I.K. Mellinghoff, and K. Cichowski. 2009. Proteasomal and genetic inactivation of the NF1 tumor suppressor in gliomagenesis. *Cancer Cell*. 16:44-54.

McPherson, J.P., L. Tamblyn, A. Elia, E. Migon, A. Shehabeldin, E. Matysiak-Zablocki, B. Lemmers, L. Salmena, A. Hakem, J. Fish, F. Kassam, J. Squire, B.G. Bruneau, M.P. Hande, and R. Hakem. 2004. Lats2/Kpm is required for embryonic development, proliferation control and genomic integrity. *Embo J*. 23:3677-88.

Mehta, S., and K.L. Gould. 2006. Identification of functional domains within the septation initiation network kinase, Cdc7. *J Biol Chem*. 281:9935-41.

Mitin, N., K.L. Rossman, and C.J. Der. 2005. Signaling interplay in Ras superfamily function. *Curr Biol*. 15:R563-74.

Mondal, S., D. Bakthavatsalam, P. Steimle, B. Gassen, F. Rivero, and A.A. Noegel. 2008. Linking Ras to myosin function: RasGEF Q, a *Dictyostelium* exchange factor for RasB, affects myosin II functions. *J Cell Biol*. 181:747-60.

Müller-Taubenberger, A., H.C. Ishikawa-Ankerhold, P.M. Kastner, E. Burghardt, and G. Gerisch. 2009. The STE group kinase SepA controls cleavage furrow formation in *Dictyostelium*. *Cell Motil Cytoskeleton*. 66:929-39.

Müller-Taubenberger, A., and M. Maniak. 2004. *Dictyostelium discoideum*: Cellular Slime Mold. *In* Encyclopedia of Molecular Cell Biology and Molecular Medicine. Vol. 3. R. Meyers, editor. Wiley-VCH. 343-349.

Müller-Taubenberger, A., M.J. Vos, A. Böttger, M. Lasi, F.P. Lai, M. Fischer, and K. Rottner. 2006. Monomeric red fluorescent protein variants used for imaging studies in different species. *Eur J Cell Biol*.

Nelson, B., C. Kurischko, J. Horecka, M. Mody, P. Nair, L. Pratt, A. Zougman, L.D. McBroom, T.R. Hughes, C. Boone, and F.C. Luca. 2003. RAM: a conserved signaling network that regulates Ace2p transcriptional activity and polarized morphogenesis. *Mol Biol Cell*. 14:3782-803.

Neujahr, R., C. Heizer, and G. Gerisch. 1997. Myosin II-independent processes in mitotic cells of *Dictyostelium discoideum*: redistribution of the nuclei, re-arrangement of the actin system and formation of the cleavage furrow. *J Cell Sci*. 110 (Pt 2):123-37.

Nigg, E.A. 2001. Mitotic kinases as regulators of cell division and its checkpoints. *Nat Rev Mol Cell Biol*. 2:21-32.

Nigg, E.A. 2006. Origins and consequences of centrosome aberrations in human cancers. *Int J Cancer*. 119:2717-23.

Noegel, A.A., R. Blau-Wasser, H. Sultana, R. Müller, L. Israel, M. Schleicher, H. Patel, and C.J. Weijer. 2004. The cyclase-associated protein CAP as regulator of cell polarity and cAMP signaling in *Dictyostelium*. *Mol Biol Cell*. 15:934-45.

Pearce, L.R., D. Komander, and D.R. Alessi. 2010. The nuts and bolts of AGC protein kinases. *Nat Rev Mol Cell Biol*. 11:9-22.

Ponchon, L., C. Dumas, A.V. Kajava, D. Fesquet, and A. Padilla. 2004. NMR solution structure of Mob1, a mitotic exit network protein and its interaction with an NDR kinase peptide. *J Mol Biol*. 337:167-82.

Rajagopalan, S., V. Wachtler, and M. Balasubramanian. 2003. Cytokinesis in fission yeast: a story of rings, rafts and walls. *Trends Genet*. 19:403-8.

Raper, K.B. 1935. *Dictyostelium discoideum*, a new species of slime mold from decaying forest leaves. *Journal Agricultural Research*. 50:135-148.

Ravanel, K., B. de Chassey, S. Cornillon, M. Benghezal, L. Zulianello, L. Gebbie, F. Letourneur, and P. Cosson. 2001. Membrane sorting in the endocytic and phagocytic pathway of *Dictyostelium discoideum*. *Eur J Cell Biol*. 80:754-64.

Reinders, Y., I. Schulz, R. Gräf, and A. Sickmann. 2006. Identification of novel centrosomal proteins in *Dictyostelium discoideum* by comparative proteomic approaches. *J Proteome Res*. 5:589-98.

Rivero, F., and M. Maniak. 2006. Quantitative and microscopic methods for studying the endocytic pathway. *Methods Mol Biol*. 346:423-38.

Robinson, D.N., and J.A. Spudich. 2004. Mechanics and regulation of cytokinesis. *Curr Opin Cell Biol*. 16:182-8.

Rohlfs, M., R. Arasada, P. Batsios, J. Janzen, and M. Schleicher. 2007. The Ste20-like kinase SvkA of *Dictyostelium discoideum* is essential for late stages of cytokinesis. *J Cell Sci*. 120:4345-54.

Ross, D.T., U. Scherf, M.B. Eisen, C.M. Perou, C. Rees, P. Spellman, V. Iyer, S.S. Jeffrey, M. Van de Rijn, M. Waltham, A. Pergamenschikov, J.C. Lee, D. Lashkari, D. Shalon, T.G. Myers, J.N. Weinstein, D. Botstein, and P.O. Brown. 2000. Systematic variation in gene expression patterns in human cancer cell lines. *Nat Genet*. 24:227-35.

Rot, G., A. Parikh, T. Curk, A. Kuspa, G. Shaulsky, and B. Zupan. 2009. dictyExpress: a *Dictyostelium discoideum* gene expression database with an explorative data analysis web-based interface. *BMC Bioinformatics*. 10:265.

Sasaki, A.T., C. Chun, K. Takeda, and R.A. Firtel. 2004. Localized Ras signaling at the leading edge regulates PI3K, cell polarity, and directional cell movement. *J Cell Biol*. 167:505-18.

Schulz, I., A. Erle, R. Graf, A. Kruger, H. Lohmeier, S. Putzler, M. Samereier, and S. Weidenthaler. 2009. Identification and cell cycle-dependent localization of nine novel, genuine centrosomal components in *Dictyostelium discoideum*. *Cell Motil Cytoskeleton*. 66:915-28.

Schulz, I., Y. Reinders, A. Sickmann, and R. Gräf. 2006. An improved method for *Dictyostelium centrosome* isolation. *Methods Mol Biol*. 346:479-89.

Seastone, D.J., L. Zhang, G. Buczynski, P. Rebstein, G. Weeks, G. Spiegelman, and J. Cardelli. 1999. The small Mr Ras-like GTPase Rap1 and the phospholipase C pathway act to regulate phagocytosis in *Dictyostelium discoideu*m. *Mol Biol Cell*. 10:393-406.

Simanis, V. 2003. Events at the end of mitosis in the budding and fission yeasts. *J Cell Sci*. 116:4263-75.

St John, M.A., W. Tao, X. Fei, R. Fukumoto, M.L. Carcangiu, D.G. Brownstein, A.F. Parlow, J. McGrath, and T. Xu. 1999. Mice deficient of Lats1 develop soft-tissue sarcomas, ovarian tumours and pituitary dysfunction. *Nat Genet*. 21:182-6.

Stavridi, E.S., K.G. Harris, Y. Huyen, J. Bothos, P.M. Verwoerd, S.E. Stayrook, N.P. Pavletich, P.D. Jeffrey, and F.C. Luca. 2003. Crystal structure of a human Mob1 protein: toward understanding Mob-regulated cell cycle pathways. *Structure*. 11:1163-70.

Stegert, M.R., A. Hergovich, R. Tamaskovic, S.J. Bichsel, and B.A. Hemmings. 2005. Regulation of NDR protein kinase by hydrophobic motif phosphorylation mediated by the mammalian Ste20-like kinase MST3. *Mol Cell Biol*. 25:11019-29.

Stork, O., A. Zhdanov, A. Kudersky, T. Yoshikawa, K. Obata, and H.C. Pape. 2004. Neuronal functions of the novel serine/threonine kinase Ndr2. *J Biol Chem*. 279:45773-81.

Sutherland, B.W., G.B. Spiegelman, and G. Weeks. 2001. A Ras subfamily GTPase shows cell cycle-dependent nuclear localization. *EMBO Rep.* 2:1024-8.

Swanson, J.A. 2008. Shaping cups into phagosomes and macropinosomes. *Nat Rev Mol Cell Biol*. 9:639-49.

Takahashi, Y., Y. Miyoshi, C. Takahata, N. Irahara, T. Taguchi, Y. Tamaki, and S. Noguchi. 2005. Down-regulation of LATS1 and LATS2 mRNA expression by promoter hypermethylation and its association with biologically aggressive phenotype in human breast cancers. *Clin Cancer Res.* 11:1380-5.

Tamaskovic, R., S.J. Bichsel, and B.A. Hemmings. 2003. NDR family of AGC kinases - essential regulators of the cell cycle and morphogenesis. *FEBS Lett*. 546:73-80.

Tamaskovic, R., S.J. Bichsel, H. Rogniaux, M.R. Stegert, and B.A. Hemmings. 2003. Mechanism of Ca2+-mediated regulation of NDR protein kinase through autophosphorylation and phosphorylation by an upstream kinase. *J Biol Chem*. 278:6710-8.

Tanaka, K., J. Petersen, F. MacIver, D.P. Mulvihill, D.M. Glover, and I.M. Hagan. 2001. The role of Plo1 kinase in mitotic commitment and septation in *Schizosaccharomyces pombe*. *Embo J*. 20:1259-70.

Tao, W., S. Zhang, G.S. Turenchalk, R.A. Stewart, M.A. St John, W. Chen, and T. Xu. 1999. Human homologue of the *Drosophila melanogaster* lats tumour suppressor modulates CDC2 activity. *Nat Genet*. 21:177-81.

Toji, S., N. Yabuta, T. Hosomi, S. Nishihara, T. Kobayashi, S. Suzuki, K. Tamai, and H. Nojima. 2004. The centrosomal protein Lats2 is a phosphorylation target of Aurora-A kinase. *Genes Cells*. 9:383-97.

Tuxworth, R.I., J.L. Cheetham, L.M. Machesky, G.B. Spiegelmann, G. Weeks, and R.H. Insall. 1997. *Dictyostelium* RasG is required for normal motility and cytokinesis, but not growth. *J Cell Biol*. 138:605-14.

Ushiba, D., and B. Magasanik. 1952. Effects of auxotrophic mutations on the adaptation to inositol degradation in *Aerobacter aerogenes*. *Proc Soc Exp Biol Med*. 80:626-32.

Watts, D.J., and J.M. Ashworth. 1970. Growth of myxameobae of the cellular slime mould *Dictyostelium discoideum* in axenic culture. *Biochem J*. 119:171-4.

Weber, I., G. Gerisch, C. Heizer, J. Murphy, K. Badelt, A. Stock, J.M. Schwartz, and J. Faix. 1999. Cytokinesis mediated through the recruitment of cortexillins into the cleavage furrow. *Embo J*. 18:586-94.

Williams, K.L. 1978. Characterization of Dominant Resistance to Cobalt Chloride in *Dictyostelium discoideum* and Its Use in Parasexual Genetic Analysis. *Genetics*. 90:37-47.

Williams, R.S., K. Boeckeler, R. Gräf, A. Müller-Taubenberger, Z. Li, R.R. Isberg, D. Wessels, D.R. Soll, H. Alexander, and S. Alexander. 2006. Towards a molecular understanding of human diseases using *Dictyostelium discoideum*. *Trends Mol Med*. 12:415-24.

Wu, S., J. Huang, J. Dong, and D. Pan. 2003. *hippo* encodes a Ste-20 family protein kinase that restricts cell proliferation and promotes apoptosis in conjunction with salvador and warts. *Cell*. 114:445-56.

Yabuta, N., N. Okada, A. Ito, T. Hosomi, S. Nishihara, Y. Sasayama, A. Fujimori, D. Okuzaki, H. Zhao, M. Ikawa, M. Okabe, and H. Nojima. 2007. Lats2 is an essential mitotic regulator required for the coordination of cell division. *J Biol Chem*. 282:19259-71.

Yang, X., D.M. Li, W. Chen, and T. Xu. 2001. Human homologue of *Drosophila* lats, LATS1, negatively regulate growth by inducing G(2)/M arrest or apoptosis. *Oncogene*. 20:6516-23.

Yang, X., K. Yu, Y. Hao, D.M. Li, R. Stewart, K.L. Insogna, and T. Xu. 2004. LATS1 tumour suppressor affects cytokinesis by inhibiting LIMK1. *Nat Cell Biol*. 6:609-17.

Yumura, S., M. Yoshida, V. Betapudi, L.S. Licate, Y. Iwadate, A. Nagasaki, T.Q. Uyeda, and T.T. Egelhoff. 2005. Multiple myosin II heavy chain kinases: roles in filament assembly control and proper cytokinesis in *Dictyostelium*. *Mol Biol Cell*. 16:4256-66.

Zhang, S., P.G. Charest, and R.A. Firtel. 2008. Spatiotemporal regulation of Ras activity provides directional sensing. *Curr Biol*. 18:1587-93.

Zhao, B., Q.Y. Lei, and K.L. Guan. 2008. The Hippo-YAP pathway: new connections between regulation of organ size and cancer. *Curr Opin Cell Biol*. 20:638-46.

Ziv, C., G. Kra-Oz, R. Gorovits, S. Marz, S. Seiler, and O. Yarden. 2009. Cell elongation and branching are regulated by differential phosphorylation states of the nuclear Dbf2-related kinase COT1 in *Neurospora crassa*. *Mol Microbiol*. 74:974-89.

List of figures

Acknowledgments

Curriculum vitae

Personal details

Name
    Peter Michael Kastner

Date of birth
    1980, January 17th in Schongau, Germany

University training

April 2006 - Aug. 2010
    Post-graduate studies at the Institute for Anatomy and Cell Biology, Ludwig-Maximilians-Universität München in the laboratory of Prof. Dr. Michael Schleicher
    Degree: Dr. rer. nat.

Oct. 1999 - Feb. 2006
    Studies in Biology at the Ludwig-Maximilians-Universität München with topics Zoology / Cell Biology, Biochemistry, Immunology and Genetics
    Degree: Dipl. biol.

May 2005 - Feb. 2006
    Diploma thesis at the Wellcome Trust Biocentre, University of Dundee, Scotland, in the laboratory of Prof. Dr. Cornelis Weijer

School training

Sept. 1990 - June 1999
    Welfen-Gymnasium Schongau
    Degree: Abitur

Sept. 1986 - July 1990
    Grundschule Schongau

Fellowships, prizes

May 2007 - Dec. 2010
    Member and speaker of the graduate program "Protein Dynamics in Health and Disease" in the Elite Network of Bavaria ENB

June 2007 - May 2010
    "Stipendium nach dem Bayerischen Eliteförderungsgesetz" of the bavarian government to perform a PhD thesis at the Ludwig-Maximilians-Universität München

Sept. / Dec. 2008
    Travel scholarships by the JSPS (Japan Society for the Promotion of Science) and the DFG (Deutsche Forschungsgemeinschaft)

Sept. 2007
    "Presentation Award" for a talk, given at the 9th DGZ young scientist meeting in Münster

Aug. 2005 - Dec. 2005
    Scholarship to perform a Diploma thesis at the University of Dundee by the DAAD (Deutscher Akademischer Austausch Dienst)